UNIVERSIDADE FEDERAL FLUMINENSE

INSTITUTO DE GEOCIÊNCIAS

DEPARTAMENTO DE GEOLOGIA E GEOFÍSICA

PROGRAMA DE PÓS-GRADUAÇÃO EM DINÂMICAS DOS OCEANOS E DA TERRA

EDUARDO THOMAZ DE AQUINO RIBEIRO

CONTROLES ESTRUTURAIS NA MORFOLOGIA DO TRECHO DISTAL DO SISTEMA DO CÂNION DE CANANÉIA, PLATÔ DE SÃO PAULO, SUDESTE DO BRASIL

Niterói
2026

EDUARDO THOMAZ DE AQUINO RIBEIRO

CONTROLES ESTRUTURAIS NA MORFOLOGIA DO TRECHO DISTAL DO SISTEMA DO CÂNION DE CANANÉIA, PLATÔ DE SÃO PAULO, SUDESTE DO BRASIL

Dissertação submetida ao Programa de Pós-Graduação em Dinâmica dos Oceanos e da Terra, da Universidade Federal Fluminense, como requisito parcial para a obtenção do título de Mestre na área de Geologia e Geofísica.

Orientador:
Prof. Dr. Cleverson Guizan Silva

Coorientador:
Prof. Dr. João Regis dos Santos Filho

Niterói
2026

Ficha catalográfica

Ficha catalográfica automática - SDC/BIG
Gerada com informações fornecidas pelo autor

R484c Ribeiro, Eduardo Thomaz de Aquino
CONTROLES ESTRUTURAIS NA MORFOLOGIA DO TRECHO DISTAL DO SISTEMA DO CÂNION DE CANANÉIA, PLATÔ DE SÃO PAULO, SUDESTE DO BRASIL / Eduardo Thomaz de Aquino Ribeiro. - 2026.
90 f.: il.

Orientador: Cleverson Guizan Silva.
Coorientador: João Regis Dos Santos Filho.
Dissertação (mestrado)-Universidade Federal Fluminense, Instituto de Geociências, Niterói, 2026.

1. Geomorfologia Marinha. 2. Geologia Marinha. 3. Controle Estrutural. 4. Bacia de Santos. 5. Produção intelectual. I. Silva, Cleverson Guizan, orientador. II. Dos Santos Filho, João Regis, coorientador. III. Universidade Federal Fluminense. Instituto de Geociências. IV. Título.

CDD - XXX

Bibliotecário responsável: Debora do Nascimento - CRB7/6368

EDUARDO THOMAZ DE AQUINO RIBEIRO

CONTROLES ESTRUTURAIS NA MORFOLOGIA DO TRECHO DISTAL DO SISTEMA DO CÂNION DE CANANÉIA, PLATÔ DE SÃO PAULO, SUDESTE DO BRASIL

Dissertação submetida ao Programa de Pós-Graduação em Dinâmica dos Oceanos e da Terra, da Universidade Federal Fluminense, como requisito parcial para a obtenção do título de Mestre na área de Geologia e Geofísica.

BANCA EXAMINADORA

Prof. Dr. Cleverson Guizan Silva – Orientador (UFF)

Prof. Dr. João Regis dos Santos Filho – Coorientador (UERJ)

Profa. Dra. Narelle Maia de Almeida – (UFC)

Prof. Dr. Alberto Garcia de Figueiredo Jr. – (UFF)

Prof. Dr. Christian Gorini – (SU/ISTEP)

DEDICATÓRIA

Dedico este trabalho aos meus avós, Lea e Celio, que sempre incentivaram em mim a curiosidade de compreender as dinâmicas do mundo.

AGRADECIMENTOS

Agradeço a toda a minha família, em especial aos meus avós, Celio e Lea, minha mãe, Adriana e meu irmão Felipe, que sempre vibram e apoiam minhas escolhas e conquistas. Sou muito grato em especial à minha irmã, Mariana e ao meu pai César, que são verdadeiras inspirações de vida pela forma como enfrentaram/enfrentam algumas lutas, e ainda assim, têm forças para me apoiar e torcer por mim. Agradeço também ao meu tio, Guilherme, que sempre foi um dos meus maiores incentivadores no caminho que estou trilhando nas geociências marinhas. Amo muito todos vocês. A caminhada pode ser dura em alguns momentos, mas estaremos sempre juntos.

À minha companheira de vida por todo apoio e incentivo incondicional durante este período, te amo. Agradeço também a minha família de axé, sou muito grato e feliz ao lado de todos vocês.

Ao meu orientador Prof. Cleverson Guizan Silva, por todo apoio, orientação e incentivo, o senhor é uma grande referência para mim, e é uma honra poder ser seu aluno. Agradeço também ao meu coorientador Prof. João Regis dos Santos Filho, que não só foi um orientador nessa etapa do mestrado, mas também foi um grande mestre desde o início da minha trajetória na geologia e geomorfologia marinha. João, sem palavras para você, só tenho a agradecer por todo apoio, conselhos e conversas ao longo desses anos, é uma honra ter sido o seu aluno e poder me considerar também seu amigo.

Ao Prof. Alberto Garcia de Figueiredo Jr. que não só é membro da banca, mas foi meu primeiro orientador na época da graduação. Professor, só tenho a agradecer ao senhor, é muito gratificante ter sido seu aluno e ver o quanto o senhor gosta do que faz e luta para que ciência continue avançando.

À Prof.ª Narelle Maia de Almeida, por aceitar compor a banca e pelas dicas e conversas durante os congressos. É uma honra poder contar com sua participação. Ao Prof. Christian Gorini, pelas orientações e pelo curso ministrado que acabou sendo muito importante não só para o desenvolvimento deste trabalho, mas também para eu me encontrar cada vez mais nessa área.

A todos os colegas do LAGEMAR, em especial ao Davy Raeder Brandão, que foi fundamental para que esse mestrado acontecesse, muito obrigado pelos ensinamentos na interpretação sísmica e por todas as ideias e conversas que tivemos. Ao meu irmão de

outra mãe, Leonardo Junius C. Santos, mais uma etapa que estamos trilhando juntos, só agradecer por todo apoio de sempre, ideias e debates de interpretação dos nossos dados. Sou eternamente grato por todos os conselhos e oportunidades que você me incluiu, graças a você, entrei no LAGEMAR na graduação e me encontrei nessa área, estamos juntos sempre, só tenho a agradecer.

A todos os amigos e colegas do DOT-UFF e aos grandes amigos que fiz na graduação, em especial Alexandre Alcazar, Daniel SQL, Mahatma Aguiar, Daniel Bruno, Braian Salvador, Claudio Lucas, e muitos outros, quem está junto sabe, amo vocês.

À TGS Brasil, em especial ao João Correa, pela disponibilização dos dados de Batimetria Multifeixe, através do acordo de cooperação com a Universidade Federal Fluminense, que possibilitou a realização deste estudo.

À ANP (Agência Nacional do Petróleo, Gás Natural e Biocombustíveis), pela disponibilização dos dados de sísmica 2D, que possibilitaram as interpretações de estruturas de subsuperfície.

Ao CNPq (Conselho Nacional de Desenvolvimento Científico e Tecnológico), pelos recursos financeiros da bolsa de mestrado.

A todos que fazem parte do programa de pós graduação Dinâmica dos Oceanos e da Terra por toda estrutura, corpo docente, funcionários e pelo apoio financeiro para apresentação de trabalhos em eventos científicos.

Ao sagrado por todas as bençãos na minha vida e pelos caminhos abertos que me levaram até aqui, por onde eu for, sei que não vou só.

RESUMO

Cânions submarinos são importantes condutos sedimentares que transferem fluxos gravitacionais das margens continentais para bacias marinhas profundas, onde geram uma variedade de feições deposicionais e erosivas. Em bacias com espessas camadas evaporíticas, a evolução e a trajetória desses condutos podem ser fortemente influenciadas pela tectônica do sal e por estruturas de subsuperfície. Este estudo investiga a morfologia e o controle estrutural de um canal submarino localizado no Platô de São Paulo (Bacia de Santos, SE do Brasil), interpretado como parte distal do sistema do Cânion de Cananéia. A análise integra batimetria multifeixe de alta resolução (15 m) com dados sísmicos de reflexão 2D regionais. O sistema de drenagem mapeado se estende por aproximadamente 194 km e compreende um setor a montante dominado por complexos de transporte em massa que evoluem a jusante para um canal submarino confinado. Os dados multifeixe revelam feições geomorfológicas proeminentes, incluindo cicatrizes de escorregamento, pockmarks, elevação intra-canal e escarpas erosivas que chegam a atingir cerca de 230 m de altura, evidenciando incisão e instabilidade das margens. As interpretações sísmicas apontam que o canal se desenvolveu sobre uma topografia irregular relacionada ao sal, controlada por reativações e falhas do Lineamento de Capricórnio e Alto de Puri. Essas estruturas governam o confinamento do canal, a deflexão do fluxo, a posição do talvegue e os padrões erosivos, com evidências que indicam um controle estrutural persistente ao longo do tempo geológico, como o preenchimento assimétrico do paleocanal. Os segmentos a montante registram episódios sucessivos de fluxos de transporte de massa e um preenchimento progressivo do cânion, enquanto que os setores a jusante apresentam maior confinamento e predominância de processos erosivos associados à influência estrutural. Esses resultados fornecem novas interpretações sobre a geomorfologia e o controle estrutural do sistema distal do Cânion de Cananéia, o principal cânion submarino da Bacia de Santos, um setor que permaneceu pouco caracterizado devido à escassez de dados de alta resolução. Os achados também reforçam a importância da tectônica do sal como um dos principais fatores de controle da evolução geomorfológica e do roteamento sedimentar em águas profundas do Platô de São Paulo.

Palavras chave: Cânion da Cananéia, Canal submarino, Controle estrutural, Tectônica do sal, Complexo de movimento de massa, Bacia de Santos

ABSTRACT

Submarine canyons are major sediment conduits that transfer gravity-driven flows from continental margins to deep-marine basins, where they generate a range of depositional and erosional elements. In salt-bearing margins, the evolution and trajectory of these conduits may be strongly influenced by halokinetic deformation and inherited structural elements. This study investigates the morphology and structural control of a submarine channel located on the São Paulo Plateau (Santos Basin, SE Brazil), interpreted as the distal continuation of the Cananéia Canyon sediment-routing system. The analysis integrates high-resolution multibeam bathymetry (15 m grid) with regional 2D seismic reflection data. The mapped drainage system extends for ~194 km and comprises a proximal sector dominated by mass-transport complexes transitioning downstream into a confined submarine channel. Multibeam data reveal prominent geomorphological features, including slide scars, pockmarks, intra-channel highs, and an erosional escarpment reaching ~230 m in height, indicating intense channel-floor incision and margin instability. Seismic interpretations show that the channel evolved over an irregular salt-related topography controlled by inherited basement structures, particularly the Puri High and faults associated with the Capricorn Lineament. These structures govern channel confinement, flow deflection, thalweg position, and erosional patterns, while asymmetric paleochannel fills indicate persistent structural control through successive stages of channel evolution. Upstream segments record repeated mass-transport deposition and progressive canyon infill, whereas downstream sectors display enhanced confinement and erosional dominance linked to structural relief. These results provide new insights into the geomorphology and structural control of the distal Cananéia Canyon system, the main submarine canyon system of the Santos Basin, a sector that has remained poorly characterized due to limited high-resolution data and highlight the key role of salt tectonics in governing deep-water sediment-routing systems on the São Paulo Plateau.

Keywords: Cananéia Canyon, Submarine channel, Structural control, Salt tectonics, Mass transport complexes, Santos Basin

SUMÁRIO

1. INTRODUÇÃO.....18
1.1. JUSTIFICATIVA 19
1.2. OBJETIVO 20
2. ESTRUTURA DA DISSERTAÇÃO 21
3. FUNDAMENTAÇÃO TEÓRICA 21
3.1. Cânions Submarinos e Sistemas Sedimentares em Ambientes Marinhos Profundos 21
3.2 Tectônica do sal 25
3.2.1. Tectônica do sal em regimes extensionais e compressivos: 28
3.2.2. Tipos de Diapirísmo: 29
3.3. Influência da tectônica do sal em canais submarinos 30
4. ARTIGO 33
5. REFERÊNCIAS 83

LISTA DE FIGURAS

Figura 1: Ilustração esquemática evidenciando algumas das principais feições erosivas e deposicionais em oceano profundo. Fonte: extraído e modificado de Posamentier & Kolla, 2003. 22

Figura 2: Ilustração esquemática evidenciando alguns tipos de processos gravitacionais de transporte sedimentar. Fonte: extraído e modificado de Shanmugan et al., 1994; Shanmugan, 2019. 23

Figura 3: Modelo esquemático ilustrando a sobrecarga sedimentar como mecanismo causador da movimentação do sal. Fonte: Extraído de Mohriak et al., 2008. 26

Figura 4: Diferentes tipos de estruturas salinas. Fonte: Extraído e modificado de Hudec & Jackson, 2007. 27

Figura 5: Comportamento de estruturas salinas em diferentes tipos de regime. Fonte: Extraído e modificado de Fossen, 2016. 28

Figura 6: Ilustração evidenciando o controle estrutural sobre sistemas canal-lobo na Bacia do Baixo Congo. Fonte: Extraído e modificado de Oluboyo et al., 2014. 30

Figura 7: Ilustração esquemática evidenciando o controle estrutural exercido pela tectônica do sal sobre canais de turbidez em ambiente de talude. Fonte: Extraído e modificado de Gee & Gawthorpe, 2006. 31

LISTA DE FIGURAS DO ARTIGO:

Fig. 1. Location map of Santos Basin (white line) and the study area outlined by a white dashed line over the multibeam bathymetric dataset. …….38

Fig. 2. Regional bathymetric map (LEPLAC dataset) illustrating the trace of the Capricorn Lineament (CL), the Puri High (PH), the Abimail Ridge (AR) and the distribution of earthquakes. The study area is delimited by the white polygon. …….40

Fig. 3. Dataset used for the analyses and interpretations. White lines represent the interpreted 2D multichannel seismic reflection lines provided by the ANP, which were used to generate the salt top, salt base, and salt thickness maps. Black-highlighted lines correspond to the seismic sections interpreted in detail and presented in the Results section. The multibeam bathymetric dataset, provided by TGS Brazil, is displayed over the study area; peripheral portions of the dataset are greyed out to mask areas not considered in this study, emphasizing the central drainage system that constitutes the main focus of the analysis. ……...42

Fig. 4**.** Examples of seismic facies identified in the study area and their respective interpretations. ……44

Fig. 5. Geomorphological map of the study area (outlined by white lines) highlighting the main features identified: slide scars (red lines), MTC boundaries (white lines), erosional scarps (blue lines), channel-base erosional surface (purple), Crestal Grabens and Ridges (green lines), pockmark cluster (green polygon), and marginal sediment deposits (yellow polygons). Line segments 1, 2 and 3 indicates the proximal, transitional and distal sectors, with different morphologies and features discussed in the text. ……...46

Fig. 6. Slope gradient map of the study area derived from bathymetric data. ……..…47

Fig. 7. (A) Salt top depth map. (B) Salt base depth map. (C) Salt thickness map. (D) Gravity anomaly map overlain by the study area (adapted from Carvalho et al., 2022). The dashed white line indicates the Cananéia channel trajectory, Abimael Ridge (AR) is represented by the red and black line (Modified from Mohriak and Szameitat, 2023), and Puri High (PH) is represented by the black line (Modified by Freitas et al., 2022). ……49

Fig. 8. (A) Detailed view of the MTC area illustrating the approximate length and geometry of several displaced blocks, and four bathymetric profiles. Black arrows indicate the measured length of individual blocks. (B) Perspective view of the relief of representative mass-transport blocks in the northwestern sector of the study area, corresponding to the yellow polygon shown in (A). Vertical exaggeration: 5×. ……...51

Fig. 9. Perspective view of a sector of the mass-transport complex (MTC), showing the 2D seismic line highlighted in yellow and its corresponding subsurface section below.

Stratigraphic markers (pink, orange, blue and yellow horizons) are constrained using the chronostratigraphic framework of (Contreras et al., 2010). The red horizon marks the basal surface of the most recent MTD events. …….…….53

Fig. 10. Morphology of channel sector (ii), highlighting Mass-Transport Complexes (MTCs), slide scars, and pockmark clusters. Bathymetric map indicating the locations of profile lines A–A', B–B', C–C', and D–D'. …….54

Fig. 11. Interpreted 2D dip longitudinal seismic line, across the proximal and transitional sectors (i) and (ii). Stratigraphic markers on the dip line (blue, yellow, and pink horizons) are constrained using the chronostratigraphic framework of Contreras et al. (2010). The red horizon marks the basal surface of the most recent MTD events. …….55

Fig. 12. (A) Eleven cross-channel bathymetric profiles illustrating preferential drainage pathways and sediment-accumulation zones. Depth (m) is shown on the left axis, and segment length (Km) is shown along the bottom axis. (B) Longitudinal profile along the channel thalweg (97.4 km in length) showing the mapped features in sector (iii). Vertical exaggeration: (5×). ……56

Fig. 13. (A) Bathymetric map showing the main erosional features of the submarine valley, including slide scars, erosional scarps and channel-base erosional surfaces. (B, C) 3D bathymetric perspective view showing erosional features of the channel (vertical exaggeration 5x). …….57

Fig.14. Interpreted 2D seismic cross-sections in the distal sector of the study area. Section A-C represent strike-oriented cross sections perpendicular to the channel axis. The sections illustrate variations in geometry, depositional architecture, and the relationship between channel incision, and salt-related structures. The red horizon marks the current seafloor in sections A–C. The yellow horizon in sections A–C represents the base of the ancient channel, while the pink horizon marks the top of the salt layer in all sections. …….59

Fig. 15. Distribution of pockmarks in the study area and A–A′ bathymetric profile highlighting the maximum depths of two representative pockmarks. ……..……..……...60

Fig. 16. (A) Cluster of pockmarks (left) and corresponding expression in the gradient map (right). (B) Perspective view of the gradient map (in degrees) highlighting sectors with the steepest slopes, including erosive scars along the elevated feature (44–58°) and the base of the erosive escarpment (48°).(C) Detailed view of an elongated positive-relief feature, likely salt-related, bounded by erosive scars and measuring ~145 m in height and ~4.3 km in length. This structure is interpreted as a morphological barrier that influences sediment bypass and controls deposition pathways.……..…….61

Fig. 17. Schematic cross-section of the Cananéia Canyon system, illustrating the structural and sedimentary framework. The section is based on 2D seismic data (upper panel and the same in Figure 7 B) but is presented as a schematic model with exaggerated vertical scale to highlight key features, including salt-related topography, forced folds, onlaps, and fluid pathways. Pockmark clusters mark zones of focused fluid escape, while the underlying Puri High represents a basement structure controlling salt uplift and canyon trajectory. Black arrows (single-sided) indicate onlaps. ……65

Fig. 18. Interpretive schematic model of the distal sector of the Cananéia Canyon system, based on the integration of seismic and bathymetric interpretations. The cross-section is based on the seismic interpretation presented in Fig. 14C. The model provides an overview of the distal study area within the limits of seismic coverage, illustrating the influence of the Puri High, faults associed with the Capricorn Lineament, salt-related deformation and their control on canyon morphology and channel evolution……67

Fig. 19. Map showing faults and features including the channel thalweg, erosional scarps, marginal sediment deposits, and the channel-base erosional surface, with cross-sections indicated by white lines. Right: two cross-sections along the channel, illustrating its asymmetric inversion. ……....69

Fig. 20. Downstream section of the current submarine channel seafloor, showing dynamics and features such as margin gradient variations, channel course changes, pockmarks, slide scars, and deflection caused by the intra-channel high. …….....70

LISTA DE TABELAS DO ARTIGO

Table 1: Summary of depth, gradient and area statistics for each mapped feature. Values represent minimum, maximum and mean estimates derived from multibeam bathymetry analysis. MTCs*- Mass Transport Complexes.....…….48

LISTA DE ABREVIATURAS E SIGLAS

AAIW - *Antarctic Intermediate Water*

ANP - Agência Nacional do Petróleo, Gás Natural e Biocombustíveis

AR - *Abimael Ridge*

CL - *Capricornio Lineament*

CPRM – Serviço Geológico do Brasil

DHN - Diretoria de Hidrografia e Navegação

ENE - *East-Northeast* (leste-nordeste)

IPT – Instituto de Pesquisas Tecnológicas do Estado de São Paulo

LEPLAC - Plano de Levantamento da Plataforma Continental Brasileira

LGM – *Last Glacial Maximum*

MTCs - *Mass Transport Complexes*

MTDs - *Mass Transport Deposits*

NADW - *North Atlantic Deep Water*

NW–SE - *Northwest–Southeast* (noroeste–sudeste)

ON – Observatório Nacional

PH - *Puri High*

SACW - *South Atlantic Central Water*

SSE - *South-Southeast* (sul-sudeste)

SW-NE – *Southwest-Northeast* (Sudoeste-Nordeste)

UFRN – Universidade do Rio Grande do Norte

UnB – Universidade de Brasília

USP – Universidade de São Paulo

WNW - *West-Northwest* (oeste-noroeste)

1. INTRODUÇÃO

Cânions submarinos são os principais condutos por meio dos quais sedimentos são transferidos das margens continentais para ambientes marinhos profundos (Normark & Carlson, 2003). Esses sistemas estão intimamente ligados a processos sedimentares controlados pela gravidade, canalizando correntes de turbidez e outros tipos de processos gravitacionais, como depósitos de movimentos de massa, que fornecem grandes volumes de sedimento aos sistemas oceânicos profundos (Normark et al., 1993; Talling et al., 2012; Wu et al., 2022; Böttner et al., 2025). O transporte sedimentar nesses ambientes é tipicamente de alta energia, sendo capaz de erodir o fundo de cânions em dezenas de metros durante eventos únicos e gerar extensas cicatrizes erosivas (Conway et al., 2012; Normandeau et al., 2025; Taylor et al., 2026).

Em ambientes marinhos profundos, os sedimentos transportados por cânions submarinos geram uma ampla variedade de feições deposicionais e erosivas, incluindo canais e lobos turbidíticos, depósitos de levees, *crevasse splays*, ondas sedimentares e complexos de transporte de massa, como deslizamentos, *slumps* e fluxos de detritos (*debris flows*) (Posamentier & Kolla, 2003; Deptuck et al., 2008; Zhang et al., 2020; Pirmez et al., 2000; Shipp et al., 2011; Zhang et al., 2026). Esses elementos registram e ajudam a compreender a variabilidade espacial e temporal do aporte sedimentar controlado pela gravidade desde o talude até o fundo da bacia.

Em bacias evaporíticas, como a Bacia de Santos, os condutos sedimentares podem ser influenciados pela halocinese. Diversos estudos documentaram o controle estrutural exercido pela tectônica do sal sobre condutos sedimentares submarinos, incluindo cânions e canais, em bacias com consideráveis camadas evaporíticas ao redor do mundo, como o Mediterrâneo oriental (Clark & Cartwright, 2009), offshore de Angola (Gee & Gawthorpe, 2006, 2007), o Golfo do México (Smith, 2004), a Bacia do Espírito Santo (Gamboa et al., 2012), a Bacia do Baixo Congo (Oluboyo et al., 2014), a Bacia de Campos (Covault et al., 2020) e o Mar do Norte (Abu et al., 2025). Quando o sal se encontra em condições compressivas, canais podem ser defletidos, represados, bloqueados ou confinados pelo surgimento de diápiros ou modificações topográficas relacionadas ao sal

(Prather et al., 2003; Clark & Cartwright, 2009; Oluboyo et al., 2014; Abu et al., 2025). Consequentemente, em margens influenciadas pelo sal, a evolução de cânions e dos sistemas de condução sedimentar associados está intrinsecamente ligada à deformação halocinética, a qual pode ser controlada por estruturas do embasamento e pela atividade (ou reativação) de falhas (Mohriak & Szameitat, 2023; Pichel et al., 2020; Silva et al., 2024).

Nesse contexto, o Cânion de Cananéia representa o principal cânion da Bacia de Santos (Zembruscki, 1979; Duarte & Viana, 2007; Hercos et al., 2023). Ele se estende do talude continental superior até a bacia profunda e é expresso na morfologia de fundo como uma grande incisão orientada a NO–SE. O cânion desempenha um papel fundamental como conduto sedimentar, influenciando na dinâmica sedimentar da plataforma continental até o oceano profundo. Estudos anteriores indicam que o cânion pode atuar capturando sedimentos finos provenientes da região proximal à quebra da plataforma, possivelmente associados às descargas do Rio da Prata, e transportando-os talude abaixo (Santos Filho et al., 2022). Em seu setor distal, esse sistema canaliza fluxos gravitacionais que contribuem para a formação de feições deposicionais, como *sediment waves* no Platô de Santa Catarina (Borisov et al., 2020). Além disso, o cânion provavelmente funcionou como uma conexão primária entre a drenagem costeira e o talude superior durante o Último Máximo Glacial (LGM), atuando como uma via eficiente de transferência de sedimentos de ambientes rasos para profundos ao longo do Quaternário tardio, inclusive durante fases de transgressão do nível do mar (Zembruscki, 1979; Borisov et al., 2020).

1.1. JUSTIFICATIVA

A caracterização de condutos sedimentares modernos em águas profundas possui grande relevância ambiental e geológica, sendo também fundamental para a segurança de infraestruturas submarinas, como cabos de fibra óptica e estruturas de fundo associadas à exploração de hidrocarbonetos. Além disso, a compreensão de sistemas deposicionais associados a paleo-canais e cânions em subsuperfície é de amplo interesse para a indústria de petróleo e gás devido ao seu potencial para hospedar reservatórios de alta qualidade (Pirmez et al., 2000; Posamentier & Kolla, 2003; Ashiru et al., 2020).

Nesse sentido, o estudo de processos gravitacionais modernos contribui tanto para a compreensão da dinâmica sedimentar atual quanto para a interpretação de sistemas análogos pretéritos em subsuperfície (Pirmez et al., 2000). O mapeamento com dados

batimétricos multifeixe de alta resolução destaca-se como uma ferramenta essencial para a identificação de feições deposicionais e erosivas, bem como para a avaliação da influência de estruturas de subsuperfície na morfologia do fundo marinho (Barnard et al., 2011; Kanari et al., 2020). No entanto, o reconhecimento e a caracterização das morfologias do fundo marinho profundo ainda constituem um desafio, em razão da necessidade de dados geofísicos de alta resolução e das limitações logísticas e econômicas associadas à aquisição de extensos levantamentos hidrográficos (Boswarva et al., 2018).

Embora estudos recentes, como o de Hercos et al. (2023), tenham avançado significativamente no mapeamento e na interpretação morfológica de grande parte da Bacia de Santos com base em dados de alta resolução, incluindo o segmento principal do cânion, do talude superior até o início do Platô de São Paulo, o setor mais distal, expresso como um vale submarino, permanece pouco caracterizado devido à limitada cobertura de dados. Estudos prévios (Duarte & Viana, 2007; Borisov et al., 2020; Hercos et al., 2023) já indicaram a conexão desse vale submarino com o Cânion de Cananéia, entretanto, nenhum desses trabalhos apresentou dados de alta resolução para o trecho nem teve como objetivo sua investigação detalhada.

Como consequência, os processos responsáveis pela evolução da porção distal do sistema do Cânion de Cananéia no Platô de São Paulo permanecem pouco compreendidos. Em particular, ainda não está estabelecido em que medida a morfologia atual do vale resulta da interação entre processos gravitacionais modernos e controles estruturais associados a estruturas de subsuperfície. A investigação desse segmento é fundamental para compreender os mecanismos que controlam a transferência sedimentar ao longo do principal conduto sedimentar da Bacia de Santos, permitindo identificar padrões erosivos e deposicionais, avaliar a influência de controles estruturais na organização do sistema sedimentar moderno e contribuir para a segurança de infraestruturas submarinas.

1.2. OBJETIVOS

Diante desse contexto, o presente trabalho tem como objetivo central caracterizar a morfologia e investigar o controle estrutural do canal submarino localizado na porção distal do sistema sedimentar do Cânion de Cananéia. Especificamente, busca-se

(i) analisar a influência de estruturas de subsuperfície na trajetória e nos padrões erosivos e deposicionais do canal;

(ii) compreender a distribuição espacial e a transição entre processos gravitacionais, incluindo complexos de transporte de massa e correntes de turbidez, ao longo do sistema;

(iii) contribuir com a caracterização e compreensão de condutos sedimentares sob influência de controle estrutural no Platô de São Paulo, ressaltando a importância da integração entre dados de batimetria multifeixe e sísmica na interpretação de sistemas deposicionais profundos em bacias evaporíticas.

2. ESTRUTURA DA DISSERTAÇÃO

A presente dissertação foi estruturada no formato de artigo científico, submetido em 15 de junho de 2026 à revista *Marine Geoscience and Energy Resources*. Inicialmente, é apresentada a fundamentação teórica, onde são abordados alguns dos conceitos evidenciados e discutidos ao longo do artigo, em seguida, é apresentado o artigo científico.

As citações utilizadas exclusivamente no artigo estão apresentadas e referenciadas em sua respectiva seção. A seção de referências ao final desta dissertação, por sua vez, reúne apenas os trabalhos citados nos capítulos de introdução e fundamentação teórica.

3. FUNDAMENTAÇÃO TEÓRICA:

3.1. Cânions Submarinos e Sistemas Sedimentares em Ambientes Marinhos Profundos

Cânions Submarinos são vales, ou incisões, normalmente entalhadas na quebra de plataforma/talude superior que atuam como principal conduto para o transporte sedimentar da plataforma para oceano profundo (Normark & Carlson, 2003). O desenvolvimento de cânions submarinos é frequentemente associado a processos de desestabilização de talude desencadeados por múltiplos fatores, incluindo suprimento sedimentar (Puig et al., 2017), variações do nível do mar (Rasmussen, 1994; Allin et al., 2018), terremotos (Kunath et al., 2025), falhamento e soerguimento tectônico (Li et al., 2023), e a topografia herdada do talude (Li et al., 2020).

Os cânions submarinos são tipicamente mais ativos durante períodos de nível do mar baixo, quando os sedimentos são mais transferidos de maneira mais eficiente para

sistemas de águas profundas (Li et al., 2023). Entretanto, muitos cânions permanecem ativos em diferentes estágios do nível do mar, a depender de fatores como o tipo do Cânion e onde ele está localizado. (Böttner et al., 2025). Cânions mais próximos da plataforma tendem a ser mais alimentados com sedimentos vindo do continente.

O trabalho de Jobe et al., (2011) definiu dois tipos principais de classificação de cânions submarinos. Os cânions Tipo I entalham a borda da plataforma continental, e conseguem um alto suprimento de sedimentos grossos, apresentam um padrão mais inciso em "V" devido a predominância de feições erosivas. Esse tipo de cânion conduz correntes de turbidez arenosas e movimentos de massa, gerando preenchimentos ricos em areia e grandes sistemas de leques submarinos talude abaixo, com alto potencial como reservatórios (Jobe et al., 2011). Já os cânions Tipo II ocorrem em áreas mais afastadas da plataforma, normalmente com cabeceiras em águas profundas e exibem morfologias suaves e agradacionais em "U" devido ao baixo aporte sedimentar. Esses condutos são dominados por deposição hemipelágica e correntes de turbidez diluídas, com preenchimentos finos, pouca erosão e ausência de leques e canais talude abaixo associados, atuando mais como selos ou intervalos geradores do que como reservatórios (Jobe et al., 2011).

Cânions submarinos são importantes componentes de sistemas sedimentares marinhos, e estão comumente associados ao desenvolvimento de canais e lobos turbidíticos, bem como a uma ampla variedade de feições erosivas e deposicionais em ambientes marinhos profundos (Figura 1). Entre essas feições, destacam-se os depósitos de transporte de massa, que desempenham papel fundamental na redistribuição sedimentar ao longo do talude e da bacia.

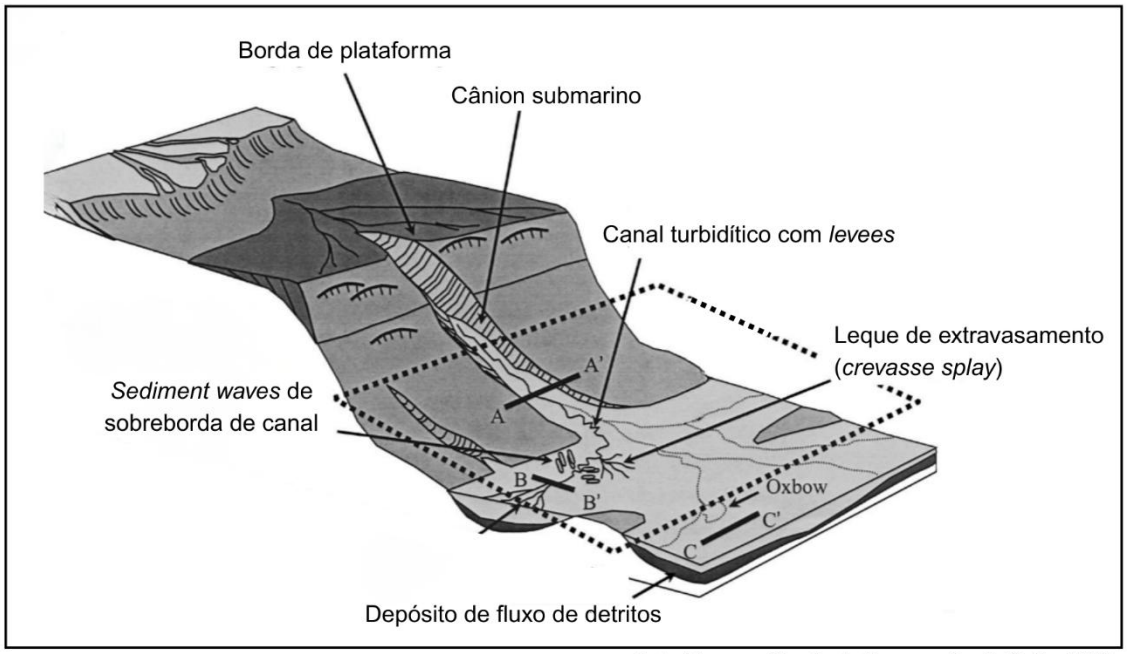

Extraído e modficado de Posamentier & Kolla, 2003.

Figura 1: Ilustração esquemática evidenciando algumas das principais feições erosivas e deposicionais em oceano profundo. Fonte: extraído e modificado de Posamentier & Kolla, 2003.

Depósito de transporte de massa é um termo geral que abrange grande parte das feições deposicionais ocasionadas por falhas induzidas pela gravidade em oceano profundo. Normalmente, nesse termo se inclui escorregamentos (*slides*), *slumps* e fluxos de detritos (*debris flow*) (Figura 2) (Moscardelli & Wood, 2007; Oluboyo et al., 2014; Shanmugan, 2019; Catuneanu, 2022). Múltiplos episódios de transporte de massa também podem ser chamados de complexos de movimento de massa

Depósitos (ou complexos) de transporte de massa, são comumente evidenciados em dados sísmicos por refletores caóticos, descontínuos e com amplitude variada, além de truncamentos erosivos em superfície basal e superfície superior irregular (Oluboyo et al., 2014; Ashiru et al., 2020).

Escorregamentos (*slides*) podem ser definidos como um movimento de massa translacional coeso de um bloco ou estrato sobre uma superfície de deslizamento plana, ou superfície de cisalhamento, com pouca ou nenhuma deformação interna ou rotação (Moscardelli & Wood, 2007; Shanmugan, 2019). *Slumps* são semelhantes aos escorregamentos, sendo diferenciados pelo plano de deslizamento, que no caso ocorrem um plano côncavo para cima que faz com que a massa sedimentar transportada seja rotacionada, podendo gerar diferentes graus de deformação (Moscardelli & Wood, 2007; Shanmugan, 2019).

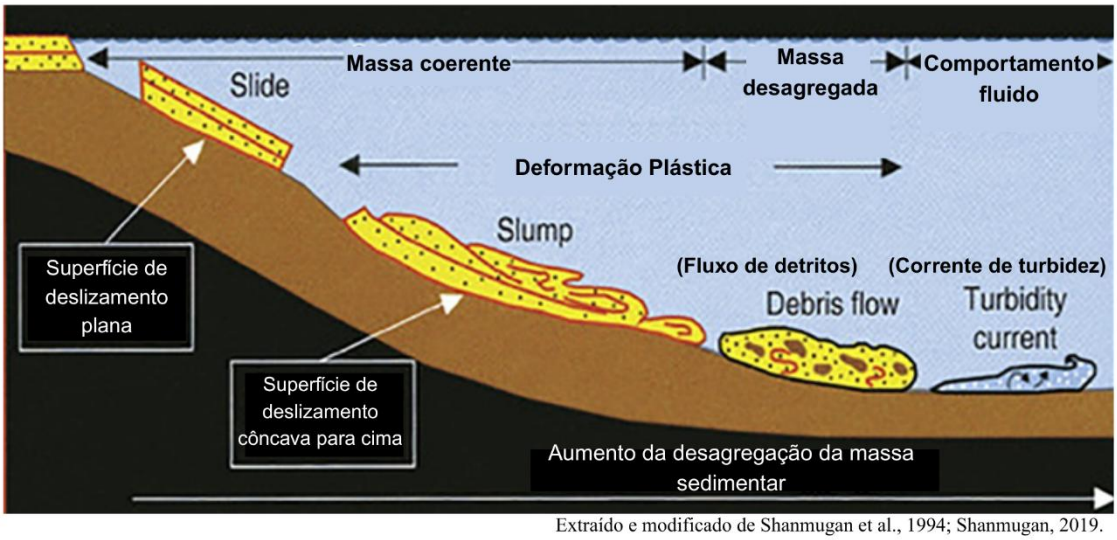

Extraído e modificado de Shanmugan et al., 1994; Shanmugan, 2019.

Figura 2: Ilustração esquemática evidenciando alguns tipos de processos gravitacionais de transporte sedimentar. Fonte: extraído e modificado de Shanmugan et al., 1994; Shanmugan, 2019.

Fluxo de detritos (*debris flow*) apresentam comportamento laminar plástico (fluido não newtoniano) com resistência controlada principalmente pela coesão associada ao teor sedimentar, normalmente composta de grãos finos, podendo receber suporte adicional por flutuabilidade da matriz (Moscardelli et al., 2006, Masson et al., 2006; Moscardelli & Wood, 2007; Shanmugan, 2019). Esses fluxos podem evoluir para correntes de turbidez newtonianas caso tenham aumento do conteúdo de fluido, embora algumas correntes de turbidez se originem diretamente de falhas sedimentares e se desenvolvam desde a borda da plataforma até ambientes distais da Bacia (Shanmugan et al., 1994).

Correntes de turbidez são fluxos gravitacionais submarinos de reologia newtoniana (comportamento fluido) e estado turbulento, nos quais os sedimentos são transportados pela suspensão turbulenta de água e sedimentos ao longo do fundo marinho (Masson et al., 2006; Moscardelli & Wood, 2007; Shanmugan, 2019). Esses fluxos são não estacionários e não uniformes, incorporando água ambiente por mistura turbulenta à medida que se deslocam talude abaixo (Heerema et al., 2020). Normalmente não possuem força suficiente para manter partículas muito grossas em suspensão, transportando principalmente areia fina a lama, que se depositam por decantação progressiva (Shanmugan et al., 1994).

Canais submarinos podem ser esculpidos pela ação de correntes de turbidez, ocorrendo normalmente do talude até porções profundas da bacia e normalmente são conectados com cânions submarinos, e podem servir de conduto sedimentar em leques submarinos

(Normark et al., 1993; Pirmez et al., 2000; Mayall et al., 2006; Deptuck et al., 2007; Ashiru et al., 2020). A arquitetura dos canais submarinos apresenta grande variabilidade em termos de escala, geometria, padrões deposicionais e capacidade erosiva, que refletem a influência de fatores como declividade, tectônica, deflexão, confinamento, entre outros. Além disso, os canais podem apresentar uma variedade de feições erosivo-deposicionais como *Levees* e *Sediment Waves* associadas, trechos de erosão basal do canal, trechos de deposições marginais intra-canal, escarpas e leques de extravasamento (*Crevasse splays*) (Posamentier & Kolla, 2003; Deptuck et al., 2007).

A interação dinâmica entre erosão, deposição e migração lateral resulta em uma arquitetura estratigráfica complexa, o que torna os canais submarinos elementos-chave tanto para a compreensão da evolução de margens continentais quanto para aplicações em geologia do petróleo (Pirmez et al., 2000; Ashiru et al., 2020). Além disso, esses condutos sedimentares podem ser influenciados e até mesmo controlados por estruturas de subsuperfície, que modificam a morfologia do fundo, como por exemplo a tectônica do sal.

3.2. Tectônica do sal

Durante o Aptiano, a progressiva restrição da comunicação oceânica entre a América do Sul e a África favoreceu o estabelecimento de um sistema lacustre-marinho restrito sob condições hipersalinas, culminando na deposição dos evaporitos (Chang et al., 1990; Davison, 2007; Moreira et al., 2007). Na Bacia de Santos, esses depósitos correspondem à Formação Ariri, que constitui a principal unidade evaporítica da margem Atlântica brasileira (Vidal et al., 2003; Jackson et al., 2015). A grande espessura e continuidade lateral desse pacote evaporítico forneceram a base mecânica para o desenvolvimento subsequente da tectônica do sal (Jackson et al., 2015).

Os depósitos evaporíticos apresentam propriedades mecânicas singulares que os diferenciam de sedimentos e rochas siliciclásticas e carbonáticas. Em escalas de tempo geológicas, o sal comporta-se de forma dúctil, fluindo como um material viscoso, o que facilita sua deformação (Weijermars et al., 1993; Mohriak et al., 2008). Além disso, é menos denso e relativamente incompressível, tornando-se efetivamente “flutuante” quando soterrado por cargas sedimentares mais densas (Jackson & Hudec, 2017). Nessas condições, seu comportamento reológico fraco promove instabilidade gravitacional e favorece a ascensão de estruturas diapíricas (Jackson & Hudec, 2017).

Assim, a baixa densidade e a reologia dúctil dos evaporitos explicam o forte controle tectônico e estratigráfico exercido em bacias evaporíticas.

A tectônica do sal refere-se à deformação que envolve corpos de sal compostos por halita, anidrita ou outros minerais evaporíticos (Hudec & Jackson, 2007). Essa deformação pode ocorrer em regimes extensionais, compressivos ou transcorrentes em escala regional. Nesse contexto, inclui-se também a halocinese, definida como o movimento de corpos evaporíticos impulsionado predominantemente pela gravidade, na ausência de forças tectônicas laterais significativas (Hudec & Jackson, 2007; Jackson & Hudec, 2017).

O entendimento da tectônica do sal é particularmente relevante para a indústria do petróleo e gás, uma vez que muitas das principais províncias petrolíferas do mundo estão associadas a bacias evaporíticas, como o Golfo do México, Golfo Pérsico, Mar do Norte, Bacia do Baixo Congo, Bacias de Campos e Santos. O fluxo de sal cria armadilhas estruturais, controla a distribuição de reservatórios e atua como selo para a migração de hidrocarbonetos. Além disso, o sal é um eficiente condutor térmico, podendo aumentar a maturidade das rochas acima das estruturas salinas e retardá-la nas regiões adjacentes ou subjacentes (Hudec & Jackson, 2007; Jackson & Hudec, 2017).

O principal mecanismo motor do fluxo salino é a sobrecarga diferencial de sedimentos, que gera gradientes de pressão e promove o deslocamento do sal em direção às zonas de menor carga (Figura 3). A flutuabilidade atua como fator complementar, contribuindo para a instabilidade gravitacional do sistema (Jackson & Hudec, 2017). Esse deslocamento diferencial pode alimentar tanto diápiros quanto a redistribuição lateral do sal na camada-fonte (Mohriak et al., 2008).

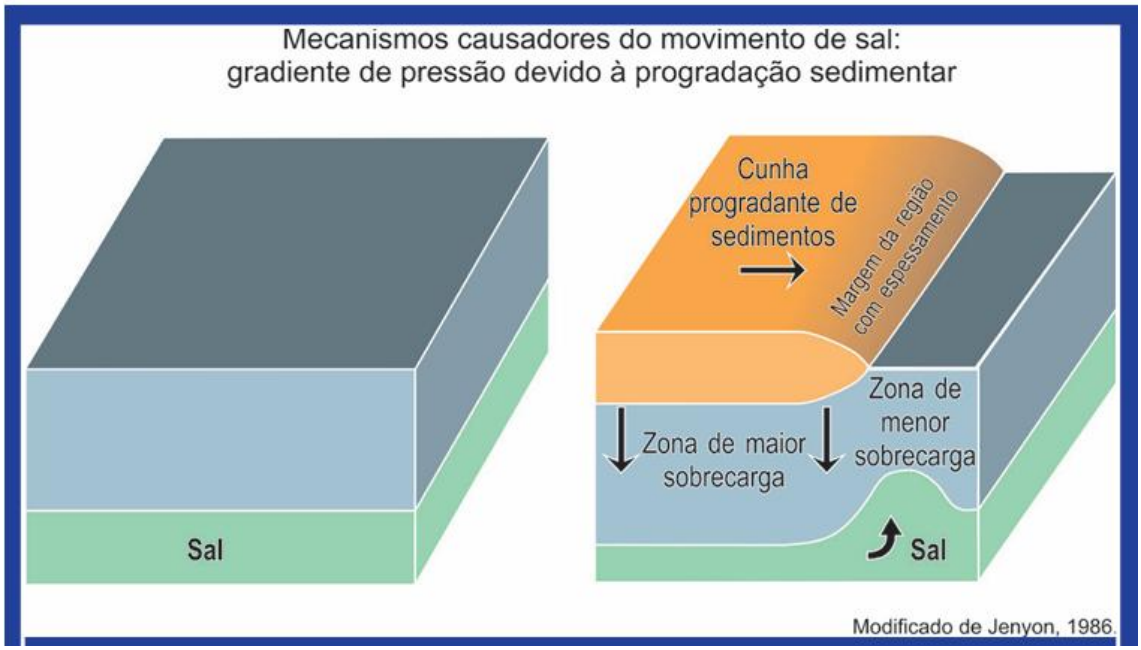

Figura 3: Modelo esquemático ilustrando a sobrecarga sedimentar como mecanismo causador da movimentação do sal. Fonte: Extraído de Mohriak et al., 2008.

A tectônica do sal pode gerar diversas estruturas salinas, que apresentam ampla variação de escala e morfologia. Sua classificação baseia-se principalmente na geometria em seção e em planta, incluindo formas alongadas, como muralhas e anticlinais de sal, e formas mais equidimensionais, como *pillows* (almofadas ou travesseiros) e *stocks*, além de geometrias mais irregulares, como lençóis e *canopies* (Figura 4) (Jackson & Hudec, 2017). Além disso, essas estruturas podem ser classificadas como autóctones, quando permanecem próximas à sua posição original e conectadas à camada fonte, ou alóctones, quando sofrem deslocamento lateral significativo, podendo se desconectar parcialmente ou totalmente de sua origem. Essa diversidade morfológica e estrutural reflete diferentes mecanismos de formação e evolução, com estruturas mais equidimensionais frequentemente associadas à halocinese, enquanto formas alongadas tendem a estar relacionadas a regimes tectônicos extensionais ou compressivos (Jackson & Hudec, 2017).

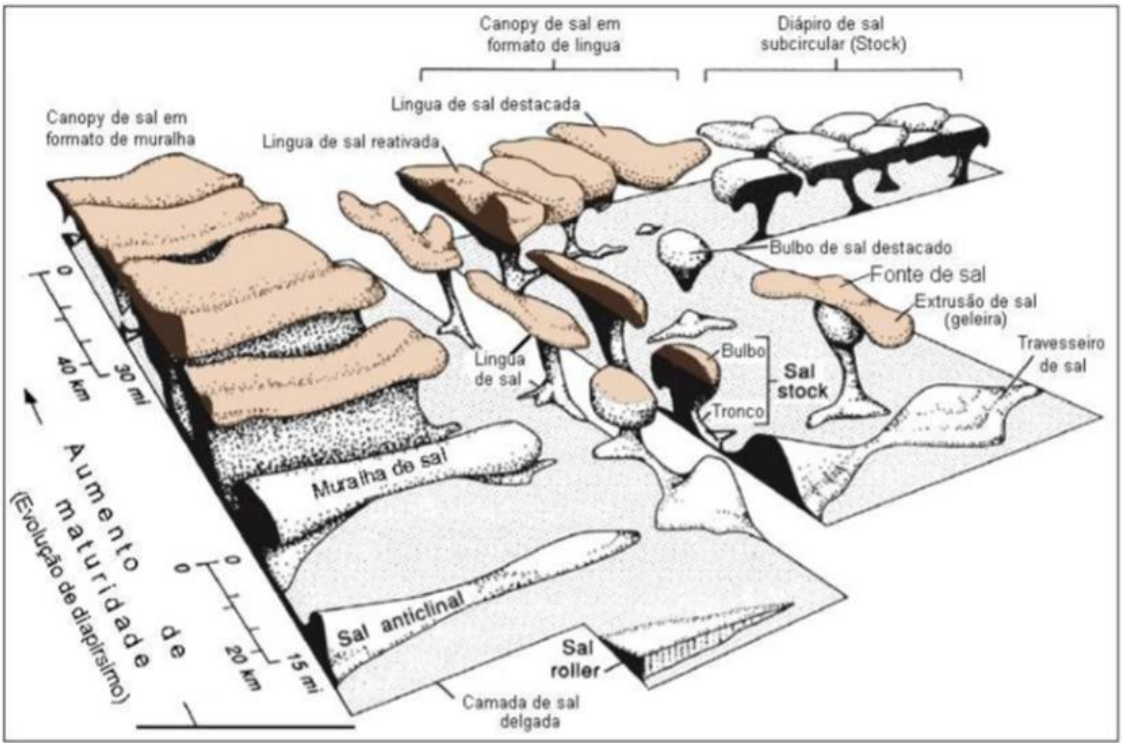

Figura 4: Diferentes tipos de estruturas salinas. Fonte: Extraído e modificado de Hudec & Jackson, 2007.

3.2.1. Tectônica do sal em regimes extensionais e compressivos:

Em regimes extensionais, típicos da plataforma externa ao talude superior de margens passivas, a tectônica de sal é dominada pela ascensão de diápiros reativos e pela evolução de diápiros extensionais (Jackson & Vendeville, 1994; Vendeville & Jackson, 1992b). Nesse contexto, a configuração estrutural resultante é controlada principalmente pela espessura da camada evaporítica. Evaporitos finos favorecem falhas lístricas de crescimento e estruturas de baixa amplitude, como *rollers* de sal, enquanto espessuras maiores possibilitam o desenvolvimento de diápiros maiores (Figura 5) (Hudec & Jackson, 2007). Esses podem evoluir progressivamente dos estágios reativo e ativo até o estágio passivo, mantendo-se próximos à superfície desde que haja suprimento contínuo de sal (Vendeville & Jackson, 1992b). Durante a extensão regional, os diápiros tendem a se alargar lateralmente, e sua evolução depende diretamente da disponibilidade de sal na camada-fonte, suprimento limitado pode levar ao colapso das estruturas e suprimento abundante permite crescimento contínuo, seja reativo ou passivo (Vendeville & Jackson, 1992b; Hudec & Jackson, 2007).

Em direção à parte distal da bacia de margens passivas, predomina o regime compressivo (Hudec & Jackson, 2007; Mohriak et al., 2008; Jackson & Hudec, 2017). Nessas condições, predominam tensões horizontais convergentes, levando ao encurtamento crustal e à espessamento da carga sedimentar, resultando em dobras, falhas de empurrão anticlinais sal (Hudec & Jackson, 2007; Mohriak et al., 2008). Assim, conforme o sal tende a fluir do talude para as regiões mais profundas da bacia, o regime compressivo tende originar estruturas cada vez maiores e mais complexas rumo ao domínio distal (Figura 5) (Mohriak et al., 2008).

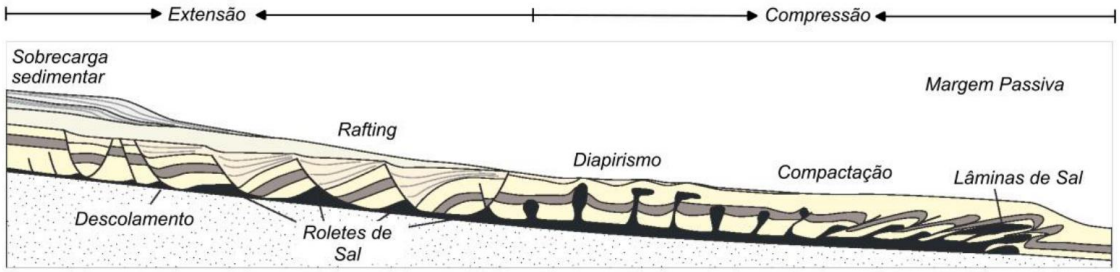

Figura 5: Comportamento de estruturas salinas em diferentes tipos de regime. Fonte: Extraído e modificado de Fossen, 2016.

3.2.2. Tipos de Diapirismo:

O diapirismo salino pode ser classificado em três tipos principais: ativo, passivo e reativo. O diapirismo ativo ocorre quando o sal rompe de forma penetrativa uma sobrecarga fina e/ou mecanicamente fraca, ascendendo independentemente de extensão regional. Esse processo pode ser impulsionado por carga diferencial de sedimentos, variações topográficas, contrastes de densidade ou por encurtamento tectônico, que aumenta as tensões compressivas e força o sal para cima (Vendeville & Jackson, 1992; Mohriak et al., 2008; Jackson & Hudec, 2017).

Já o diapirismo passivo ocorre quando diápiro atingiu o nível de equilíbrio isostático com os sedimentos encaixantes e caracteriza-se pelo crescimento do diápiro próximo à superfície deposicional, sem ruptura das camadas encaixantes, à medida que sedimentos mais densos se acumulam nas bacias periféricas por agradação lateral (Mohriak et al., 2008).

O diapirismo reativo representa a fase inicial de formação do diápiro, ocorrendo em resposta à deformação tectônica extensional, como a geração de grabens e falhas normais

que afinam e enfraquecem a sobrecarga (Jackson & Hudec, 2017). Esse afinamento cria gradientes de pressão e permite a ascensão do sal, inicialmente sob a forma de almofadas, evoluindo posteriormente para diápiros que podem cortar as camadas sobrejacentes (Vendeville & Jackson, 1992; Mohriak et al., 2008).

3.3. Influência da tectônica do sal em canais submarinos

A tectônica do sal gera deformações nas camadas sobrepostas e em muitos casos essas deformações não ficam em subsuperfície, mas se apresentam no fundo marinho atual, gerando diversas feições morfológicas como mini bacias, cristas, grabens de crista, altos e baixos topográficos, além de diápiros e línguas de sal que são exumados (Pichel et al., 2020; Mohriak et al., 2008).

Essas alterações na morfologia do fundo podem interagir e até controlar fluxos e condutos sedimentares, como cânions e canais submarinos. Esse controle estrutural se dá principalmente pelas modificações do relevo marinho, que é capaz de interagir e modificar rotas de transporte sedimentar ao longo do tempo geológico. Diversos autores já realizaram estudos sobre condutos sedimentares controlados por estruturas de subsuperfície, principalmente pela tectônica do sal. Algumas das principais evidencias desse controle são padrões de bloqueio, deflexão e confinamento por altos e baixos topográficos (Prather et al., 2003; Clark and Cartwright, 2009; Oluboyo et al., 2014; Abu et al., 2025). A interação entre canais submarinos e padrões de desvio ou confinamento, podem alterar também dinâmicas internas do canal, como trechos de deposição sedimentar, trajetória do talvegue, e a capacidade erosiva, que pode se intensificar em caso de confinamento (Gee et al., 2007; McHargue et al., 2011; Ashiru et al., 2020).

O estudo de Oluboyo et al. (2014) (Figura 6) demonstrou que a tectônica do sal exerceu forte controle estrutural sobre sistemas canal–lobo durante o Mioceno na Bacia do Baixo Congo. Os autores evidenciaram padrões sistemáticos de deflexão, bloqueio e confinamento que condicionaram as trajetórias dos canais, bem como a formação de zonas de transbordamento associadas a depressões estruturais persistentes. Além disso, reconheceram áreas de “sombra” deposicional, nas quais os fluxos gravitacionais não alcançam devido à presença de estruturas salinas que desviam ou impedem a propagação dos sistemas canalizados ao longo do talude.

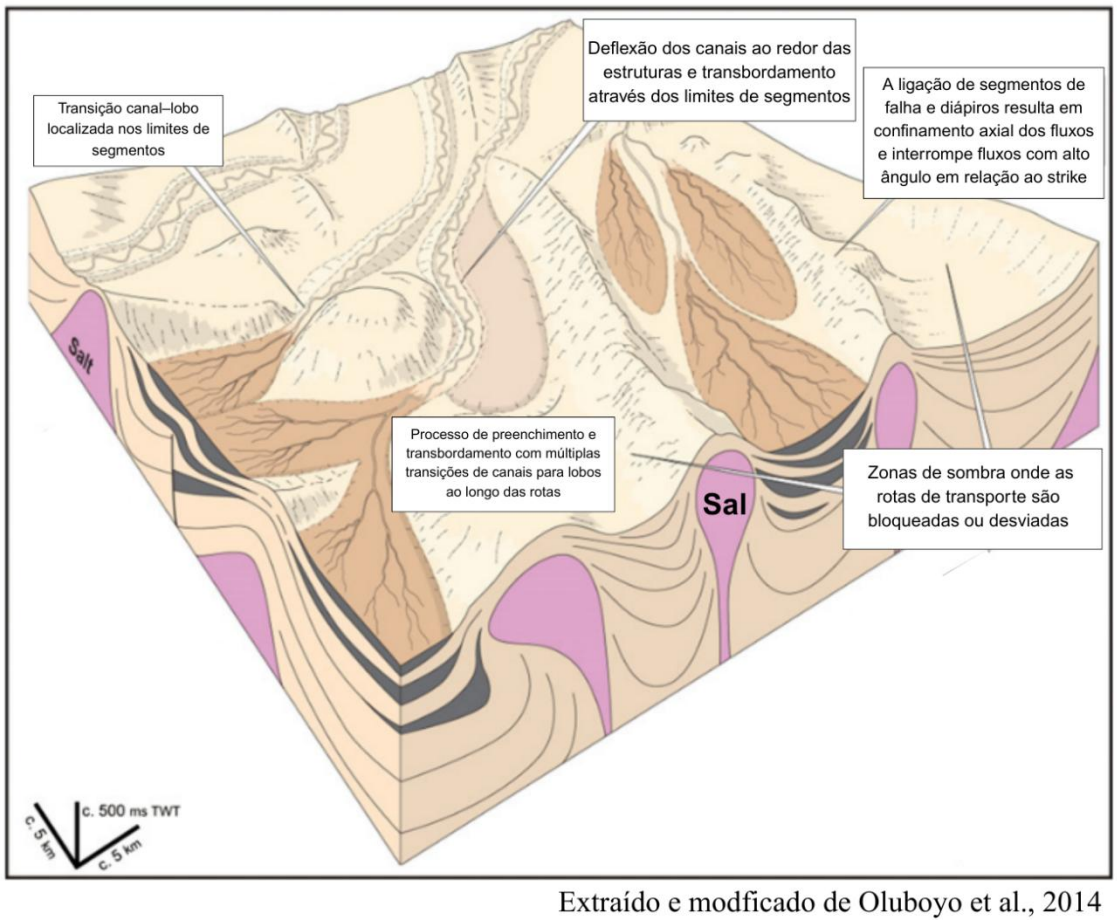

Figura 6: Ilustração evidenciando o controle estrutural sobre sistemas canal-lobo na Bacia do Baixo Congo. Fonte: Extraído e modificado de Oluboyo et al., 2014.

O trabalho de Gee & Gawthorpe (2006) evidencia um sistema de canais de turbidez no talude tendo sua geometria e evolução sendo controlados sendo controlados pela tectônica salina (Figura 7). As principais evidências que os autores apontaram incluem a relação direta entre as geometrias dos canais e o gradiente/configuração do talude moldado por estruturas de sal, o soerguimento induzido por domos e muros salinos que promove incisão local de canais profundos, e a ocorrência de estreitamentos estruturais que confinam, e tornam os fluxos mais erosivos.

Deslizamentos submarinos associados à atividade de falhas também remodelam a topografia do talude, criando ou eliminando rotas de escoamento e influenciando trajetórias subsequentes. A presença de dobras sin-sedimentares, espessamento de pacotes sedimentares em direção a falhas relacionadas ao movimento do sal e episódios de avulsão próximos a domos salinos reforçam que a arquitetura dos canais registra diretamente a atividade tectônica, evidenciando que a evolução planimétrica e

longitudinal dos sistemas é controlada pela interação entre fluxo sedimentar e estruturas salinas ativas (Gee & Gawthorpe, 2006).

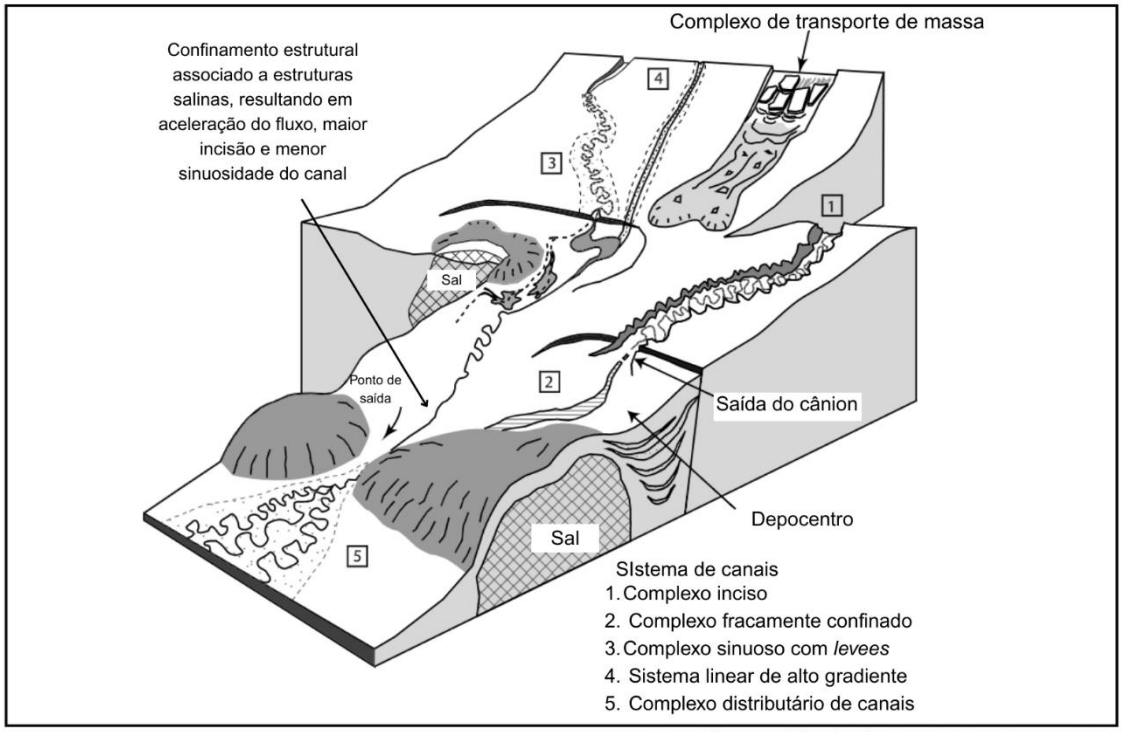

Extraído e modficado de Gee & Gawthorpe, 2006

Figura 7: Ilustração esquemática evidenciando o controle estrutural exercido pela tectônica do sal sobre canais de turbidez em ambiente de talude. Fonte: Extraído e modificado de Gee & Gawthorpe, 2006.

Além disso, a redução da carga sedimentar pelos cortes erosivos de condutos sedimentares, como cânions e canais, é atrativa para o deslocamento e formação de diápiros (Jackson, 1995; Mohriak et al., 2008). Ou seja, em bacias evaporíticas com forte controle estrutural, fluxos sedimentares não só são controlados pela tectônica do sal, como também podem influenciar no soerguimento de estruturas salinas sob eles, o que pode intensificar esse controle.

4. ARTIGO

Structural Controls on the Morphology of the Distal Cananéia Canyon System, São Paulo Plateau, Southeastern Brazil

Eduardo Thomaz de Aquino Ribeiro[1], Davy Raeder Brandão[1], Leonardo Junius Chapeta Santos[1], João Regis dos Santos Filho[2], Christian Gorini[3], Narelle Maia de Almeida[4], João Correa[5], Cleverson Guizan Silva[1]

[1-] Graduate Program in Ocean and Earth Dynamics, Marine Geology and Geophysics Laboratory (LAGEMAR), Geosciences Institute, Fluminense Federal University (UFF), Brazil.
[2-] Department of Geological Oceanography, Oceanography Faculty, Rio de Janeiro State University, Brazil.
[3-] Institut des Sciences de la Terre Paris (ISTEP), UMR 7193, Sorbonne Université, France.
[4-] Department of Geology, Federal University of Ceará (UFC), Brazil.
[5-] TGS Brazil.

ABSTRACT

Submarine canyons are major sediment conduits that transfer gravity-driven flows from continental margins to deep-marine basins, where they generate a range of depositional and erosional elements. In salt-bearing margins, the evolution and trajectory of these conduits may be strongly influenced by halokinetic deformation and inherited structural elements. This study investigates the morphology and structural control of a submarine channel located on the São Paulo Plateau (Santos Basin, SE Brazil), interpreted as the distal continuation of the Cananéia Canyon sediment-routing system. The analysis integrates high-resolution multibeam bathymetry (15 m grid) with regional 2D seismic reflection data. The mapped drainage system extends for ~194 km and comprises a proximal sector dominated by mass-transport complexes transitioning downstream into a confined submarine channel. Multibeam data reveal prominent geomorphological features, including slide scars, pockmarks, intra-channel highs, and an erosional escarpment reaching ~230 m in height, indicating intense channel-floor incision and margin instability. Seismic interpretations show that the channel evolved over an irregular salt-related topography controlled by inherited basement structures, particularly the Puri High and faults associated with the Capricorn Lineament. These structures govern channel confinement, flow deflection, thalweg position, and erosional patterns, while asymmetric paleochannel fills indicate persistent structural control through successive stages of channel evolution. Upstream segments record repeated mass-transport deposition and progressive canyon infill, whereas downstream sectors display enhanced

confinement and erosional dominance linked to structural relief. These results provide new insights into the geomorphology and structural control of the distal Cananéia Canyon system, the main submarine canyon system of the Santos Basin, a sector that has remained poorly characterized due to limited high-resolution data and highlight the key role of salt tectonics in governing deep-water sediment-routing systems on the São Paulo Plateau.

KEYWORDS: Cananéia Canyon, Submarine channel, Structural control, Salt tectonics, Mass transport complexes, Santos Basin

1. INTRODUCTION

Submarine canyons are the main conduits through which sediments are transferred from continental margins to deep-marine environments (Normark and Carlson, 2003). These systems are closely linked to gravity-driven sedimentary processes, funneling turbidity currents and other gravity-driven flows, such as debris flow, which deliver large volumes of sediment to deep-ocean systems (Normark et al., 1993; Talling et al., 2012; Wu et al., 2022; Böttner et al., 2025). High-energy gravity flows can erode canyon floors by tens of meters during single events, leaving large erosional scars (Conway et al., 2012; Normandeau et al., 2025; Taylor et al., 2026). The development of submarine canyons is controlled by multiple factors, including sediment supply (Puig et al., 2017), sea-level fluctuations (Rasmussen, 1994; Allin et al., 2018), earthquakes (Kunath et al., 2025), faulting and tectonic uplift (Li et al., 2023), and inherited slope topography (Li et al., 2020). Submarine canyons are typically more active during sea-level lowstands, when sediments are more efficiently delivered to deep-water systems (Li et al., 2023), however, many canyons remain active across different sea-level stages (Böttner et al., 2025). Sediments routed through submarine canyons in deep-marine environments generates a range of depositional elements, including turbidite channels and lobes, levee-overbank deposits, crevasse splays, sediment waves, and mass-transport complexes (Posamentier and Kolla, 2003; Deptuck et al., 2008; Silva et al., 2016; dos Reis et al., 2016; Zhang et al., 2020; Pirmez et al., 2000; Shipp et al., 2011; Zhang et al., 2026). These elements collectively record the spatial and temporal variability of gravity-driven sediment delivery from the slope to the basin floor.

Understanding deep-water depositional systems is of broad interest to the oil and gas industry due to their potential to host high-quality reservoirs (Pirmez et al., 2000; Posamentier and Kolla, 2003; Ashiru et al., 2020). In addition, investigations of modern

sediment gravity-flow processes provide critical constraints for interpreting ancient subsurface analogues (Pirmez et al., 2000) and for the safety of submarine infrastructure. In this context, high-resolution multibeam bathymetric mapping has become a key tool for unraveling depositional and erosional processes, as well as assessing the influence of subsurface dynamics on seafloor morphology (Barnard et al., 2011; Kanari et al., 2020).

In sedimentary basins containing thick evaporitic sequences, such as the Santos Basin, sediment conduits are commonly influenced by salt tectonics. Several studies have documented the structural control exerted by halokinesis on submarine sediment conduits, including canyons and turbidite channels, in salt-bearing basins worldwide, such as the eastern Mediterranean (Clark and Cartwright, 2009), offshore Angola (Gee and Gawthorpe, 2006, 2007), the Gulf of Mexico (Smith, 2004), the Espírito Santo Basin (Gamboa et al., 2012), the southern Barbados accretionary prism (Huyghe et al., 2004), the Lower Congo Basin (Oluboyo et al., 2014), the offshore Western Niger Delta (Ashiru et al., 2020), the Campos Basin (Covault et al., 2020), and the North Sea (Abu et al., 2025). Under compressional conditions, turbidite channels may be deflected, ponded, blocked, or confined by the growth of salt-cored or salt-related structures (Prather et al., 2003; Clark and Cartwright, 2009; Oluboyo et al., 2014; Abu et al., 2025). Consequently, on salt-influenced margins, canyon evolution and associated sediment-routing systems are intrinsically coupled with halokinetic deformation.

Cananéia Canyon represents the major canyon of the Santos Basin (Zembruscki, 1979; Duarte and Viana, 2007; Hercos et al., 2023). It extends from the upper continental slope to the deep basin and is expressed in bathymetric data as a major NW–SE-oriented incision (Fig. 2). The canyon plays a fundamental role as a sediment conduit linking the continental shelf to the deep ocean. Previous studies suggest that it may capture fine-grained sediments sourced from the La Plata River and transport them downslope (Santos Filho et al., 2022). Additionally, gravity-driven flows routed through the distal canyon sector contribute to the formation of depositional features such as sediment waves on the Santa Catarina Plateau (Borisov et al., 2020). Moreover, the canyon likely functioned as a primary connection between coastal drainage and the upper slope during the Last Glacial Maximum (LGM), acting as an efficient pathway for sediment transfer from shallow to deep waters throughout the Late Quaternary, including periods of sea-level transgression (Zembruscki, 1979; Borisov et al., 2020).

Despite their importance, the recognition and characterization of deep-marine seafloor morphologies remain challenging due to the requirement for high-resolution geophysical data and the logistical and economic constraints associated with extensive hydrographic surveys. Although recent work by Hercos et al. (2023) provided high-resolution imagery and morphological interpretations of the Santos Basin, including the main canyon segment from the upper slope to part of the São Paulo Plateau, the more distal sector remains poorly constrained due to limited data coverage. This distal segment, expressed as a broad submarine valley across the São Paulo Plateau, remains poorly characterized, particularly regarding the role of subsurface structures, such as salt tectonics, in controlling channel morphology and sediment routing.

This study presents novel high-resolution multibeam bathymetric data (15 m cell size) provided by TGS Brazil in cooperation with Federal Fluminense University, integrated with regional 2D seismic data made available by the National Agency of Petroleum, Natural Gas and Biofuels (ANP). Using these datasets, we investigate the morphology and structural controls of a submarine channel located on the São Paulo Plateau and genetically linked to the Cananéia Canyon sediment-routing system. Our results indicate that the morphology and trajectory of the channel are strongly influenced by first-order basement structures, including the Puri High and the Capricorn Lineament, as well as by salt-related topography, which together exert a major control on channel confinement and sediment-routing patterns across the plateau.

2. STUDY AREA

The study area is located in the south–southwestern sector of the São Paulo Plateau, within the Santos Basin, offshore southeastern Brazil, between 26.3°–27.7°S and 45.3°–43.5°W (Fig. 1). Water depths range from ~2,230 to 3,350 m, corresponding to the outer plateau domain, which is characterized by salt-tectonic morphologies including ridges, minibasins, diapir-related scarps, and structural volcanic highs (Kumar et al., 1977; Duarte and Viana, 2007; Pichel et al., 2020; Hercos et al., 2023).

2.1. Oceanography

At these depths, the São Paulo Plateau is influenced by complex deep-water circulation associated with the Deep Brazil Current, composed of South Atlantic Central Water

(SACW), Antarctic Intermediate Water (AAIW), and predominantly North Atlantic Deep Water (NADW), as well as mesoscale vortical features (Duarte and Viana, 2007; Silveira et al., 2023). These hydrodynamic conditions interact with the irregular salt-tectonic relief, contributing to the redistribution and reworking of gravity-driven deposits across the plateau.

2.2. Geomorphology

The Cananéia Canyon System comprises the Cananéia Canyon (Zembruscki, 1979; Duarte and Viana, 2007; Hercos et al., 2023) and the Cananéia Channel, which forms the distal continuation of the canyon system and is expressed in the study area as a submarine valley (Fig. 1).

The Cananéia Canyon, the main erosive conduit incising the continental slope of the Santos Basin, was originally described by Zembruscki (1979) and Duarte and Viana (2007). According to Hercos et al. (2023), the canyon extends for ~85 km, with a head located between the shelf break and the upper continental slope, reaching ~23 km in width and ~370 m in relief (Fig. 1). The canyon incision is largely infilled by mass-transport deposits (MTDs/MTCs) with runout distances exceeding 140 km (Hercos et al., 2023), which propagate basinward toward the São Paulo Plateau and significantly modify seabed roughness.

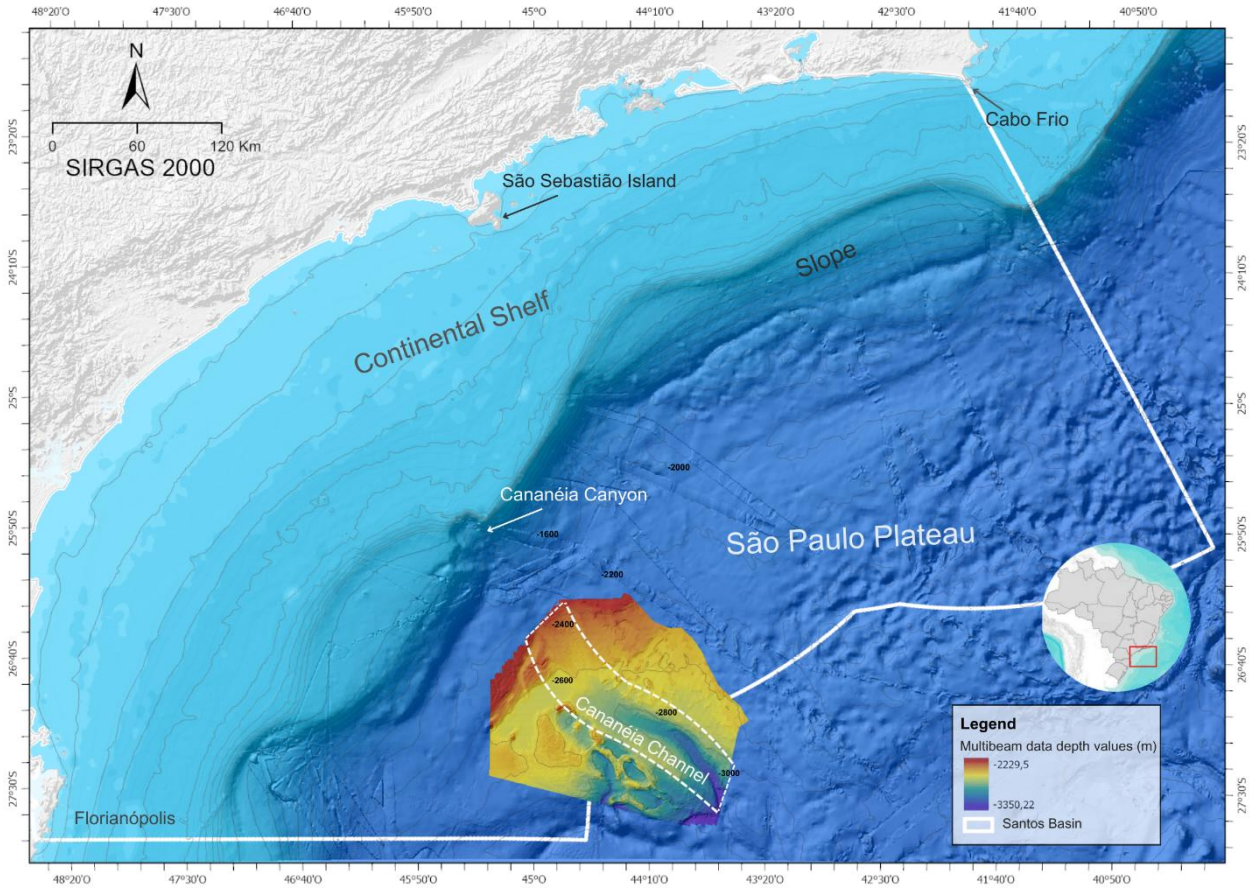

Fig. 1. Location map of Santos Basin (white line) and the study area outlined by a white dashed line over the multibeam bathymetric dataset.

The northwestern boundary of the study area lies approximately 95 km downslope from the canyon head, highlighting the large spatial reach of gravity-driven sediment transfer across the outer São Paulo Plateau. Considering the distance from the canyon head to the distal limit of the mapped submarine valley, the system exhibits a minimum length of ~286 km and likely extends further downslope, as suggested by regional bathymetric data from LEPLAC (Fig. 2).

2.3. Geological settings

The Santos Basin was formed during the Early Cretaceous in the context of the breakup of Western Gondwana and the opening of the South Atlantic Ocean. Initial rifting resulted from lithospheric extension associated with the separation of the South American and African plates, intensified by the activity of the Tristan da Cunha mantle plume, responsible for regional thermal anomaly, crustal uplift, and significant magmatism (White and McKenzie, 1989; Mohriak et al., 2010, 2021; Quirk et al., 2013).

The structural architecture established during rifting constituted the tectonic framework that conditioned post-rift sedimentation and later controlled evaporite mobilization in the basin. In the Aptian, the progressive restriction of oceanic communication between South America and Africa led to the establishment of a restricted lacustrine–marine system, culminating in the deposition of the Ariri Formation evaporites under hypersaline conditions (Chang et al., 1990; Davison, 2007; Moreira et al., 2007). The Santos Basin represents the most significant evaporitic province along the Brazilian Atlantic margin (Vidal et al., 2003; Jackson et al., 2015), and the great thickness and lateral continuity of this evaporitic package provided the mechanical foundation for the subsequent development of salt tectonics.

From the Albian to the Recent, the basin evolved into a fully marine passive margin, characterized by the alternating deposition of carbonate and siliciclastic sediments (Moreira et al., 2007). Regional salt deformation began as early as the Albian, shortly after evaporite deposition (Magee et al., 2021), evolving into a kinematic system dominated by up-dip extension, intermediate translation, and down-dip contraction (Demercian et al., 1993; Davison et al., 2012; Jackson et al., 2015; Pichel et al., 2019; Rodriguez et al., 2018). On the São Paulo Plateau, this evolution is associated with contractional domains of halokinesis, expressed by ridges, crest grabens, fault scarps, topographic highs and lows, minibasin systems, and locally exhumed diapirs (Mahiques et al., 2017).

In addition to gravitational halokinesis, inherited basement structural features exert a strong control on the architecture and dynamics of the evaporitic layer in the Santos Basin (Mohriak and Szameitat, 2023; Pichel et al., 2020; Silva et al., 2024). In the study area, the Abimael Ridge, the Puri High, and the Capricorn Lineament stand out as first-order structural elements capable of influencing the distribution, thickness, and segmentation of the evaporites, thereby exerting a fundamental structural control on the development and confinement of the submarine valley.

The Abimael Ridge is a prominent structural feature interpreted as an oceanic propagator or an aborted spreading axis, developed from the late Aptian to the early Albian (Mohriak, 2001; Gamboa et al.,2021). This structure displays a V-shaped geometry with n orthward propagation (Fig.2), suggesting the advance of a proto-oceanic ridge from the Pelotas Basin toward the Santos Basin (Mohriak et al., 2022; Mohriak and Szameitat, 2023;

Gamboa et al., 2021). Gravity and magnetic data reveal associated structural highs, as well as the local absence of autochthonous salt over newly formed volcanic basement (Mohriak and Leroy, 2013).

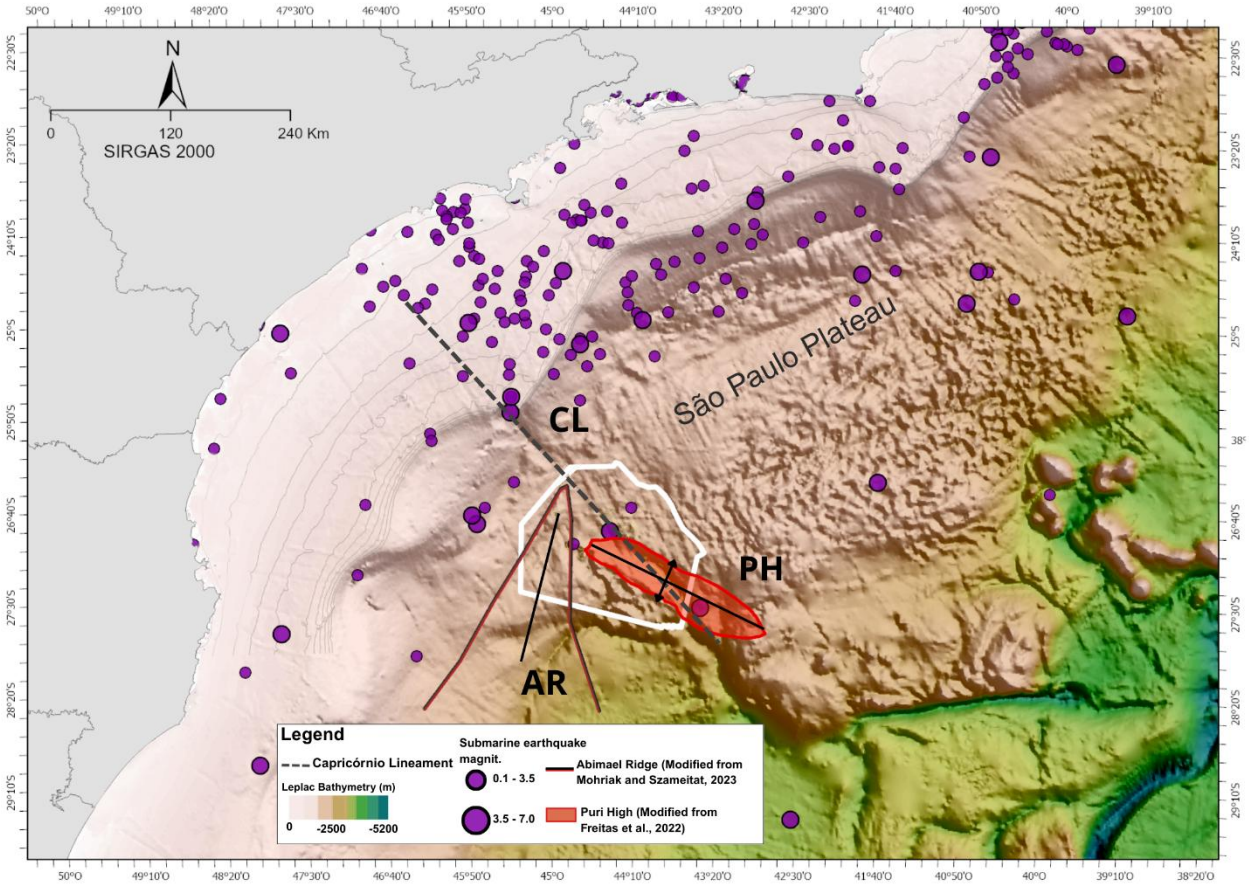

Fig. 2. Regional bathymetric map (LEPLAC dataset) illustrating the trace of the Capricorn Lineament (CL), the Puri High (PH), the Abimail Ridge (AR) and the distribution of earthquakes. The study area is delimited by the white polygon.

The Capricorn Lineament corresponds to a NW–SE-oriented crustal lineament described by Bueno et al. (2004), with significant regional expression along the southeastern Brazilian margin. In addition to influencing the organization of the evaporitic layer, this lineament is strongly associated with seismic activity in the Santos Basin. The 2008 São Vicente earthquake (Mb 5.2) is located proximal to the lineament (Assumpção et al., 2011), as are other seismic events possibly related to flexural stresses induced by sedimentary loading and reactivation of crustal faults. Part of this seismicity has also been recorded near the Cananéia Canyon, whose orientation coincides with the trace of the Capricorn Lineament (Duarte and Viana, 2007).

3. METHODS AND MATERIALS

3.1. Data sources and processing

3.1.1. Multibeam data

The 15-m grid multibeam bathymetric data used in this study were provided by TGS Brazil through a cooperation agreement with Fluminense Federal University. The data were acquired as part of the BRAZIL MULTIBEAM AND SEEP CORING & HEAT FLOW MULTI-CLIENT SURVEY, conducted by TGS Brazil between 2018 and 2019, covering an area of approximately 213,627 km². Data acquisition was carried out by Fugro using Kongsberg EM302, EM2040, and EM3002 multibeam echo sounder systems deployed aboard the vessels *Fugro Brasilis* and *Fugro Searcher*. Initial processing, including tidal corrections, sound-velocity corrections, and quality control procedures, was performed by the data provider during the survey and subsequent onshore workflows prior to data delivery.

No reprocessing of the multibeam data was undertaken in the present study, as only fully processed bathymetric and backscatter products were made available. The final bathymetric grids, with a spatial resolution of 15 m, were used for geomorphometric analyses, geomorphological interpretations, and the generation of derivative products aimed at characterizing the seafloor morphology of the study area. Although the full dataset comprises approximately 21,400 km², this study focuses exclusively on the sector corresponding to the distal part of the Cananeia Canyon system (white dashed line in Fig. 1).

3.1.2. 2D seismic data

The 2D depth-converted seismic data were obtained from the Brazilian National Agency of Petroleum, Natural Gas and Biofuels (ANP), which publicly provides regional seismic datasets for academic research purposes. The seismic grid in the study area (Fig. 3) consists of regional 2D lines with spacing ranging from 3 to 7 km. The seismic data were primarily used to map the evaporitic layer, identify mass-transport deposits (MTDs/MTCs), and to understand the subsurface geometry of the submarine canyon system.

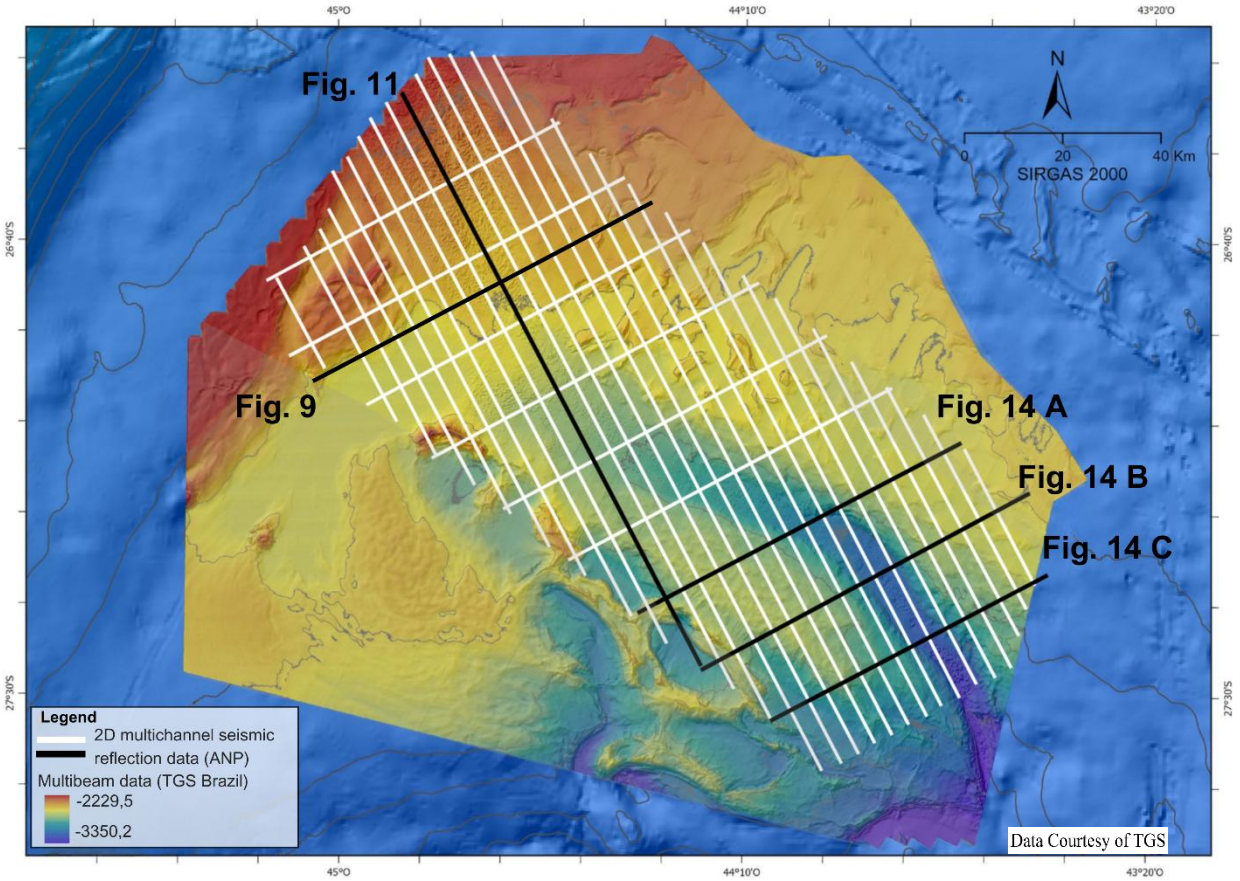

Fig. 3. Dataset used for the analyses and interpretations. The multibeam bathymetric dataset provided by TGS Brazil is displayed over the study area. White lines represent the interpreted 2D multichannel seismic reflection profiles provided by the ANP, which were used to generate the top-salt, base-salt, and salt-thickness maps. Black-highlighted lines correspond to the seismic sections selected for detailed interpretation and presented in the Results section.

3.1.3. Regional bathymetric and earthquake data

The bathymetric framework used as regional geomorphological background in this study (Fig.2) is derived from the Brazilian Continental Shelf Survey Plan (LEPLAC), conducted by the Diretoria de Hidrografia e Navegação (DHN). This dataset integrates multibeam hydrographic surveys, nautical charts, and global ocean relief models, enabling a broad-scale representation of the seafloor morphology along the southeastern Brazilian margin. The LEPLAC bathymetric products were employed as a regional reference to contextualize the physiography of the São Paulo Plateau and the location of the Cananéia Canyon system, supporting the integration and interpretation of the high-resolution seismic and bathymetric data used in this study.

The earthquake data used in this study are derived from the Brazilian Seismic Catalog, initially compiled by Berrocal et al. (1984) and continuously updated by seismological

centers affiliated with the University of Brasília (UnB), University of São Paulo (USP), University of Rio Grande do Norte (UFRN), Technological Research Institute of São Paulo State (IPT), National Observatory (ON) and Brazilian Geological Survey (CPRM) (Carvalho et al., 2020).

3.2. Data analysis

3.2.1. Bathymetric analysis

Bathymetric data visualization, morphometric analyses, and the generation of derivative maps were carried out using ArcGIS Pro software (Esri). Slope, hillshade, and relative relief maps were produced to assist in the identification of geomorphological features, such as mass-transport-related features (MTCs/MTDs), scarps, slide scars, thalweg, pockmarks, marginal deposits, and erosional features on the channel floor. These products were integrated with seismic interpretations to evaluate the relationship between seafloor morphology and subsurface structural controls.

3.2.2. Seismic interpretation workflow

Seismic interpretation was performed using DecisionSpace Geosciences software (Halliburton). The interpretations focused on: (i) the top and base of the evaporitic sequence, (ii) mass-transport deposits (MTCs), and (iii) the architecture of the submarine canyon. The salt-top generally shows good seismic imaging, whereas the base of salt is locally difficult to interpret due to seismic signal attenuation and the complex internal deformation of the salt. In areas where the base of salt could not be reliably identified, interpretative uncertainty was explicitly acknowledged, and these intervals were treated with caution in thickness calculations.

In the sector corresponding to the Abimael Ridge propagator, where the evaporitic layer is absent, the pre-salt horizon was interpreted and used simultaneously as both top and base, to avoid the generation of artificial thickness anomalies in the derived maps. From the interpreted horizons, top, base, and thickness maps were generated to support the discussion on salt tectonics and the interaction between the canyon and the salt (Fig.11).

The chronostratigraphic framework adopted in this study is based on the regional seismic stratigraphy proposed by Contreras et al. (2010), who calibrated key seismic horizons

using well data located on the continental shelf of the Santos Basin. The dated regional horizons defined in that study were traced into the study area.

3.2.3. Interpretation criteria and limitations

The interpretation of mass-transport deposits was based on seismic facies characterized by chaotic internal reflections, irregular basal surfaces, and lateral continuity consistent with deposits generated by gravitational processes (Fig.4). Submarine canyon elements were identified based on erosional geometries, truncation of stratigraphic reflectors, and alignment with features observed in seafloor bathymetry.

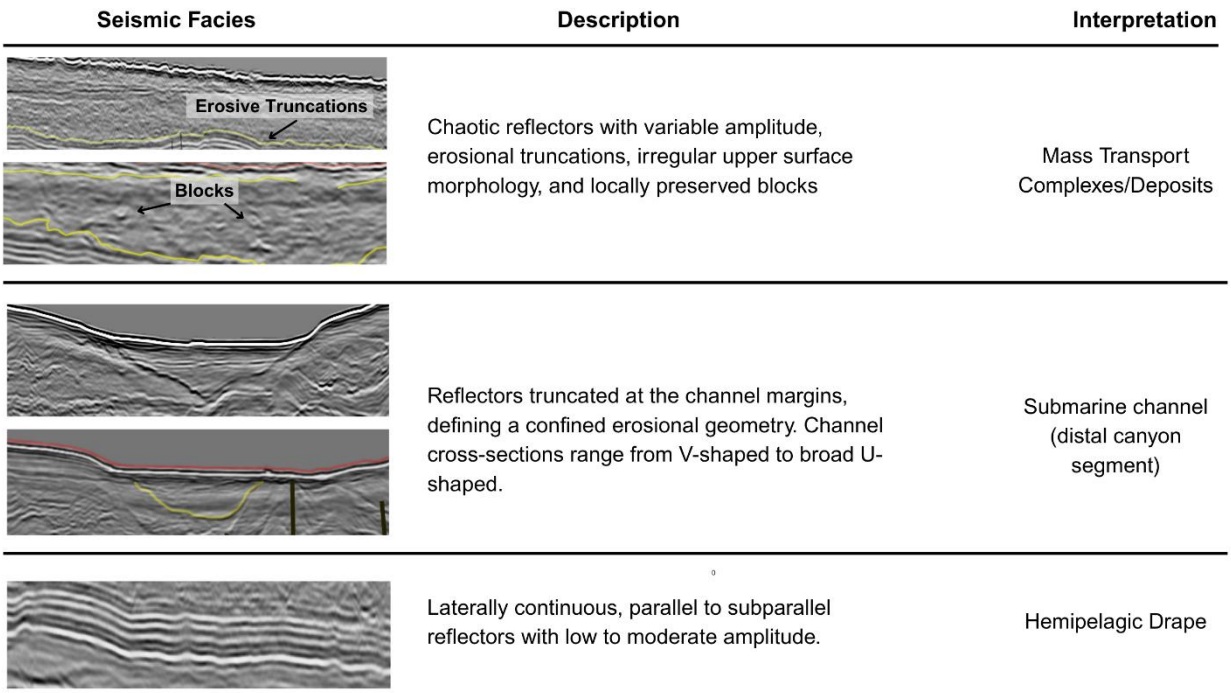

Fig. 4. Examples of seismic facies identified in the study area and their respective interpretations.

The main limitations of this study are related to: (i) the regional nature of the 2D seismic grid, (ii) variability in the imaging quality of the base of the evaporitic sequence, and (iii) the lack of direct well control in the deep-water study area. Despite these limitations, the integration of high-resolution multibeam bathymetry, regional seismic data, and chronostratigraphic information provides a robust framework to characterize the morphology and to highlight the structural and salt-tectonic controls on the development of the distal portion of the Cananéia Canyon system.

4. RESULTS

4.1. Seafloor geomorphology

The entire sector mapped in the multibeam dataset extends for approximately 194 km, comprising the Cananéia Channel and the mass-transport complex (MTC) (Fig. 5). This region can be subdivided into three main geomorphological sectors: (i) a proximal north–northwestern sector dominated by MTDs; (ii) a transitional sector where the channel valley becomes progressively narrower and more confined; and (iii) a distal sector characterized by a fully developed submarine-valley morphology. Some halokinetic-related features such as ridges and crestal grabens (Fig. 5.) appear to influence the distribution of the MTDs in sector (i), possibly acting as barriers that hinder lateral dispersal and accommodation during deposition of these gravitational processes.

Downstream from the main depositional sector of the MTC, which represents the largest area within the study region (Table 1), sector (ii) is characterized by a channel deflection and progressively increasing confinement (Fig. 5), until reaching sector (iii), where the system transitions into a more typical submarine-channel morphology, marked by a narrower planform and steeper channel flanks.

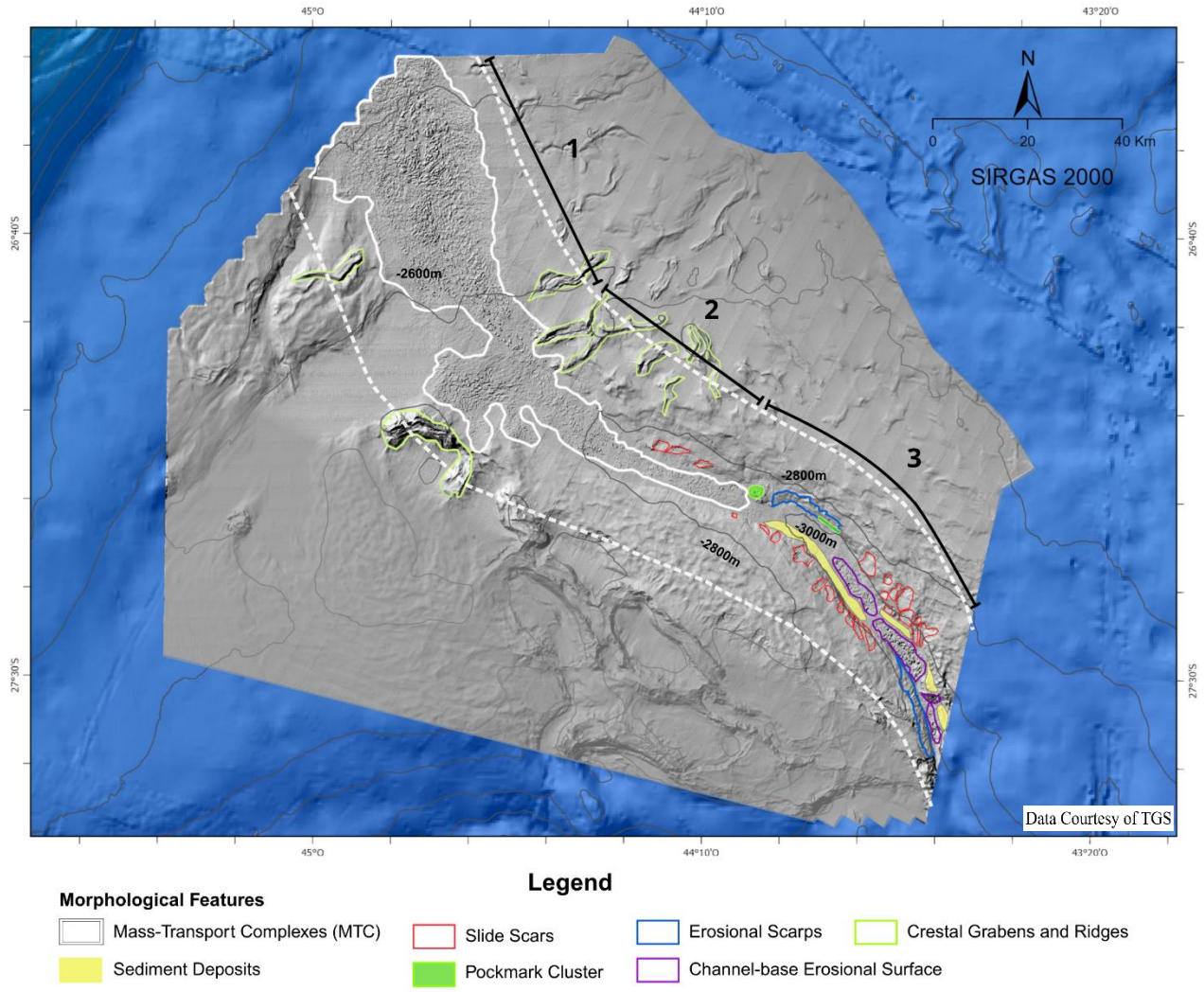

Fig. 5. Geomorphological map of the study area (outlined by white lines) highlighting the main features identified: slide scars (red lines), MTC boundaries (white lines), erosional scarps (blue lines), channel-base erosional surface (purple), Crestal Grabens and Ridges (green lines), pockmark cluster (green polygon), and marginal sediment deposits (yellow polygons). Line segments 1, 2 and 3 indicates the proximal, transitional and distal sectors, with different morphologies and features discussed in the text.

From the 3,000 m isobath basinward, the channel width ranges from approximately 8.4 km to about 4 km at its narrowest point. With increasing depth, the channel develops a more incised morphology, characterized by a deeper thalweg and progressively higher channel margins. Within the channel, seafloor erosional features coexist with localized marginal sediment accumulations, Along the channel margins, slide scars and erosional scarps are present as well as a small pockmark cluster located adjacent to the erosional scarp near the 2,800 m isobath (Fig.5).

The slope gradient map (in degrees) highlights the spatial distribution of slope values within the channel system and its adjacent margins. Slope gradients within the study area

range from near-zero values to a maximum of 58° (Fig. 6). The steepest sectors are mainly associated with structural and tectonic features, including ridges and crestal grabens, which locally reach maximum gradients of approximately 58° and 45°, respectively (Table 1). These high-gradient zones are spatially restricted and occur independently of the submarine channel system.

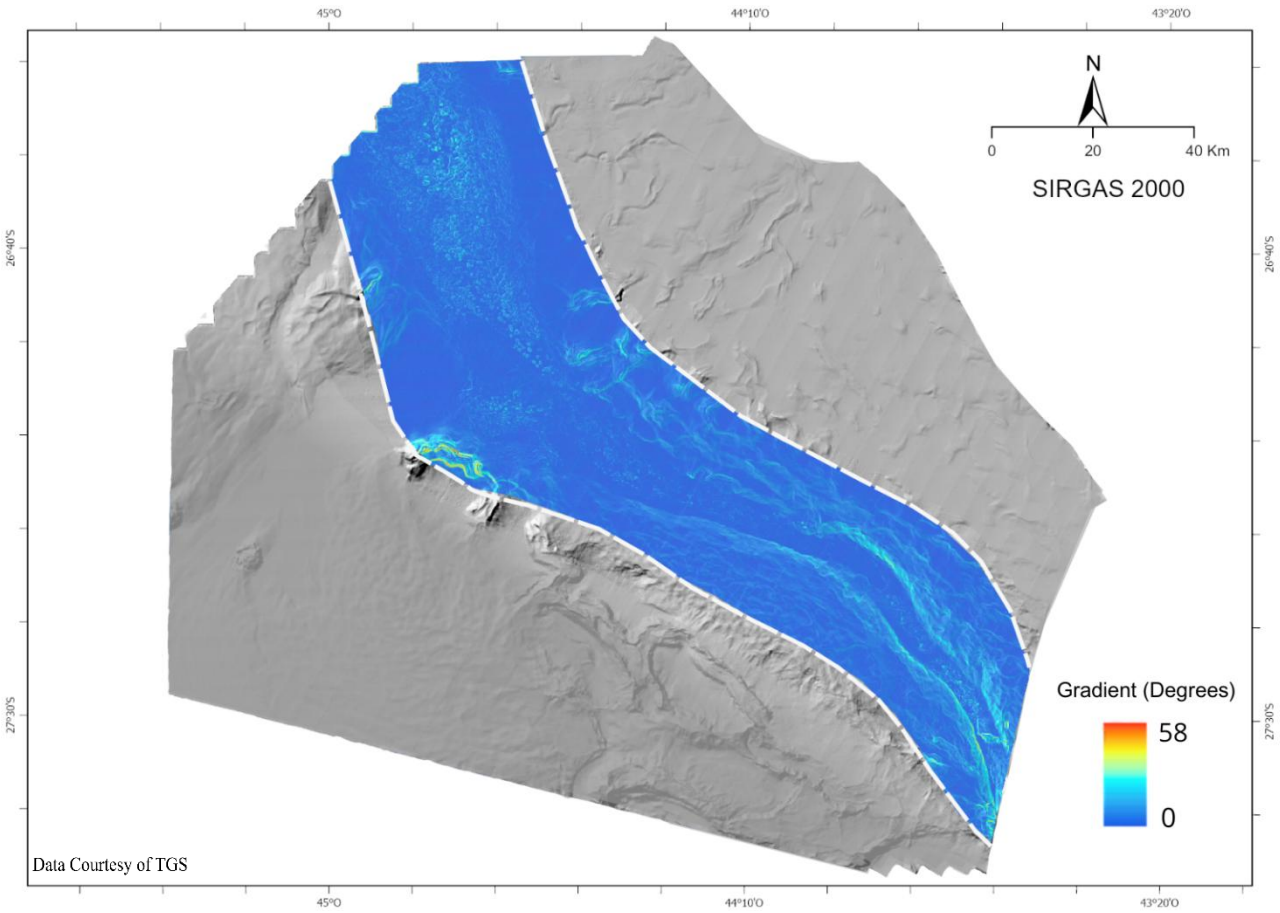

Fig. 6. Slope gradient map of the study area derived from bathymetric data.

Considering features directly associated with the submarine channel, higher gradients generally occur along the channel flanks and local scarps, whereas the channel floor is characterized by relatively low slope values (Fig. 6).

Table 1: Summary of depth, gradient and area statistics for each mapped feature. Values represent minimum, maximum and mean estimates derived from multibeam bathymetry analysis. MTCs*- Mass Transport Complexes

	Gradient (Degrees)			Depth (Meters)			Area (Km²)
	min	max	mean	max	min	mean	
Erosional Scarps	0.02	49.9	5.9	-3,314.5	-2,787.3	-3,016.2	68.2
Slide Scar	0.006	26.3	3.6	-3,114.8	-2,772.8	-2,921.9	113.5
Erosional Surface	0.001	58.1	4.3	-3,283.9	-3,027.6	-3,121.6	98.7
MTCs*	0.0009	45.6	3.1	-2,946.4	-2,301.7	-2,570.5	2098
Sediment deposits	0.002	25.7	2.4	-3,212.1	-2,964.3	-3,056.3	79.6
Pockmarks	0,01	31.3	2.4	-2,951.2	-2,867.9	-2,900.8	7.5
Crestal Grabens and Ridges	0.01	58.9	7.8	-2,808.7	-2,291.9	-2,580.4	375.6

To further investigate the structural framework underlying the seafloor morphology described above, salt top, salt base, and salt thickness maps derived from seismic interpretation were analyzed (Fig.7).

4.2 Subsurface structure and salt distribution

The subsurface structure of the study area is illustrated by salt top, salt base, and salt thickness maps (Fig. 7A–C). Most of the area occupied by the submarine channel overlies subsurface salt. This condition becomes more pronounced downstream of the first major channel bend, where the feature exhibits a more confined morphology. The channel bend is salt tectonic influenced in the portions where there is an increment in the salt thickness, which the most representative is the salt walls at the southern portion of the area.

In contrast, the northwestern sector of the study area, where the main mass-transport deposits are concentrated (Fig.8A) and where the Abimael Ridge is present (Mohriak and Szameitat, 2023) (Fig. 7D), shows a reduced expression of the subsurface evaporite layer.

Comparison between the distal WNW-ENE trajectory of the submarine channel (dashed white line) and the structural datasets, including the salt top, salt base, and gravity anomaly maps (Fig. 7A, B, and D), reveals a marked spatial parallelism, also coinciding with the Puri High (Freitas et al., 2022), which is also controlled by deeper structures that elevates the basement reducing the salt thickness in this area

The top-saltreaches its shallowest depth at approximately –2,700 m, located above a salt-related crestal graben between the margins of adjacent minibasins. Mean top-salt depths across the study area range from –4,700 to –8,700 m. The salt base is shallowest at approximately –5,000 m, with average depths ranging from –5,500 to –8,000 m.

Although the top-salt and base values indicate that in some sectors the evaporite layer occurs relatively close to the seafloor, the salt thickness map does not display particularly high thickness values. Instead, salt thickness generally ranges between approximately 1,000 m and 2,000 m along the channel trajectory, decreasing to near-zero values in the sector adjacent to the Abimael Ridge (Fig. 7C).

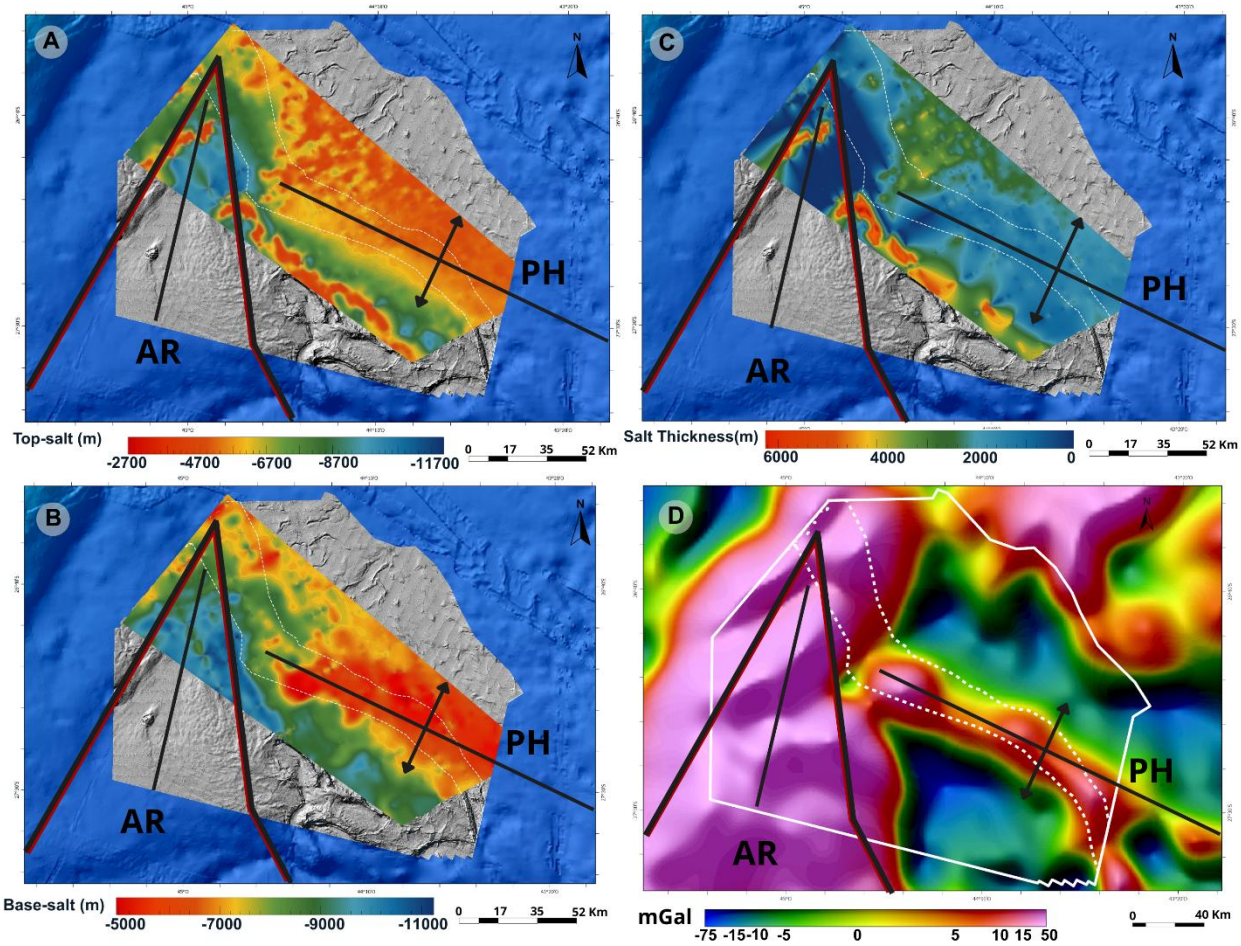

Fig. 7. (A) Top-salt depth map. (B) Base-salt depth map. (C) Salt thickness map. (D) Gravity anomaly map overlain by the study area (adapted from Carvalho et al., 2022). The dashed white line indicates the Cananéia channel trajectory, Abimael Ridge (AR) is represented by the red and black line (Modified from Mohriak and Szameitat, 2023), and Puri High (PH) is represented by the black line (Modified by Freitas et al., 2022).

4.3 Proximal sector: MTC-dominated domain

The proximal sector (Fig. 5) contains an extensive mass-transport complex (MTC) that extends for approximately 115 km, reaching a maximum width of 30 km and covering an estimated total area of 2,098 km² (Table 1). On the seafloor, this unit is expressed as a highly irregular and chaotic morphology composed of numerous cohesive sedimentary blocks of variable shapes and sizes (Figs. 8 and 9).

The blocks transported by gravitational processes are not entirely isolated and are interpreted as cohesive sediment masses transported downslope during large-scale mass-transport events (Fig. 8A, B).

The spatial distribution of the relief associated with the mass-transport complex is illustrated in Fig. 8. The deposit exhibits a highly irregular morphology characterized by numerous mounds and depressions that form a hummocky seafloor topography formed by the presence of cohesive sedimentary blocks.

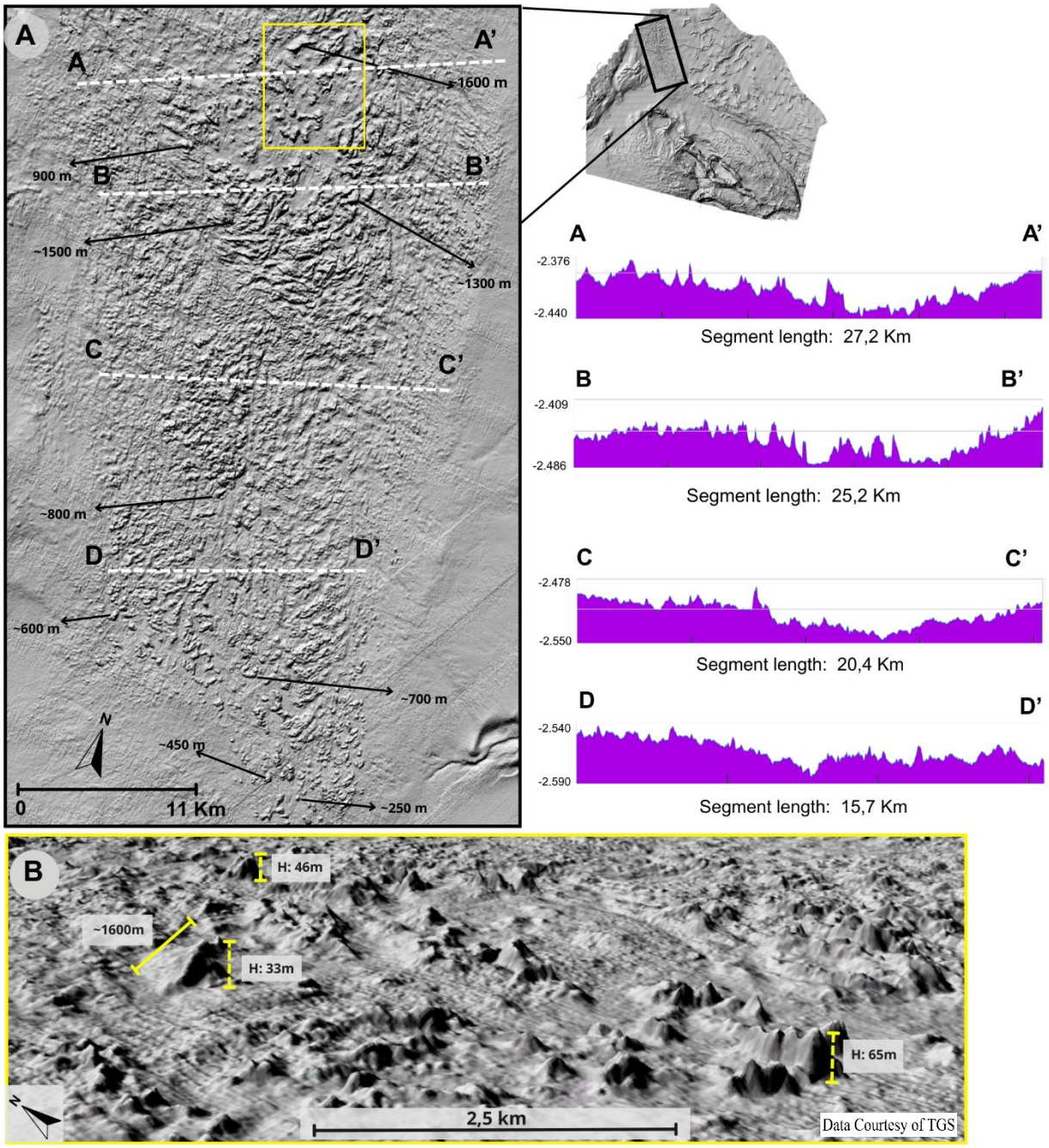

Fig. 8. (A) Detailed view of the MTC area illustrating the approximate length and geometry of several displaced blocks, and four bathymetric profiles. Black arrows indicate the measured length of individual blocks. (B) Perspective view of the relief of representative mass-transport blocks in the northwestern sector of the study area, corresponding to the yellow polygon shown in (A). Vertical exaggeration: 5×.

Four transverse bathymetric profiles (A–A,' B–B', C–C', and D–D') were extracted along the main axis of the deposit (Fig. 8A). These profiles show that the relief associated with the blocks is more pronounced in proximal sectors and becomes progressively smoother toward the distal portions of the deposit. In the proximal sector (profile A–A'), the relief

is characterized by higher mounds and greater topographic roughness. Toward profiles B–B,' C–C', and D–D', a progressive reduction in both the height and lateral extent of these features is observed.

The perspective view (Fig. 8B) highlights the irregular geometry of these sedimentary blocks, which reach heights of approximately 30–65 m, separated by lower-relief depressions. In the northwestern portion of the study area, closer to the inferred source area on the continental slope, the blocks are larger and more cohesive, reaching 800–1,600 m in length. Toward the south–southeast, the blocks become progressively smaller and less coherent, ranging from 4–12 m in height and 200–400 m in length.

The integrated analysis of the bathymetric profiles indicates that from profile A–A' to D–D' there is a progressive reduction in both the height and lateral extent of the irregular relief associated with the MTC deposits. This trend reflects a gradual decrease in the size of the transported blocks, accompanied by progressive confinement of the conduit filled by the MTC, which becomes narrower toward the distal sectors.

The seismic profile exhibited in Figure 9 indicates that this sector experienced multiple mass-transport events throughout geological time. Three MTDs are observed in the seismic section expressed as intervals of chaotic reflections. In conjunction these MTD events are named here as the Cananéia Mass Transport Complex.

The subparallel unit above this prominent erosional unconformity (yellow horizon), represented by the blue horizon, is interpreted here as a hemipelagic drape and represents a continuous stratigraphic marker separating two distinct phases of mass-transport deposition. The lower one is limited at the base by the early Miocene erosional unconformity (orange horizon in figure 9). The upper one occurs above the late Miocene-Pliocene unconformity, that eroded the top of the hemipelagic unit drape showing pronounced reflector truncations (yellow horizon in figure 9). The uppermost superficial MTD, with undefined Quaternary age, is confined within the Cananéia Channel, containing preserved cohesive blocks, giving the irregular morphology of the present seafloor revealed by the multibeam bathymetry (red polygon in figure 9).

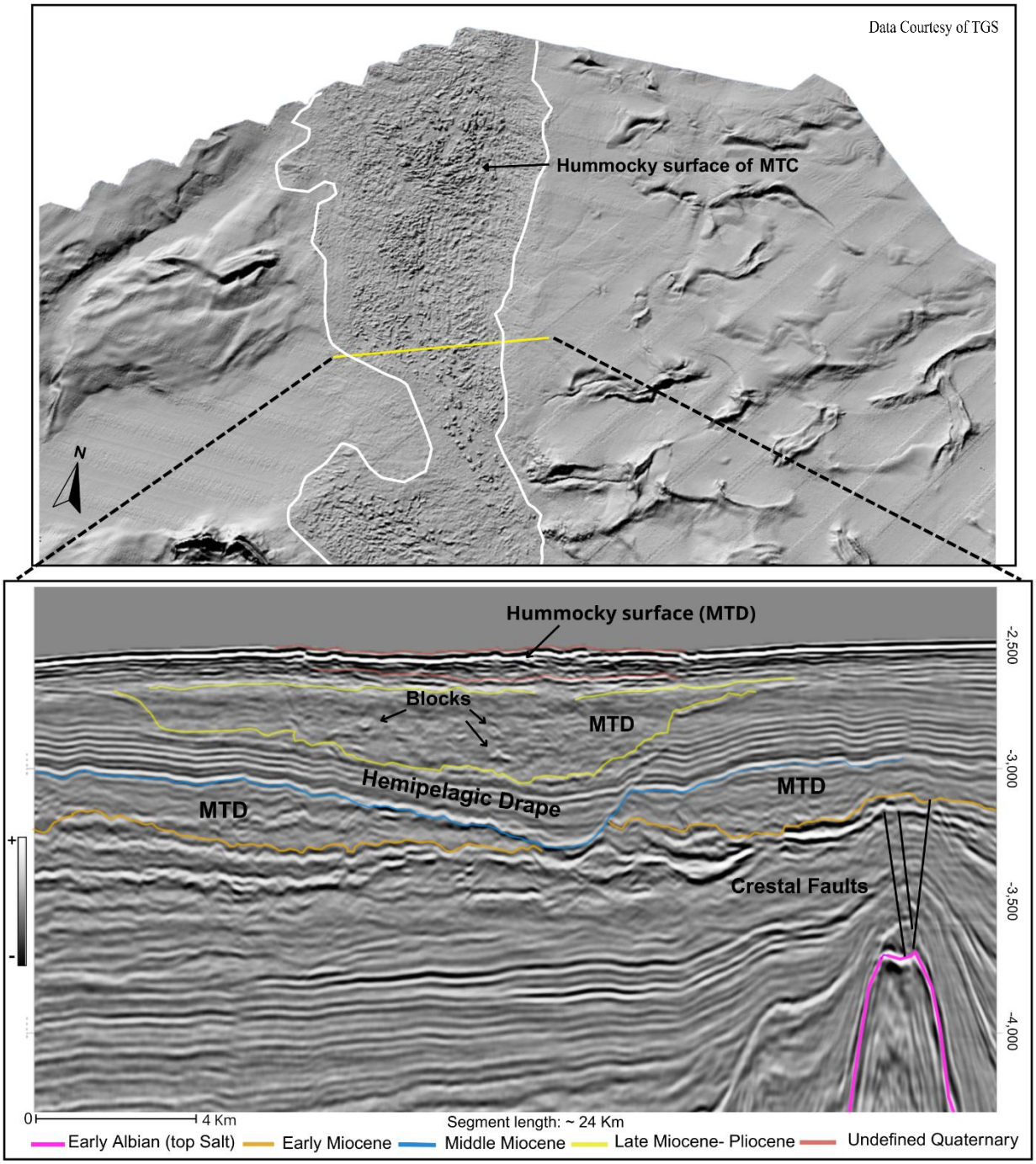

Fig. 9. Perspective view of a sector of the mass-transport complex (MTC), showing the 2D seismic line highlighted in yellow and its corresponding subsurface section below. Stratigraphic markers (pink, orange, blue and yellow horizons) are constrained using the chronostratigraphic framework of Contreras et al., (2010). The red horizon marks the basal surface of the most recent MTD events.

Additionally, the seismic data indicate that the stratigraphic succession was deformed in response to the uplift of an underlying salt structure, represented by the pink horizon corresponding to the Early Albian top-salt surface. This deformation generated crestal

faulting and localized structural relief, particularly visible on the right side of the seismic section.

4.4 Transitional sector: Deflected and progressively confined valley

The sector (ii) is characterized by a deflection of the sediment-routing conduit, reflected in the geometry of the MTC deposits within this portion of the study area (Fig. 10). The blocks forming the irregular MTC morphology continue to show a progressive reduction in size downslope, as was also observed in the proximal sector. The MTDs also exhibit a higher degree of fragmentation, with numerous smaller and less cohesive blocks that appear partially displaced relative to the surrounding sediments.

The bathymetric profiles shown in Fig. 10 (A–A', B–B', C–C', and D–D') further illustrate this pattern. In profiles B–B' and C–C', several of these isolated blocks can be identified as small topographic highs standing above a relatively smoother seafloor surface.

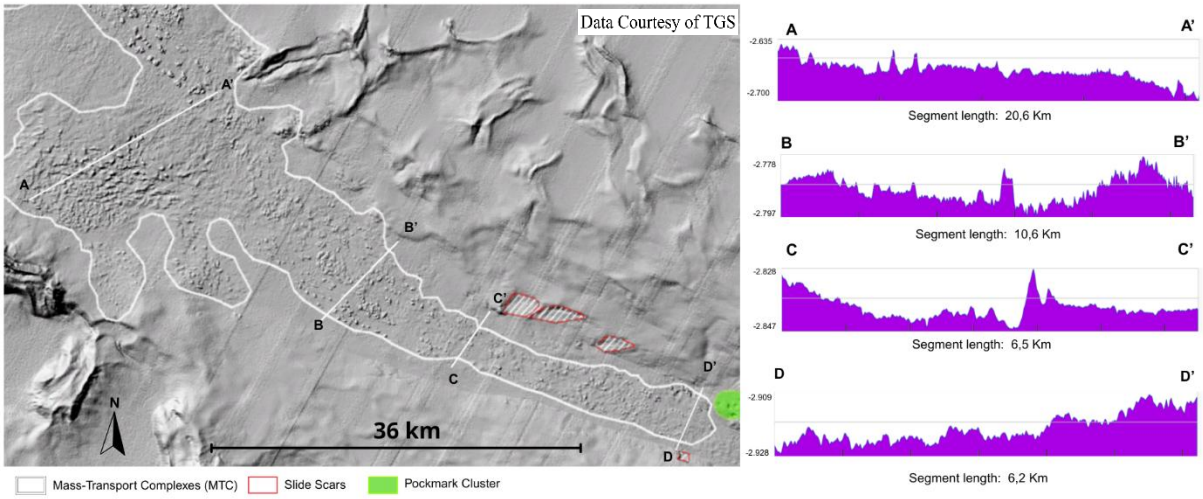

Fig. 10. Morphology of channel sector (ii), highlighting Mass-Transport Complexes (MTCs), slide scars, and pockmark clusters. Bathymetric map indicating the locations of profile lines A–A', B–B', C–C', and D–D'.

In addition, this sector shows a progressive increase in valley confinement, with the submarine valley margins becoming more clearly defined compared to those observed in the proximal sector. This enhanced confinement is accompanied by the development of slope-instability features along the channel flanks, including slide scars mapped along the

valley margins (Fig. 10). A pockmark cluster is observed in the transition to the distal sector.

The dip seismic line (Fig. 11), which crosses the entire transitional sector shows the dominance of mass-transport deposits (MTCs) and in its SSE portion enters sector (ii), reveals the subsurface architecture associated with the channel deflection.

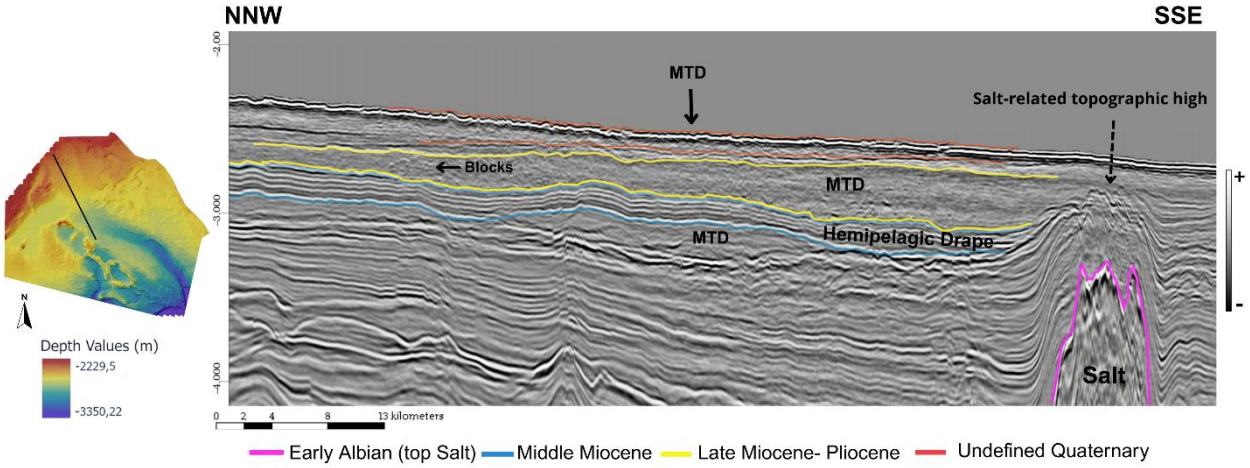

Fig. 11. Interpreted 2D dip longitudinal seismic line, across the proximal and transitional sectors (i) and (ii). Stratigraphic markers on the dip line (blue, yellow, and pink horizons) are constrained using the chronostratigraphic framework of Contreras et al. (2010). The red horizon marks the basal surface of the most recent MTD events

The horizon highlighted in yellow corresponds to a thick MTD whose base is assigned to the Upper Miocene–Pliocene interval. This unit displays numerous erosional truncations. Along the longitudinal profile, progressive infill is observed, with the accumulation of sediments and blocks transported by gravitational flows. A clear gradient contrast is observed between the canyon base, which is steeper, and the upper portion, which appears more flattened and smoothed.

Furthermore, the package bounded by the yellow horizons appears to terminate against a topographic high related to a salt structure. The shallower chaotic reflectors (red horizons), indicate the more recent MTD also visible in the multibeam data, show a significant reduction in thickness and extent.

4.5. Distal sector: confined submarine valley

In the distal sector the channel segment extends for approximately 97 km, (Fig.12 B), in water depths ranging from ~2,800 m to ~3,350 m. Cross-sectional bathymetric profiles along the channel floor (Fig. 12. A) delineate preferential zones of erosion and localized marginal sediment accumulation. From profiles A–A′ to D–D′, the thalweg is positioned toward the right margin of the channel, whereas from E–E′ to K–K′ it shifts to the opposite side. This lateral migration of the thalweg corresponds to a reorientation of the depositional pattern observed in plan view. Between profiles B–B′ and D–D′, the marginal depositional sector is interbedded with slide deposits, one of which can be observed as a still-coherent mass in Fig.13 B.

When comparing the bathymetric profiles in Fig. 10 (B–B′ and C–C′), which intersect isolated MTD blocks, with profiles F–F′ and G–G′ (channel-base erosional features) in Fig. 12, clear morphological differences are observed. Cross-sections intersecting the MTD blocks display sharper and more irregular relief, whereas the channel-floor erosional features exhibit smoother and more rounded morphologies.

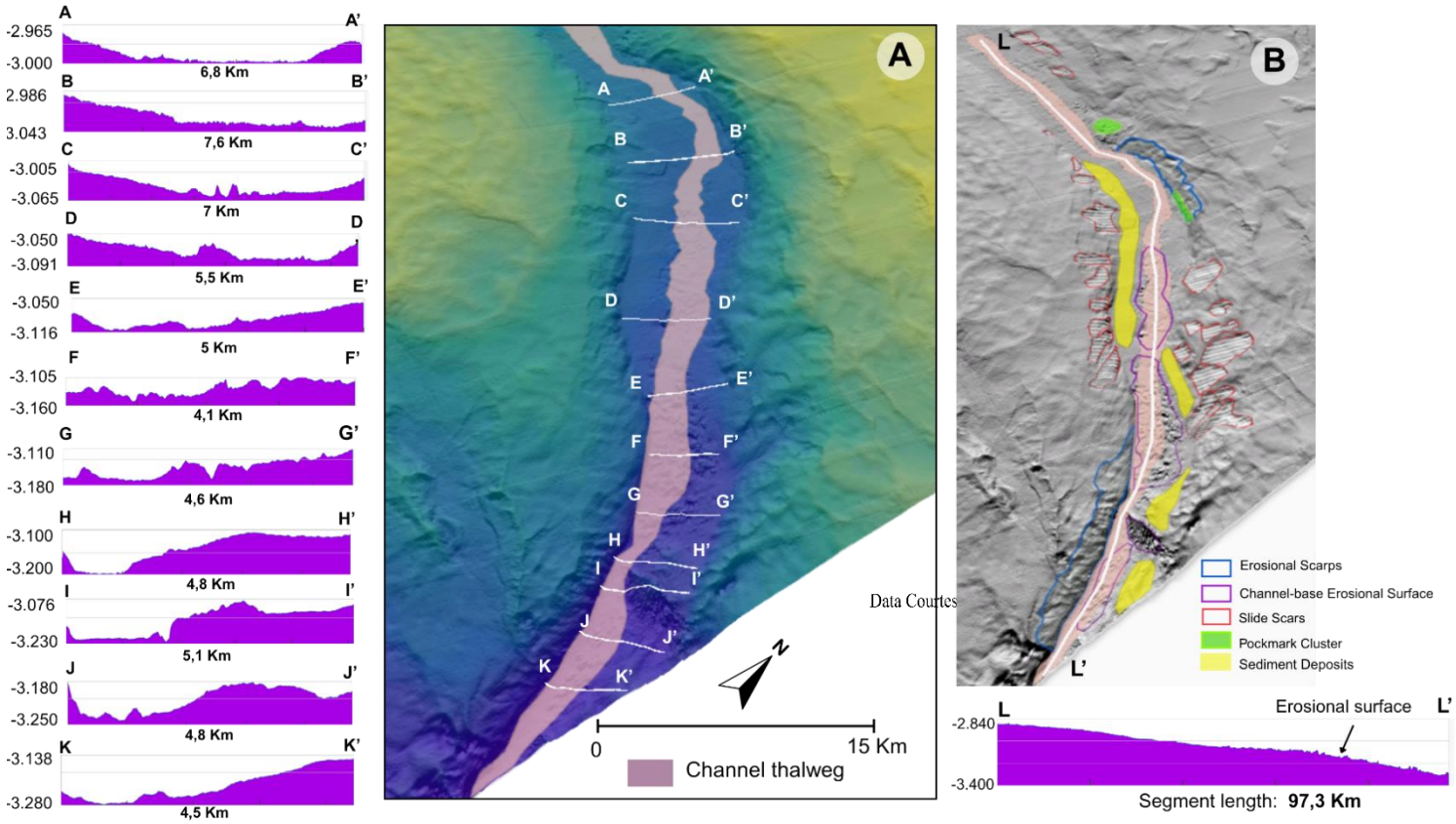

Fig. 12. (A) Eleven cross-channel bathymetric profiles illustrating preferential drainage pathways and sediment-accumulation zones. Depth (m) is shown on the left axis, and segment length (Km) is shown along

the bottom axis. (B) Longitudinal profile along the channel thalweg (97.4 km in length) showing the mapped features in sector (iii). Vertical exaggeration: (5×).

Along the segment intersected by profile H-H' to J-J' (Fig.12.A) a prominent positive-relief feature is observed, reaching approximately 145 m in height and extending for about 4.3 km in length (Fig. 13. C). This feature is located within the channel and coincides with a local deviation of the thalweg.

Erosional scarps are prominent morphological features along the channel margins and define the steepest sectors of the channel flanks. These scarps extend for approximately 15–23 km downstream and reach heights ranging from ~170 m to a maximum of ~230 m in the most distal sector (Fig. 13. B, C). They occur systematically adjacent to the thalweg, marking zones of enhanced incision and lateral erosion.

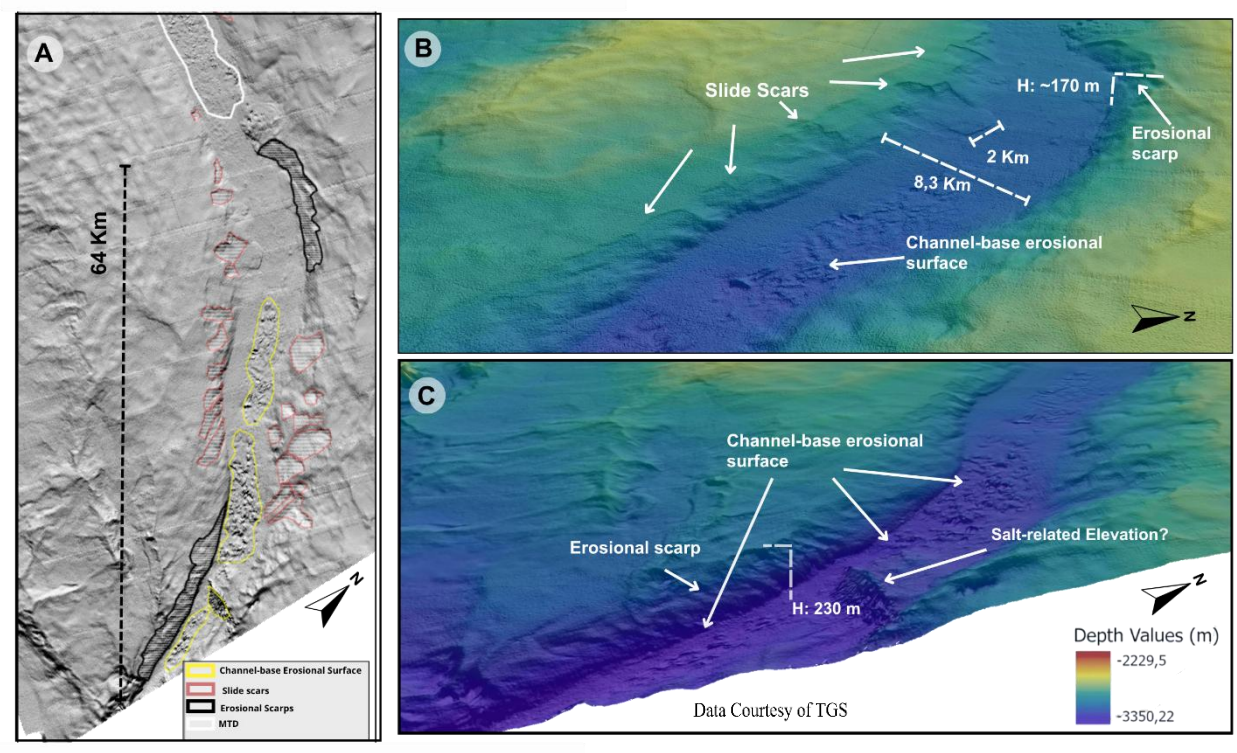

Fig. 13. (A) Bathymetric map showing the main erosional features of the submarine valley, including slide scars, erosional scarps and channel-base erosional surfaces. (B, C) 3D bathymetric perspective view showing erosional features of the channel (vertical exaggeration 5x).

The channel margins associated with slide scars are relatively smoother (Fig.12.B, Fig.13.A). These scars result from cohesive sediment blocks detaching and moving downslope while largely preserving their internal structure, leaving scars comparable in size to the displaced masses. The mapped slide scars vary in areal extent from

approximately 2.8 km² to 11.5 km², totaling ~113.5 km² (Table 1). In Fig. 13. B, one scar is visible, with the displaced mass still preserved downslope. The slide deposit extends to approximately 2 km in length.

To further investigate the subsurface configuration associated with these morphologies, seismic profiles crossing the distal sector were analyzed (Fig.14). Along Line A, the former morphology of the canyon (yellow horizon) exhibits a U-shaped pattern. On the canyon's right-hand margin, a topographic high associated with the underlying salt is observed, while adjacent topographic lows are also present. Several faults cut through the evaporite package, with one reaching the seafloor on the right-hand margin and corresponding to a scarp observed in the bathymetry.

In the downstream sections, the canyon displays a V-shaped geometry (Fig. 14.B) and, further downstream, a broader V-shaped pattern (Fig. 14.C). Faults associated with the regional structural framework are also observed in these sections and coincide with the progressive widening of the valley.

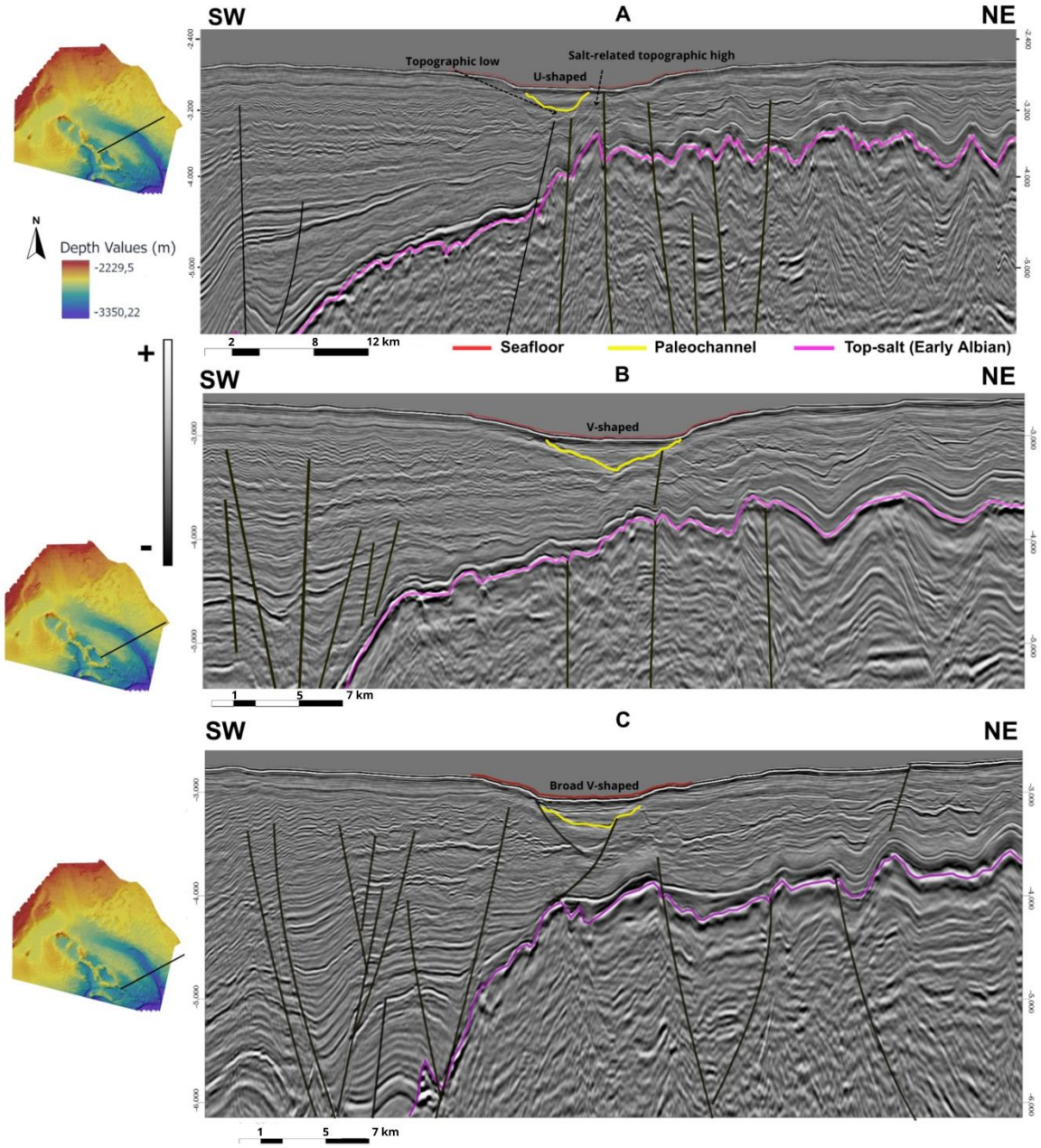

Fig.14. Interpreted 2D seismic cross-sections in the distal sector of the study area. Section A-C represent strike-oriented cross sections perpendicular to the channel axis. The sections illustrate variations in geometry, depositional architecture, and the relationship between channel incision, and salt-related structures. The red horizon marks the current seafloor in sections A–C. The yellow horizon in sections A–C represents the base of the ancient channel, while the pink horizon marks the top of the salt layer in all sections.

In addition to these morphologic characteristics, other seafloor features are present within this sector. A total of 11 pockmarks were mapped proximal to the erosive escarpment near the ~2,800 m isobath (Fig.15). Seven of these features are clustered along the escarpment rim, whereas four are aligned along the escarpment face within the inner portion of the channel. Most pockmarks display sub-elliptical planforms, while others are more circular

in shape. The largest features range from 250 to 400 m in diameter, and one prominent pockmark (P7) reaches a maximum depth of ~40 m, as measured from the transverse bathymetric profile A–A′(Fig.15) extracted from the multibeam dataset. Notably, this deepest pockmark also exhibits high slope-gradient values, reaching angles of up to 31°, as shown in Fig. 16.

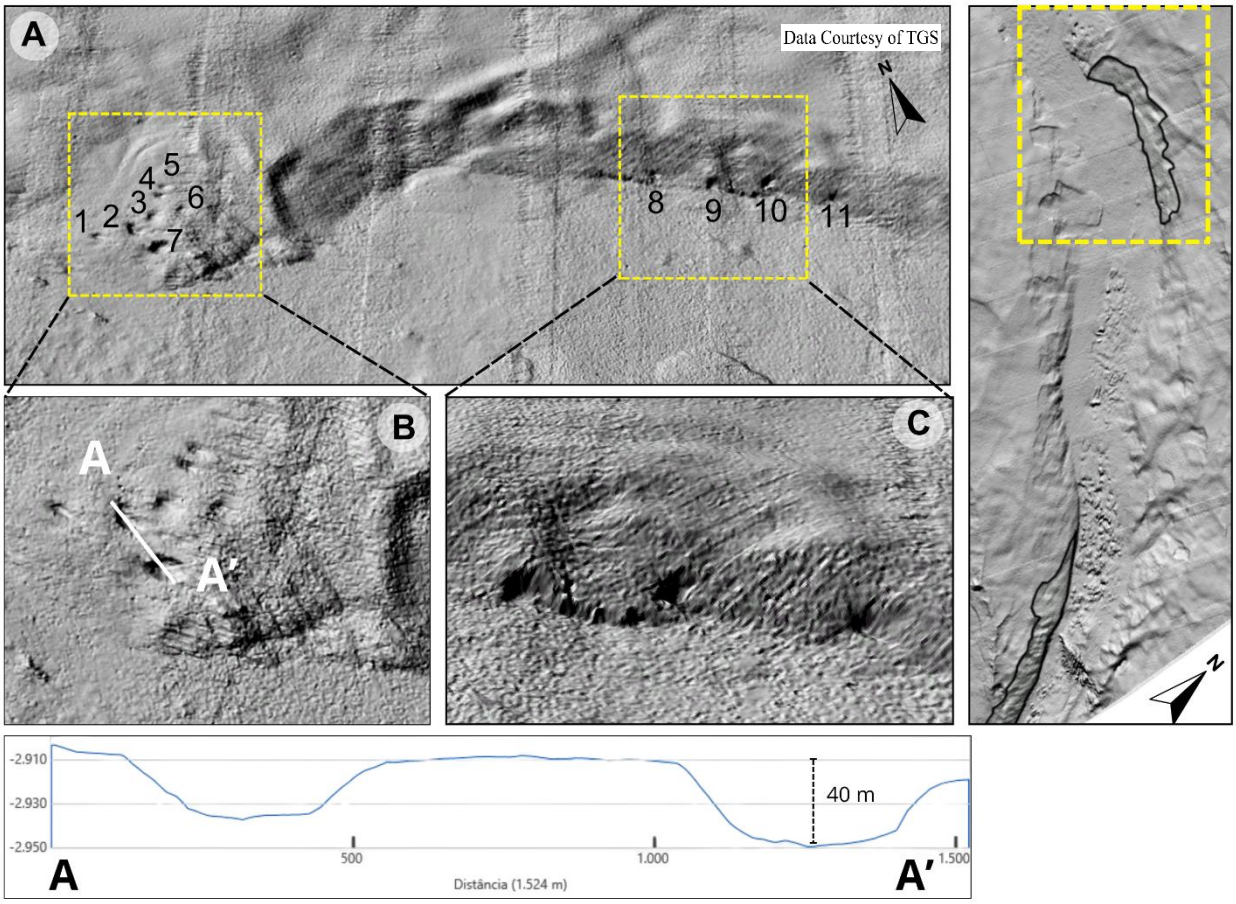

Fig. 15. Distribution of pockmarks in the study area. (A) Regional location of the area displayed in panels B and C. (B) Detailed view of the pockmark cluster and location of the A–A′ bathymetric profile. (C) Close-up of the pockmarks occurring along the erosional scarp. The A–A′ bathymetric profile highlights the maximum depths of two representative pockmarks

4.5.1 Slope gradient distribution and morphometric analysis

Considering features directly associated with the submarine channel, the highest gradient values occur on erosional scars developed over intra-channel positive relief and on the erosional scarp located farther downstream. The erosional scars, grouped under the erosional surface feature category in Table 1, display maximum gradient values ranging from approximately 44° to 58°, whereas the downstream erosional scarp reaches maximum values of up to ~48° (Fig. 16B). In contrast, the upstream erosional scarp

exhibits comparatively lower gradient values, with maximum angles of up to approximately 30°.

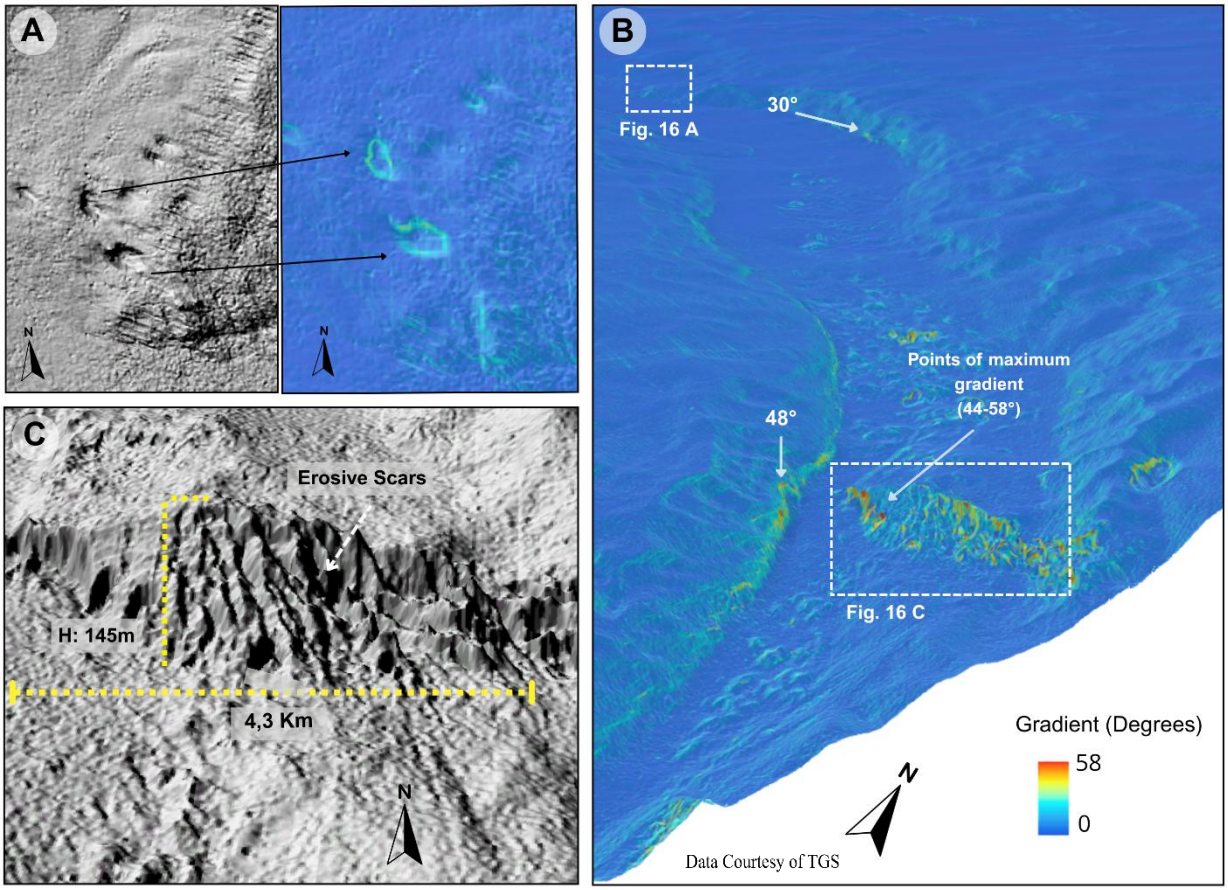

Fig. 16. (A) Cluster of pockmarks (left) and corresponding expression in the gradient map (right). (B) Perspective view of the gradient map (in degrees) highlighting sectors with the steepest slopes, including erosive scars along the elevated feature (44–58°) and the base of the erosive escarpment (48°).(C) Detailed view of an elongated positive-relief feature, likely salt-related, bounded by erosive scars and measuring ~145 m in height and ~4.3 km in length. This structure is interpreted as a morphological barrier that influences sediment bypass and controls deposition pathways

Isolated pockmarks within the study area also show locally elevated gradients (Fig. 16A), reaching values close to 31° (Table 1). The downstream erosional scarp, adjacent to the intra-channel high, is both higher and steeper, reflecting a marked increase in slope angle toward the channel margin. This increase in steepness is accompanied by more pronounced erosive patterns on the channel floor adjacent to the scarp and by a morphological trend of progressively higher channel margins along this sector of the channel.

5. DISCUSSION

5.1 Structural control on channel trajectory

The northwestern sector of the top, base, and isopach maps of salt (Fig. 7. A-C) over the Abimael Ridge stands out due to the pronounced thinning and local absence of the evaporite section. Previous studies by Mohriak and Szameitat (2023) and by Silva et al. (2024) have already identified the propagator as a key structural component controlling the segmentation and compartmentalization of the evaporitic package, leading to the partitioning and local removal of salt along this sector. Downstream, in the transitional sector, the deflection observed (Fig. 7. A, Fig.11) is interpreted as resulting from structural control exerted by a salt diapir, whose uplift induced deformation of the overlying strata and generated a topographic high. This feature acted as a barrier to gravitational flow, deflecting the thalweg toward morphodynamically more favorable areas.

The seismic horizon highlighted by yellow markers (Fig. 11, Fig. 9) shows recurrent erosional truncations and progressive canyon infill, reflecting the cumulative deposition of sediments and blocks transported by gravity-driven flows. Differences in gradient between the steeper base and the smoother, flattened top corroborate continuous infill processes and highlight the capacity of massive or recurrent MTDs events to modify pre-existing topography (Covault et al., 2020). Similar patterns were described by Gee and Gawthorpe (2006), who documented high sedimentation rates during the Late Miocene–Pliocene along the Angolan margin, considered a structural and stratigraphic analogue of the Santos Basin.

The most recent MTDs, visible in multibeam data, are marked in red on the seismic section (Fig. 11). According to Hercos et al. (2023), most mass-transport deposits shaping the modern seabed in the Santos Basin are older than ~10 ky (Pleistocene or earlier) and are now partially draped by Holocene pelagic to hemipelagic sediments.

The absence of seismic markers associated with mass-transport and block deposits in the distal sector, as illustrated by cross sections (Figs. 14. A– C) suggests a change in the depositional regime and dominant processes along the system. While upstream segments are characterized by instability and MTDs deposition, downstream reaches display greater incision by channelized flows, such as turbidity currents. This segment of the canyon develops over an irregular salt top, and seismic interpretation indicates that salt-

tectonics-related topography conditions the canyon trajectory. The cross sections (Figs. 14. A – C) also exhibit increased incision and flow confinement, with V-shaped and broad V-shaped cutting patterns. This transition suggests a local gradient increase and flow focusing, enhancing the erosive capacity of the Cananéia system as was also observed in different localities (Gee et al., 2007; McHargue et al., 2011; Ashiru et al., 2020).

The submarine valley morphology is further controlled by topographic highs associated with underlying salt uplift, which act as preferential corridors or barriers, depending on the configuration of adjacent lows (Fig. 14). This structural control not only influences the thalweg trajectory but also governs patterns of marginal erosion and lateral deposition, resulting in geometric asymmetry and variations in sediment infill. Faults cutting the evaporite package additionally contribute to localized flow deflection, flow confinement, and enhanced erosion, supporting interpretations of submarine canyon development under structural control (Clark and Cartwright, 2009; Covault et al., 2020; Gee and Gawthorpe, 2006; Oluboyo et al., 2014; Posamentier and Kolla, 2003).

5.1.2 Puri High and Capricorn Lineament influence

The faults responsible for structural control of the canyon morphology are associated with reactivations of faults along the Capricorn Lineament (Fig.2), described by Bueno et al. (2004) as a crustal lineament-oriented NW–SE. Previous studies have shown that the Cananéia Canyon coincides with the Capricorn Lineament (Duarte and Viana, 2007), and that its faults exhibit post-Aptian activity, controlling sediment depocenters (Mohriak et al., 2022). In addition, studies such as Assumpção et al. (2011) report proximal earthquakes along the lineament, some reaching 5.2 mb (Fig.2), which are associated with reactivation of these faults.

These earthquakes, particularly along continental-slope settings, can act as an important trigger for large mass-transport complexes (MTCs) and submarine landslides (Masson et al., 2006; Moscardelli and Wood, 2008). These processes may, in turn, play a key role in the initiation and early-stage development of submarine canyons (Kunath et al., 2025). According to Hercos et al. (2023), the origin of the Cananéia Canyon is likely associated with successive retrogressive collapses (slumps). In this context, paleo-earthquakes related to fault reactivation may have contributed to slope failures at the canyon head, ultimately influencing the genesis and progressive headward growth of the Cananéia

Canyon. Supporting this interpretation, Fig. 2 shows two seismic events exceeding magnitude 3.5 located near the canyon head region.

The evolution of the canyon system is also modulated by the regional basement structural framework, which governs the deformation and mobility of the overlying evaporitic layer. The Capricorn Lineament, together with inherited structures such as the Puri High, exerts a first-order control on salt distribution and kinematics, directly influencing seafloor morphology and the dynamics of deep-water depositional systems. Within the study area, the Puri High is responsible for the uplift of the salt base (Figs. 7B, 17, and 18), which exhibits geometric parallelism with the top salt, as previously described. This configuration suggests structural control exerted by reactivated faults, possibly rooted in the basement or pre-salt units, which have influenced both the architecture of the salt layer and its flow dynamics. Previous studies have consistently demonstrated that reactivated basement faults can control salt distribution, thickness, and kinematic behavior (Peel et al., 1998; Pichel et al., 2020), supporting the interpretation proposed in this study.

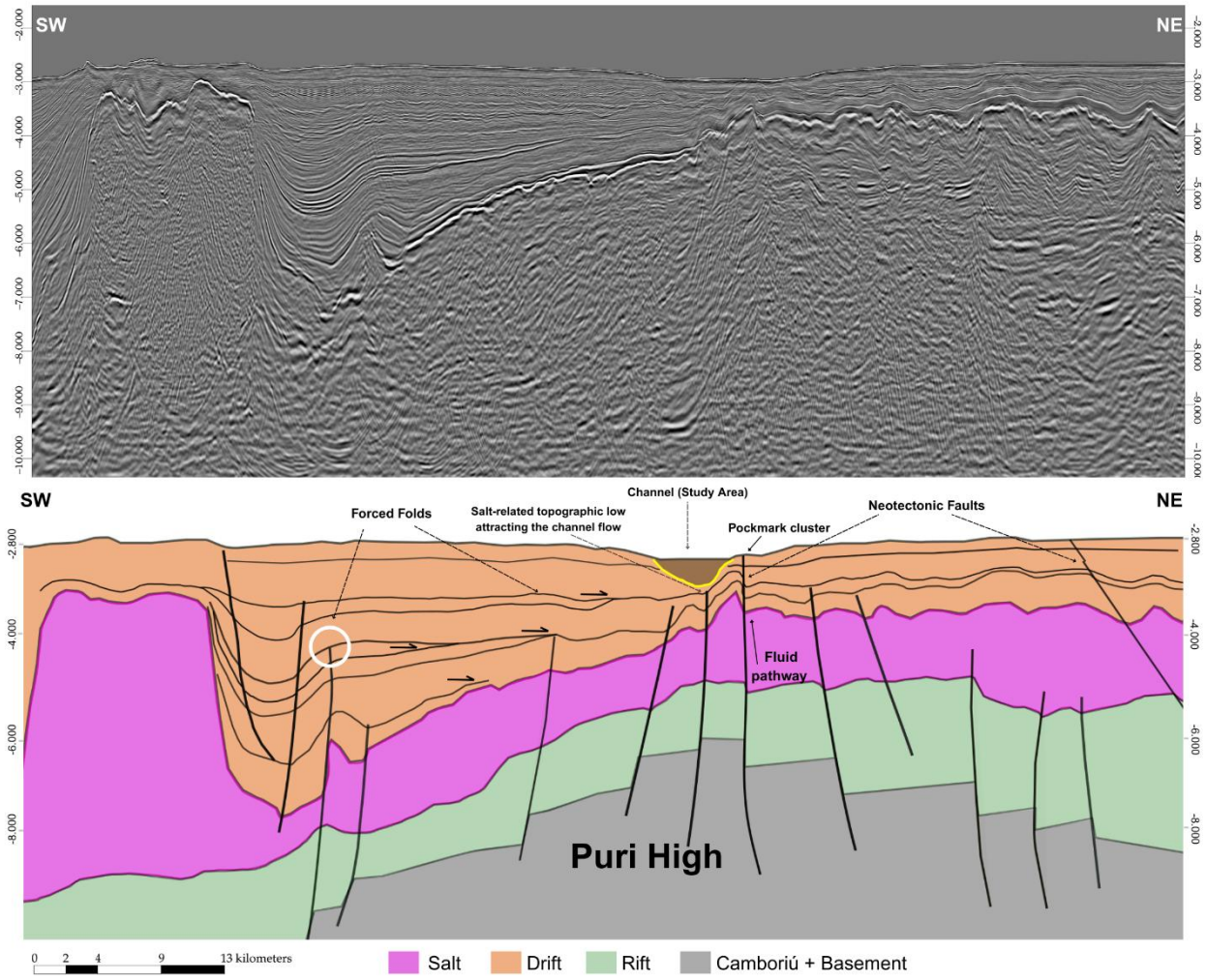

Fig. 17. Schematic cross-section of the Cananéia Canyon system, illustrating the structural and sedimentary framework. The section is based on 2D seismic data (upper panel and the same in Figure 7 B) but is presented as a schematic model with exaggerated vertical scale to highlight key features, including salt-related topography, forced folds, onlaps, and fluid pathways. Pockmark clusters mark zones of focused fluid escape, while the underlying Puri High represents a basement structure controlling salt uplift and canyon trajectory. Black arrows (single-sided) indicate onlaps.

The development of the downstream segment of the Cananéia Canyon system reflects the interaction between inherited structural controls and deformation of the evaporitic succession. Salt movement, influenced by fault activity, indicates the persistence of an active tectonic regime and promotes the formation of forced folds and salt-related topographic highs and lows that condition preferential flow pathways and the geomorphological configuration of the canyon. This behavior is consistent with that observed in other structurally controlled submarine channel systems (Covault et al., 2020; Oluboyo et al., 2014). Onlapping reflectors indicate the presence of syn-depositional relief associated with continued salt movement during sedimentation (Soutter et al.,

2019), while faults cutting the evaporitic layer may act as preferential pathways for fluid migration (Chand et al., 2008), as evidenced by the spatial association between structurally controlled scarps and clusters of pockmarks observed on the seafloor (Figs. 17, 18, and 19). Similarly, Böttner et al. (2025) documented onlap patterns related to salt tectonics that influenced the evolution of the Agadir Canyon.

Additional evidence of this structural control is provided by seismic interpretations, which indicate that faults associated with the Capricorn Lineament and the Puri High directly influenced the position of the thalweg during different stages of channel-system evolution. This influence is evidenced by the asymmetric geometry and thickening of the paleochannel fill adjacent to the faults (Fig. 14C), represented by the yellow and orange sedimentary packages (Fig. 18), which characterize a structurally controlled channel fill. The yellow stratigraphic package identified within the paleochannel (Fig. 18) suggests that an antithetic fault controlled and confined the thalweg during its deposition. Notably, the most recent thalweg remains positioned within the same sector of the valley, adjacent to the scarp generated by this fault, indicating the persistence of structural control through time. The recurrence of this pattern suggests that inherited faults, subsequently reactivated, played a fundamental role in both the depositional architecture of the paleochannel and the configuration of the modern system.

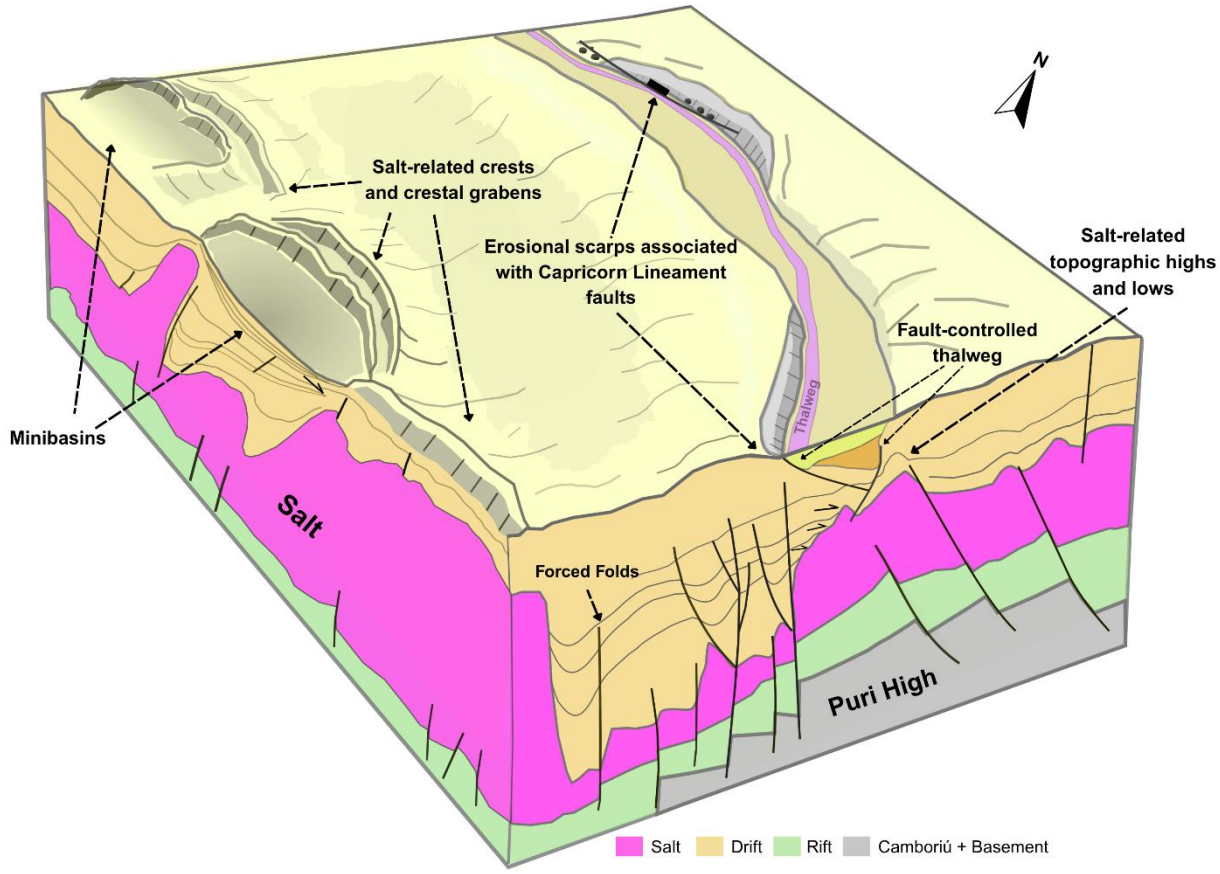

Fig. 18. Interpretive schematic model of the distal sector of the Cananéia Canyon system, based on the integration of seismic and bathymetric interpretations. The cross-section is based on the seismic interpretation presented in Fig. 14C. The model provides an overview of the distal study area within the limits of seismic coverage, illustrating the influence of the Puri High, faults associed with the Capricorn Lineament, salt-related deformation and their control on canyon morphology and channel evolution.

Taken together, these observations demonstrate a strong coupling between deep-seated structural inheritance, salt tectonics, and sedimentary processes, indicating that canyon evolution is governed by an integrated, multiscale structural control rather than solely by autogenic sedimentary dynamics. This structural framework plays a fundamental role not only in determining canyon trajectory and morphology, but also in modulating erosional efficiency and fluid release in deep-water environments.

5.2 Channel dynamics versus structural control

As discussed above, the two main erosional scarps identified from the multibeam data exhibit a clear spatial association with the mapped faults in the study area (Figs. 18 and 19). The channel thalweg follows these scarps along a large portion of its course, consistently positioning near their base, where erosion is most intense. This

morphological arrangement indicates direct structural control on the location of the current/recent thalweg, as observed in the multibeam data, promoting the concentration of basal erosion along structurally controlled margins and contributing to the development of gravitational instability processes, including localized scarp collapses. Consequently, these segments display higher system slope angles compared to adjacent sectors. The influence of faults on flow deflection, channel confinement, and enhancement of marginal erosion has been widely documented in submarine channels of the Levant Basin, Lower Congo Basin, and Western Niger Delta, supporting the interpretation proposed here (Clark and Cartwright, 2009; Oluboyo et al., 2014; Ashiru et al., 2020).

Downstream, the right-hand channel margin, where the first erosive scarp develops, shows a progressive reduction in slope angle, accompanied by an increase in the frequency of slide scars. In contrast, the left-hand margin exhibits a gradual slope increase, culminating further downstream in the development of a second erosive scarp on this side of the channel. This morphological pattern indicates a progressive inversion of valley asymmetry along the canyon-system trajectory (Fig.19, A-A', B-B'), interpreted as resulting from variations in structural control exerted by faults along the system. Such deformation locally modifies the gradients of the channel floor and flanks, promoting lateral migration of the thalweg toward zones of higher topographic gradient, with direct implications for the distribution of erosional and gravitational processes (Gee et al., 2007; Ashiru et al., 2020).

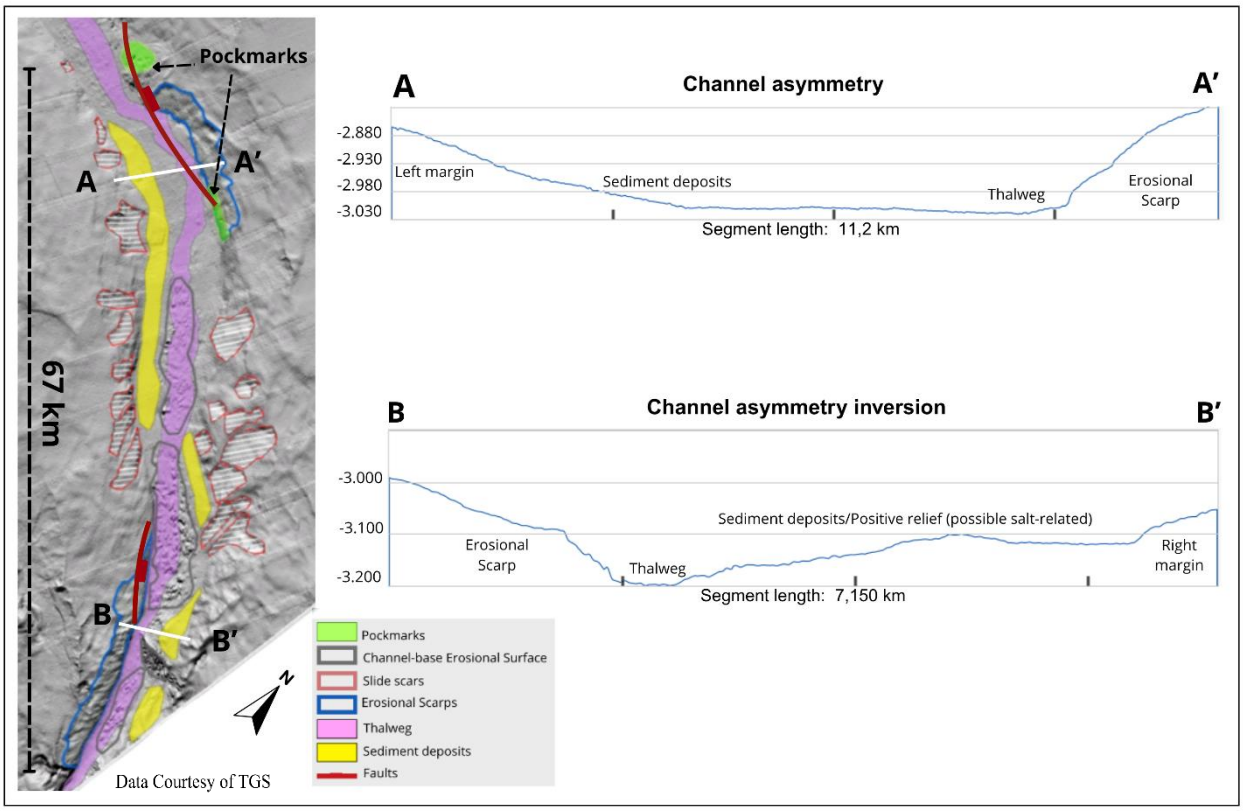

Fig. 19. Map showing faults and features including the channel thalweg, erosional scarps, marginal sediment deposits, and the channel-base erosional surface, with cross-sections indicated by white lines. Right: two cross-sections along the channel, illustrating its asymmetric inversion

Slide scars are more frequent in segments characterized by lower slope angles (Table 1) compared to the main scarps and occur predominantly in positions approximately opposite the thalweg. These sectors, highlighted by yellow polygons in Figs. 19, 20 are interpreted as marginal sedimentation zones within the valley, where some of the material mobilized by margin collapse tends to accumulate, at least temporarily. In Fig. 13B, one segment shows that the slid material exhibits a high degree of cohesion, potentially indicating a relatively recent instability event that has not yet been fully reworked by subsequent flows. This pattern suggests that the interaction between margin instability and thalweg position controls not only erosion but also local sediment retention along this system.

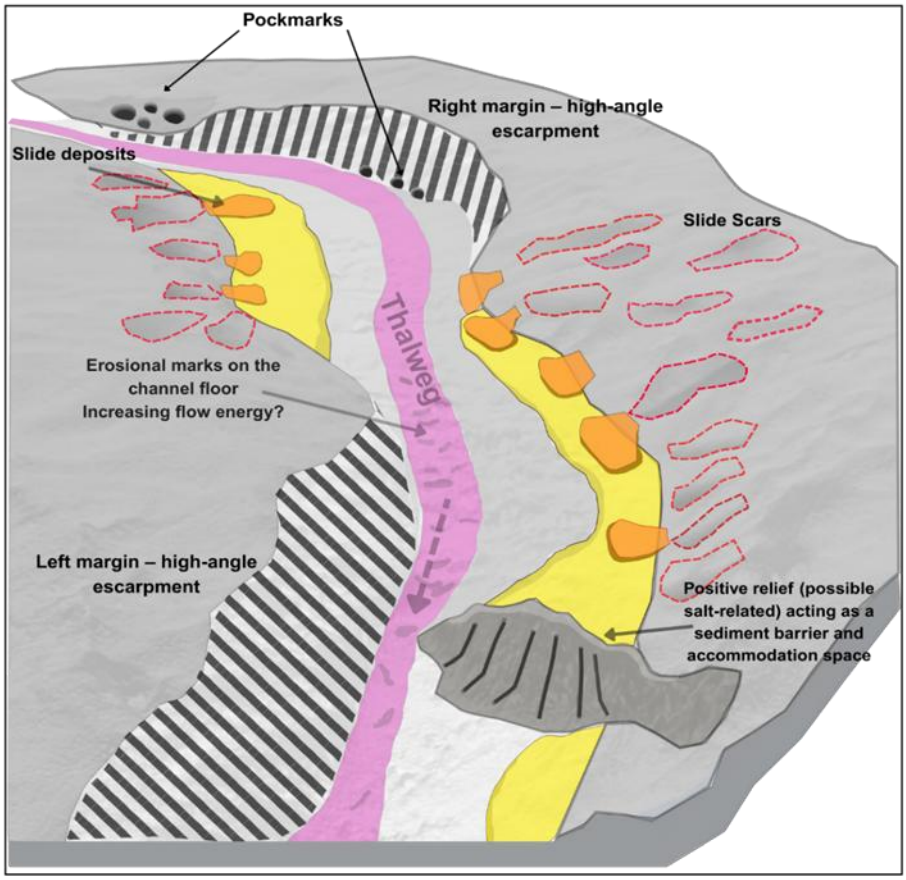

Fig. 20. Downstream section of the current submarine channel seafloor, showing dynamics and features such as margin gradient variations, channel course changes, pockmarks, slide scars, and deflection caused by the intra-channel high

In the distal sector of the study area, where valley asymmetry is inverted, morphology becomes influenced by shallow salt-related structures. This interpretation is supported by the presence of an intra-channel high (Fig.13.C, Fig.16.C) and a well-defined scarp along the left canyon margin. Although seismic coverage does not extend over this segment, multibeam data indicate that the thalweg is deflected and remains confined along the scarp associated with the structural high. Erosive scars oriented along the flow direction, observed on this high (Fig. 16. C) indicate significant erosive capacity beyond the thalweg and suggest that confinement imposed by the structure may locally enhance flow erosive efficiency. Similar conditions of flow-topography interaction have been well documented in previous studies of slope and deep-water channel settings (Gee and Gawthorpe, 2006; Pirmez et al., 2000; Prather, 2003). This intra-channel high is substantial, it also acts as a barrier to part of the sediment transport, contributing to an increase in marginal deposition areas (Fig.12, Fig.20).

In addition to these sedimentary and morphological features, the small cluster of eleven pockmarks identified adjacent to an erosional scarp (Fig. 15) exhibits a restricted spatial distribution and occurs in close association with fault-related erosional scarps and structurally elevated domains, coinciding with areas where the thalweg is deflected and confined. The limited number and clustered arrangement of these pockmarks suggest localized and discrete fluid escape events, rather than a regionally extensive seepage system such as the pockmark field mapped by by Mahiques et al. (2017) on the Santos Basin continental slope. Although the seismic resolution of the regional 2D dataset does not allow the identification of typical seismic indicators of fluid escape, the characteristic circular morphology of these features and their spatial association with scarps related to deep-seated faults (Fig. 17) reinforce their interpretation as pockmarks expressed on the present-day seafloor morphology (Fig. 19). The relationship between pockmarks and fault-controlled fluid migration has been widely documented in the literature (Chand et al., 2008; Benjamin et al., 2015).

The pockmarks within the submarine valley are predominantly located along its margins or scarps (Fig. 15). The study by Benjamin et al. (2015) describes pockmarks occurring both along canyon margins and within the canyon interior on the Niger Delta Slope, noting that the number of pockmarks along the margins was substantially higher than within the canyon. This distribution was interpreted as related to the higher efficiency of stratigraphic discontinuities generated by erosive canyon margins as preferential fluid pathways. Similarly, Frisicchio et al. (2025) documented pockmark occurrences associated with canyon pathways in a salt-tectonic setting. In the context of the present study, the pockmark distribution suggests combined control exerted both by faults mapped in seismic data and by the erosive scarp, which may have favored the formation of truncation surfaces and enhanced hydraulic connectivity, facilitating fluid migration and release at the seafloor.

In a deep canyon system subject to spatial and temporal variations in flow energy, the preservation of pockmarks indicates that structural control plays a fundamental role not only in the channel's trajectory and morphology but also in the dynamics of fluid circulation within the substrate. Thus, even when scarce, pockmarks provide independent geomorphological evidence supporting the influence of recent or still-active tectonics on the evolution of the deep-water channel system.

6 CONCLUSIONS

This study presents the first detailed morphological characterization of the distal segment of the Cananéia Canyon system on the São Paulo Plateau, based on the integration of novel high-resolution multibeam bathymetry and 2D seismic data. The results highlight the strong interplay between structural inheritance, salt tectonics, and sedimentary processes in shaping deep-water depositional systems, which are summarized as follows:

i) Structural control and influence of salt tectonics

The morphology and trajectory of the submarine channel are strongly influenced by first-order basement structures, including the Puri High and the Capricorn Lineament, as well as by salt-related topography. Salt-related topographic highs and lows act both as barriers and as preferential corridors for sediment transport, controlling thalweg position, flow confinement, and patterns of lateral erosion. Faults cutting the evaporitic layer further contribute to flow deflection and localized erosional intensification, demonstrating that canyon evolution is not purely autogenic but structurally controlled.

ii) Gravity-driven sedimentary processes

Mass-transport complexes dominate the proximal sector of the canyon, reflecting multiple episodes of gravitational instability. Deposited blocks show systematic variation in size and cohesion along the system, indicating progressive infill and modification of the canyon floor over time. In the more distal and confined reaches, turbidity currents appear to govern channel dynamics, marking a transition from widespread mass-wasting deposition to more focused erosional processes.

iii) Morphological responses and fluid interaction

Erosional scarps, slide scars, and pockmark clusters reveal the spatial coupling between seafloor morphology, structural control, and fluid escape. Variations in slope gradient and valley asymmetry along the channel demonstrate that structural topography strongly modulates sediment retention, lateral migration of the thalweg, and erosive efficiency. These lines of evidence indicate a system that remains active but is in an evolutionary maturation stage, in which seismic interpretations suggest that activity was more intense in the past and has progressively decreased, accompanied by gradual infill of the canyon over time. The presence of pockmarks along structurally controlled scarps indicates that fluid migration is closely linked to the same tectonic framework that shapes canyon morphology.

iv) Geological implications

The integration of bathymetric and seismic datasets allows a detailed understanding of a previously poorly constrained distal canyon-system segment. These findings underscore the importance of considering multiscale structural controls, halokinesis, and sedimentary dynamics when interpreting deep-water depositional systems in evaporite-bearing basins.

In summary, the Cananéia Canyon system exemplifies a deep-water depositional system governed by a complex combination of structural inheritance, salt tectonics, and sedimentary processes, emphasizing the need for integrated morpho-structural analyses in evaluating the evolution of submarine canyons and their associated sedimentary architectures.

In this context, this study provides insights into modern deep-water systems that may serve as analogues for subsurface reservoirs in salt-bearing margins. The interplay between structural controls and sediment routing also has direct implications for seafloor stability in areas of submarine infrastructure, highlighting the applied value of integrated morpho-structural analyses.

7 ACKNOWLEDGEMENT

The authors are grateful to TGS Brazil for providing the 15 m grid multibeam bathymetric data through a cooperation agreement with Fluminense Federal University and the Brazilian National Agency of Petroleum, Natural Gas and Biofuels (ANP), which makes regional seismic datasets publicly available for academic research. We also thank the LEPLAC Program conducted by the Diretoria de Hidrografia e Navegação (DHN) of the Brazilian Navy for providing bathymetric data used for the regional context map. Additionally, we acknowledge the Marine Geology and Geophysics Laboratory (LAGEMAR-UFF) and the Graduate Program in Ocean and Earth Dynamics (DOT-UFF) for logistical and structural support. This study was supported by CNPq and CAPES through research grants and scholarships.

8 REFERENCES

Abu, C., Jackson, C. A. L., & Francis, M. (2025). The role of salt diapirism in controlling the stratigraphic architecture and distribution of deep-water deposits, Pierce Field, East Central Graben, North Sea. Journal of Sedimentary Research, 95(4), 643-674. https://doi.org/10.2110/jsr.2024.022

Allin, J.R., Hunt, J.E., Clare, M.A., Talling, P.J., 2018. Eustatic sea-level controls on the f lushing of a shelf-incising submarine canyon. GSA Bull. 130 (1–2), 222–237. https://doi.org/10.1130/B31658.1

Ashiru, O.R., Qin, Y., Wu, S., 2020. Structural controls on submarine channel morphology, evolution, and architecture, offshore Western Niger delta. Mar. Pet. Geol. 118. https://doi.org/10.1016/j.marpetgeo.2020.104413

Assumpção, M., Dourado, J. C., Ribotta, L. C., Mohriak, W. U., Dias, F. L., & Barbosa, J. R. (2011). The São Vicente earthquake of 2008 April and seismicity in the continental shelf off SE Brazil: further evidence for flexural stresses. *Geophysical Journal International*, *187*(3), 1076-1088. https://doi.org/10.1111/j.1365-246X.2011.05198.x

Barnard, P.L., Erikson, L.H., Kvitek, R.G., 2011. Small-scale sediment transport patterns and bedform morphodynamics: new insights from high-resolution multibeam bathymetry. Geo Mar. Lett. 31 (4), 227–236. DOI 10.1007/s00367-011-0227-1

Benjamin, U., Huuse, M., Hodgetts, D., 2015. Canyon-confined pockmarks on the western Niger Delta slope. Journal of African Earth Sciences 107, 15–27. https://doi.org/10.1016/j.jafrearsci.2015.03.019

Berrocal, J., Assumpção, M., Artezana, R., Dias Neto, C.M., Ortega, R., França, H., Veloso, J.A.V., Antezana, R., Neto, C.M.D., Franca, H., 1984. Sismicidade Do Brasil. Instituto Astronômico e Geofísico, Sao Paulo.

Borisov, D., Frey, D., & Levchenko, O. (2020). Sediment waves on the Santa Catarina plateau (western South Atlantic). *Journal of South American Earth Sciences*, *102*, 102698. https://doi.org/10.1016/j.jsames.2020.102698

Böttner C, Stevenson CJ, Geersen J and Krastel S (2025) The spatiotemporal evolution of a giant submarine canyon system– the Agadir Canyon. Front. Earth Sci. 13:1400289. doi: 10.3389/feart.2025.1400289

Bueno, G.V., Machado, D.L., Jr, Oliveira, J.A.B. & Marques, E.J.J., 2004. A influência do Lineamento de Capricornio na evolução tectono-sedimentar da bacia de Santos. Abstracts, 42nd Brazilian Geological Congress, Araxá, MG, Brazil.

Carvalho, J. M., Barros, L. V., Zahradník, J., Von Huelsen, M. G., & Ferreira, V. M. (2020). Earthquake relocation, focal mechanism and stress field determination in central

Brazil. Journal of South American Earth Sciences, 97, 102411. https://doi.org/10.1016/j.jsames.2019.102411

Carvalho, M., Ferraz, A., Ferrari, A. L., de Matos Mello, S. L., & Gambôa, L. A. P. (2022). Regional-residual separation and enhancement methods applied to regional analysis of potential data: Structure of Florianopolis and Rio de Janeiro fracture zones in the western South Atlantic. Brazilian Journal of Geophysics, 40(2), 287-298.

Chang, H. K., Kowsmanm, R. O., and Figueiredo, A. M. F. (1990). Novos conceitos sobre o desenvolvimento das bacias marginais do Leste brasileiro. *In:* Origem e evolução de bacias sedimentares. Eds. (Pederneiras, G; Gabaglia, R; Milana, E.J.). – Rio de Janeiro. Ed. Gávea: R. Redisch Prog. Viasual Prod. Graf. E Editoração: Petrobras.

Chand, S., Rise, L., Ottesen, D., Dolan, M.F.J., Bellec, V., Boe, R., 2008. Pockmark-like depressions near the Goliat hydrocarbon field, Barents Sea: morphology and genesis. Mar. Pet. Geol. 26, 1035–1042. https://doi.org/10.1016/j.marpetgeo.2008.09.002

Clark, I.R., Cartwright, J.A., 2009. Interactions between submarine channel systems and deformation in deepwater fold belts: Examples from the Levant Basin, Eastern Mediterranean sea. Mar. Pet. Geol. 26, 1465–1482. https://doi.org/10.1016/j.marpetgeo.2009.05.004

Conway, K.W., Barrie, J.V., Picard, K., and Bornhold, B.D., 2012, Submarine channel evolution: Active channels in fjords, British Columbia, Canada: Geo- Marine Letters, v. 32, p. 301–312, https:// doi .org /10 .1007 /s00367 -012 -0280-4.

Contreras, J., Zühlke, R., Bowman, S., Bechstädt, T., 2010. Seismic stratigraphy and subsidence analysis of the southern Brazilian margin (Campos, Santos and Pelotas basins). Mar. Pet. Geol. 27, 1952–1980. https://doi.org/10.1016/j.marpetgeo.2010.06.007

Covault, J.A., Sylvester, Z., Hudec, M.R., Ceyhan, C., Dunlap, D., 2020. Submarine channels 'swept' downstream after bend cutoff in salt basins. Depositional Record 6, 259–272. https://doi.org/10.1002/dep2.75

Davison, I., 2007. Geology and tectonics of the South Atlantic Brazilian salt basins. Geological Society 272 (1), 345–359. London, Special Publications. https://doi.org/10.1144/GSL.SP.2007.272.01.18

Davison, I., Anderson, L., Nuttall, P., 2012. Salt deposition, loading and gravity drainage in the Campos and Santos salt basins. Geological Society, London, Special Publications 363 (1), 159–174. https://doi.org/10.1144/SP363.8

Deptuck ME, Piper DJ, Savoye B, et al. Dimensions and architecture of late Pleistocene submarine lobes off the northern margin of East Corsica. Sedimentology. 2008;55(4):869–98. https ://doi.org/10.1 111/j.1365-3091.2007.00926 .

Demercian, S., Szatmari, P., Cobbold, P.R., 1993. Style and pattern of salt diapirs due to thin-skinned gravitational gliding, Campos and Santos basins, offshore Brazil. Tectonophysics 228 (3), 393–433.

dos Reis, A. T., Silva, C. G., Gorini, M. A., Leaõ, R., Pinto, N., Perovano, R., Santos, M. V. M., Guerra, J. V., Jeck, I. K., & Tavares, A. A. A. (2016). The chuí megaslide complex: Regional-scale submarine landslides on the southern Brazilian margin. In *Advances in Natural and Technological Hazards Research* (Vol. 41). https://doi.org/10.1007/978-3-319-20979-1_11

Duarte and Viana, 2007. Santos Drift System: stratigraphic organization and implications for late Cenozoic palaeocirculation in the Santos Basin, SW Atlantic Ocean. In: Economic and Palaeoceanographic Significance of Contourite Deposits. Eds (Viana, A. R.; Rebesco, M.). Geological Society of London. https://doi.org/10.1144/GSL.SP.2007.276.01.09

Freitas, V.A., Vital, J.C.S., Rodrigues, B.R., Rodrigues, R., 2022. Source rock potential, main depocenters, and CO2 occurrence in the pre-salt section of Santos Basin, Southeast Brazil. J. S. Am. Earth Sci. 115 https://doi.org/10.1016/j. jsames.2022.103760.

Frisicchio, V., Del Ben, A., Geletti, R., Caradonna, M. C., Rebesco, M., & Bellucci, M. (2025). Tectono-sedimentary processes shaping the West Sardinian margin and adjacent oceanic basin during the Plio-Quaternary (Western Mediterranean Sea). Marine Geology, 480, 107450. https://doi.org/10.1016/j.margeo.2024.107450

Gamboa, D., Alves, T.M. & Cartwright, J. (2012) A submarine channel confluence classification for topographically confined slopes. Mar. Petrol. Geol., 35, 176–189. https://doi.org/10.1016/j.marpetgeo.2012.02.011

Gamboa, L. A. P., Ferraz, A. E. P. P. D., Drehmer, L. H., & Demercian, L. S. (2021). Seismic, magnetic, and gravity evidence of marine incursions in the Santos Basin during the early Aptian. doi: 10.1306/13722322MSB.10.1853

Gee, M.J.R., Gawthorpe, R.L., 2006. Submarine channels controlled by salt tectonics: Examples from 3D seismic data offshore Angola. Mar. Pet. Geol. 23, 443–458. https://doi.org/10.1016/j.marpetgeo.2006.01.002

Gee, M.J.R., Gawthorpe, R.L., Bakke, K., Friedmann, S.J., 2007. Seismic geomorphology and evolution of submarine channels from the Angolan continental margin. Journal of Sedimentary Research 77, 433–446. https://doi.org/10.2110/jsr.2007.042

Hercos, C.M., Schreiner, S., Ferreira, E.T.I., 2023. Deep-water seafloor geomorphic features of the Santos Basin, Southeastern Brazilian Margin, shown by analyses and integration of an extensive 3-D seismic data set. Ocean and Coastal Research 71. https://doi.org/10.1590/2675-2824071.22067cmh

Huyghe, P., Foata, M., Deville, E.&Mascle, G. (2004) Channel profiles through the active thrust front of the southern Barbados prism. Geology, 32, 429–432. https://doi.org/10.1130/G20000.1

Jackson, C.A.-L., Lewis, M.M., Reeve, M.T., Evans, A.M., 2015. Enigmatic structures within salt walls of the Santos Basin—Part 1: geometry and kinematics from 3D seismic reflection and well data. J. Struct. Geol. 75, 135–162. https://doi.org/10.1016/j.jsg.2015.01.010

Kanari, M., Tibor, G., Hall, J.K., Ketter, T., Lang, G., Schattner, U., 2020. Sediment transport mechanisms revealed by quantitative analyses of seafloor morphology: New evidence from multibeam bathymetry of the Israel exclusive economic zone. Mar. Pet. Geol. 114. https://doi.org/10.1016/j.marpetgeo.2020.104224

Kunath, P., Talling, P. J., Urlaub, M., Berndt, C., Chi, W. C., & Baker, M., 2025. Ocean-bottom seismometers document how submarine landslides develop and grow. Communications Earth & Environment, 6(1), 871. https://doi.org/10.1038/s43247-025-02918-6

Kumar, N., Gamboa, L.A.P., Schreiber, BC, & Mascle, J. (1977). Geologic History And Origin Of Sao Paulo Plateau (Southeastern Brazilian Margin), Comparison With The Angolan Margin, And The Early Evolution Of The Northern South Atlantic. Init. Repts of the D.S.D.P., Washington, U.S. Gvt Printing Office, vol. 39 (1977), pp. 927-945

Li, W., Alves, T.M., Rebesco, M., Sun, J., Li, J., Li, S., Wu, S., 2020. The Baiyun Slide Complex, South China Sea: a modern example of slope instability controlling submarine-channel incision on continental slopes. Mar. Pet. Geol. 114, 104231. https://doi.org/10.1016/j.marpetgeo.2020.104231

Li, W., Li, S., Alves, T. M., Jing, S., Chen, H., & Zhan, W. (2023). Initiation and evolution of an isolated submarine canyon system on a low-gradient continental slope. Geomorphology, 434, 108746. doi.org/10.1016/j.geomorph.2023.108746

Magee, C., Pichel, L.M., Madden-Nadeau, A.L., Jackson, C.A.-L., Mohriak, W., 2021. Salt–magma interactions influence intrusion distribution and salt tectonics in the Santos Basin, offshore Brazil. Basin Res. 33 (3), 1820–1843. https://doi.org/ 10.1111/bre.12537.

Mahiques, M. M., Schattner, U., Lazar, M., Yukio Gomes Sumida, P., Antonio Pereira de Souza, L., 2017. An extensive pockmark field on the upper Atlantic margin of Southeast Brazil: spatial analysis and its relationship with salt diapirism. Heliyon 3, 257. https://doi.org/10.1016/j.heliyon.2017

Masson, D.G., Harbitz, C.B., Wynn, R.B., Pedersen, G., Løvholt, F., 2006. Submarine landslides: Processes, triggers and hazard prediction. Philosophical Transactions of the Royal Society A: Mathematical, Physical and Engineering Sciences 364, 2009–2039. https://doi.org/10.1098/rsta.2006.1810

McHargue, T., Pyrcz, M.J., Sullivan, M.D., Clark, J.D., Fildani, A., Romans, B.W., Covault, J.A., Levy, M., Posamentier, H.W., Drinkwater, N.J., 2011. Architecture of turbidite channel systems on the continental slope: Patterns and predictions. Mar. Pet. Geol. 28, 728–743. https://doi.org/10.1016/j.marpetgeo.2010.07.008

Mohriak, W.U., 2001. Salt tectonics, volcanic centers, fracture zones and their relationship with the origin and evolution of the South Atlantic Ocean: geophysical evidence in the Brazilian and West African margins. 7th International Congress of the Brazilian Geophysical Society, Salvador, Bahia, Expanded Abstract, pp. 1594–1597.

Mohriak, W. U., Nóbrega, M., Odegard, M. E., Gomes, B. S., & Dickson, W. G., 2010. Geological and Geophysical Interpretation of the Rio Grande Rise, South-Eastern Brazilian Margin: Extensional Tectonics and Rifting of Continental and Oceanic Crusts, pp. 231–245. https://doi.org/10.1144/1354-079309-910

Mohriak, W.U., Leroy, S., 2013. Architecture of rifted continental margins and break-up evolution: insights from the South atlantic, north atlantic and Red Sea–gulf of aden conjugate margins. Geological Society, London, Special Publications 369 (1), 497–535. https://doi.org/10.1144/SP369.17

Mohriak, W.U., Gordon, A.C., Mello, M.R., 2021. Origin and petroleum system of the cabo frio high between the Santos and campos basins: reviewed integration of structural and paleogeographic reconstruction with the oil and gas systems.

Mohriak, W. U.; De Almeida, J. C. H.; Gordon, A. C., 2022. South Atlantic Ocean: postbreakup configuration and Cenozoic magmatism. In: Meso-Cenozoic Brazilian Offshore Magmatism. Cham: Academic Press,. p. 1-45. https://doi.org/10.1016/B978-0-12-823988-9.00007-1

Mohriak, W.U., Szameitat, L., 2023. The anomalous magmatism in the southern part of the Santos basin, and the non-continuous salt layer over Abimael ridge. J. S. Am. Earth Sci., 104435. https://doi.org/10.1016/j.jsames.2023.104435

Moreira, J.L.P., Madeira, C.V., Gil, J.A., Machado, M.A.P., 2007. Bacia de Santos. Bol. Geociências Petrobras 15 (2), 531–549.

Moscardelli, L., Wood, L., 2008. New classification system for mass transport complexes in offshore Trinidad. Basin Research, 20: 73-98.

Normandeau, A., Jenner, K.A., Desiage, P.-A., De Moura Neves, B., Edinger, E., Van Nieuwenhove, N., Limoges, A., Cote, D., and Sherwood, O.A., 2025, Holocene earthquake-triggered submarine landslides and turbidites in western Baffin Bay: Canadian Journal of Earth Sciences, v. 62, p. 1043–1061, https:// doi .org /10 .1139 /cjes -2024 -0068.

Normark, W.R., Carlson, P.R., 2003. Giant submarine canyons, is size any clue to their importance in the rock record? In: Chan, M.A., Archer, A.W. (Eds.), Extreme Depositional Environments, Mega End Members in Geologic Time. Boulder, CO, Geological Society of America, Geological Society of America Special Paper, vol. 370, pp. 175e190. DOI: 10.1130/0-8137-2370-1.175

Normark, W.R., Posamentier, H., Mutti, E., 1993. Turbidite systems: State of the art and future directions. Reviews of Geophysics. https://doi.org/10.1029/93RG02832

Oluboyo, A.P., Gawthorpe, R.L., Bakke, K., Hadler-Jacobsen, F., 2014. Salt tectonic controls on deep-water turbidite depositional systems: Miocene, southwestern Lower Congo Basin, offshore Angola. Basin Research 26, 597–620. https://doi.org/10.1111/bre.12051

Peel, F., Jackson, M. P., & Ormerod, D. (1998). Influence of major steps in the base of salt on the structural style of overlying thin-skinned structures in deep water Angola. In American Association of Petroleum Geologists International Conference and Exhibition (pp. 366–367). Extended Abstracts Volume. Rio de Janeiro, Brazil.

Pichel, L. M., Finch, E., & Gawthorpe, R. (2019). Impacts of pre-salt rift topography on salt tectonics. Tectonics, 38 (2019), pp. 1466-1488. https://doi.org/10.1029/2018TC005174

Pichel, L.M., Jackson, C.A.L., Peel, F., Dooley, T.P., 2020. Base-salt relief controls salt-tectonic structural style, São Paulo Plateau, Santos Basin, Brazil. Basin Research 32, 453–484. https://doi.org/10.1111/bre.12375

Pichel, L.M., Jackson, C.A.L., Peel, F., Ferrer, O., 2021. The Merluza Graben: how a failed spreading center influenced margin structure, and salt deposition and tectonics in the Santos Basin, Brazil. Tectonics 40 (10), e2020TC006640. https://doi.org/10.1029/2020TC006640

Pirmez, C., Beaubouef, R.T., Friedmann, S.J., Mohrig, D.C., 2000. Equilibrium profile and baselevel in submarine channels: examples from Late Pleistocene systems and implications for the architecture of deepwater reservoirs. Deep-water Reservoirs of the World. GCSSEPM Foundation 20th Annual Research Conference.

Posamentier, H.W., Kolla, V., 2003. Seismic geomorphology and stratigraphy of depositional elements in deep-water settings. Journal of Sedimentary Research 73, 367–388. https://doi.org/10.1306/111302730367

Prather, B.E., 2003. Controls on reservoir distribution, architecture and stratigraphic trapping in slope settings. Mar. Pet. Geol. 20, 529–545. https://doi.org/10.1016/j.marpetgeo.2003.03.009

Puig, P., Durán, R., Muñoz, A., Elvira, E., Guillén, J., 2017. Submarine canyon-head morphologies and inferred sediment transport processes in the Alías-Almanzora canyon

system (SW Mediterranean): on the role of the sediment supply. Mar. Geol. 393, 21–34. https://doi.org/10.1016/j.margeo.2017.02.009

Quirk, D.G., Hertle, M., Jeppesen, J.W., Raven, M., Mohriak, W.U., Kann, D.J., et al., 2013. Rifting, subsidence and continental break-up above a mantle plume in the central South Atlantic. Geological Society, London, Special Publications 369 (1), 185–214. https://doi.org/10.1144/SP369.20

Rasmussen, E.S., 1994. The relationship between submarine canyon fill and sea-level change: an example from Middle Miocene offshore Gabon, West Africa. Sediment. Geol. 90 (1–2), 61–75. https://doi.org/10.1016/0037-0738(94)90017-5

Rodriguez, C. R., Jackson, C. L., Rotevatn, A., Bell, R. E., & Francis, M. (2018). Dual tectonic-climatic controls on salt giant deposition in the Santos Basin, offshore Brazil. Geosphere, 14(1), 215–242. https://doi.org/10.1130/GES01434.1

Santos Filho, J.R., Figueiredo Júnior, A.G., Carneiro, J.C., Dias, G.T.M., Ramalho, A.S. (2022). Mesophotic bioclastics and bioconstructions at the continental shelf of Santos Basin, Brazil. Sedimentary Geology, 442, 106294. https://doi.org/10.1016/j.sedgeo.2022.106294

Scotchman, I.C., Gilchrist, G., Kusznir, N.J., Roberts, A.M., Fletcher, R., 2010. The breakup of the South Atlantic Ocean: formation of failed spreading axes and blocks of thinned continental crust in the Santos Basin, Brazil and its consequences for petroleum system development. In: Vining, B.A., Pickering, S.C. (Eds.), Petroleum Geology: from Mature Basins to New Frontiers – Proceedings of the 7th Petroleum Geology Conference. Geological Society, London, pp. 855–866. https://doi.org/10.1144/0070855

Shipp, R. C., Weimer, P., & Posamentier, H. W. (2011). Mass-transport deposits in deepwater settings: an introduction. SEPM Special Publication, Tulsa, OK (2011), p. 96 https://doi.org/10.2110/sepmsp.096.003

Silva, C. C., dos Reis, A. T., Perovano, R. J., Gorini, M. A., dos Santos, M. V. M., Jeck, I. K., Tavares, A. A. A., & Gorini, C. (2016). Multiple megaslide complexes and their significance for the Miocene stratigraphic evolution of the offshore Amazon Basin. *Submarine Mass Movements and Their Consequences, 7th International Symposium*. https://doi.org/10.1007/978-3-319-20979-1_5

Silva, F. C., Mohriak, W. U., Porto, A. L., & Gordon, A. C. (2024). The impact of the Abimael Ridge on the salt tectonics in the southern Santos Basin, Brazil: The Esmeralda exploration block case. *Journal of South American Earth Sciences*, *148*, 105094. https://doi.org/10.1016/j.jsames.2024.105094

Silveira, I.C., Bernardo, P.S., Lazaneo, C.Z., Amorim, J.P., Borges-Silva, M., Martins, R.C., Santos, D., Dottori, M., Belo, W.C., Martins, R.P., et al., 2022. Oceanographic conditions of the continental slope and deep Waters in Santos Basin: the SANSED cruise (winter 2019). Ocean and Coastal Research 71.

Smith, R. (2004) Silled sub-basins to connected tortuous corridors: sediment distribution systems on topographically complex sub-aqueous slopes. In: Confined Turbidite Systems (Ed. by S.A. Lomas & P. Joseph) Geol. Soc. London Spec. Publ., 222,23–44. https://doi.org/10.1144/GSL.SP.2004.222.01.03

Soutter, E.L., Kane, I.A., Fuhrmann, A., Cumberpatch, Z.A., Huuse, M., 2019. The stratigraphic evolution of OnLAP in siliciclastic deep-water systems: Autogenic modulation of allogenic signals. Journal of Sedimentary Research 89, 890–917. https://doi.org/10.2110/jsr.2019.49

Talling, P. J., Masson, D. G., Sumner, E. J., and Malgesini, G. (2012). Subaqueous sediment density flows: depositional processes and deposit types. Sedimentology 59 (7), 1937–2003. doi:10.1111/j.1365-3091.2012.01353.x

Taylor, W.J., Hodgson, D.M., Peakall, J., Kane, I.A., Flint, S.S., Bouwmeester, M.J., Marsh, J.R., Soutter, E.L., Poyatos-Moré, M., McArthur, A.D., Keavney, E., Brunt, R.L., and Valdez-Buso, V., 2026, Spilling into confinement: Submarine canyon-confined overbank processes and architecture: Geosphere, v. 22, no. 1, p. 70–100, https://doi.org/10.1130/GES02900.1

Vidal, A.C., Kiang, C.H., Corrêa, F.S., Fernandes, F.L., Castro, J.D., Tinen, J.S., et al., 2003. Interpretação e mapeamento dos sistemas petrolíferos da Bacia de Santos, vol. 1. ANP/UNESP/LEBAC, p. 170.

White, R., McKenzie, D., 1989. Magmatism at rift zones: the generation of volcanic continental margins and flood basalts. J. Geophys. Res. Solid Earth 94 (B6). https://doi.org/10.1029/JB094iB06p07685

Wu, N., Nugraha, H. D., Zhong, G., & Steventon, M. J. (2022). The role of mass-transport complexes in the initiation and evolution of submarine canyons. Sedimentology, 69(5), 2181-2202. https://doi.org/10.1111/sed.12987

Zembruscki, S.G. (1979). Geomorfologia da margem continental sul brasileira e das bacias adjacentes. In: Chaves, H.A.F. (Ed.), Projeto REMAC – Geomorfologia da margem continental brasileira e das áreas adjacentes (Relatório Final). PETROBRÁS, CENPES, DINTEP, 7, 129–177.

Zhang, L. F., Pan, M., & Li, Z. L. (2020). 3D modeling of deepwater turbidite lobes: a review of the research status and progress. Petroleum Science, 17(2), 317-333. https://doi.org/10.1007/s12182-019-00415-y

Zhang, J., Zhao, J., Gao, Z., Shen, W., Wei, F., Meng, X., Yan, X., Zhang, X., Wu, W., Zhao, Z., Cao, L. & Bai, Y. (2026). Characterization of gravity-flow deposits in the Chang 7–9 oil groups in the Yanchang Formation, Ganquan County, Ordos Basin. Energy Geoscience, 100520. https://doi.org/10.1016/j.engeos.2026.100520

5. REFERÊNCIAS

ABU, C., JACKSON, C. A. L., & FRANCIS, M. (2025). The role of salt diapirism in controlling the stratigraphic architecture and distribution of deep-water deposits, Pierce Field, East Central Graben, North Sea. Journal of Sedimentary Research, 95(4), 643-674. https://doi.org/10.2110/jsr.2024.022

ALLIN, J.R., HUNT, J.E., CLARE, M.A., TALLING, P.J., 2018. Eustatic sea-level controls on the f lushing of a shelf-incising submarine canyon. GSA Bull. 130 (1–2), 222–237. https://doi.org/10.1130/B31658.1

ASHIRU, O.R., QIN, Y., WU, S., 2020. Structural controls on submarine channel morphology, evolution, and architecture, offshore Western Niger delta. Mar. Pet. Geol. 118. https://doi.org/10.1016/j.marpetgeo.2020.104413

BARNARD, P.L., ERIKSON, L.H., KVITEK, R.G., 2011. Small-scale sediment transport patterns and bedform morphodynamics: new insights from high-resolution

multibeam bathymetry. Geo Mar. Lett. 31 (4), 227–236. DOI 10.1007/s00367-011-0227-1

BORISOV, D., FREY, D., & LEVCHENKO, O. (2020). Sediment waves on the Santa Catarina plateau (western South Atlantic). Journal of South American Earth Sciences, 102, 102698. https://doi.org/10.1016/j.jsames.2020.102698

BOSWARVA, K.; BUTTERS, A.; FOX, C. J.; HOWE, J. A.; NARAYANASWAMY, B. Improving marine habitat mapping using high-resolution acoustic data: a predictive habitat map for the Firth of Lorn, Scotland. Continental Shelf Research, v. 168, p. 39–47, 2018. DOI: 10.1016/j.csr.2018.09.005.

BÖTTNER C, STEVENSON CJ, GEERSEN J and KRASTEL S (2025) The spatiotemporal evolution of a giant submarine canyon system– the Agadir Canyon. Front. Earth Sci. 13:1400289. doi: 10.3389/feart.2025.1400289

CATUNEANU, O. Principles of sequence stratigraphy. 2. ed. Amsterdam: Elsevier, 2022. ISBN 978-0-444-53353-1.

CLARK, I.R., CARTWRIGHT, J.A., 2009. Interactions between submarine channel systems and deformation in deepwater fold belts: Examples from the Levant Basin, Eastern Mediterranean sea. Mar. Pet. Geol. 26, 1465–1482. https://doi.org/10.1016/j.marpetgeo.2009.05.004

CONWAY, K.W., BARRIE, J.V., PICARD, K., and BORNHOLD, B.D., 2012, Submarine channel evolution: Active channels in fjords, British Columbia, Canada: Geo- Marine Letters, v. 32, p. 301–312, https:// doi .org /10 .1007 /s00367 -012 -0280-4.

COVAULT, J.A., SYLVESTER, Z., HUDEC, M.R., CEYHAN, C., DUNLAP, D., 2020. Submarine channels ‘swept’ downstream after bend cutoff in salt basins. Depositional Record 6, 259–272. https://doi.org/10.1002/dep2.75

DEPTUCK ME, PIPER DJ, SAVOYE B, et al. Dimensions and architecture of late Pleistocene submarine lobes off the northern margin of East Corsica. Sedimentology. 2008;55(4):869–98. https ://doi.org/10.1 111/j.1365-3091.2007.00926 .x.

DEPTUCK, M. E.; SYLVESTER, Z.; PIRMEZ, C.; O'BYRNE, C. Migration–aggradation history and 3-D seismic geomorphology of submarine channels in the

Pleistocene Benin-major Canyon, western Niger Delta slope. Marine and Petroleum Geology, v. 24, n. 6–9, p. 406–433, 2007.

DUARTE and VIANA, 2007. Santos Drift System: stratigraphic organization and implications for late Cenozoic palaeocirculation in the Santos Basin, SW Atlantic Ocean. In: Economic and Palaeoceanographic Significance of Contourite Deposits. Eds (Viana, A. R.; Rebesco, M.). Geological Society of London. https://doi.org/10.1144/GSL.SP.2007.276.01.09

FOSSEN, H. Structural geology. Cambridge: Cambridge University Press, 2016.

GAMBOA, D., ALVES, T.M. & CARTWRIGHT, J. (2012) A submarine channel confluence classification for topographically confined slopes. Mar. Petrol. Geol., 35, 176–189. https://doi.org/10.1016/j.marpetgeo.2012.02.011

GEE, M.J.R., GAWTHORPE, R.L., 2006. Submarine channels controlled by salt tectonics: Examples from 3D seismic data offshore Angola. Mar. Pet. Geol. 23, 443–458. https://doi.org/10.1016/j.marpetgeo.2006.01.002

GEE, M.J.R., GAWTHORPE, R.L., BAKKE, K., FRIEDMANN, S.J., 2007. Seismic geomorphology and evolution of submarine channels from the Angolan continental margin. Journal of Sedimentary Research 77, 433–446. https://doi.org/10.2110/jsr.2007.042

HEEREMA, C. J.; TALLING, P. J.; CARTIGNY, M. J.; PAULL, C. K.; BAILEY, L.; SIMMONS, S. M.; PARSONS, D. R.; CLARE, M. A.; GWIAZDA, R.; LUNDSTEN, E.; ANDERSEN, K.; MAIER, K. L.; XU, J. P.; SUMNER, E. J.; ROSENBERGER, K.; GALES, J.; MCGANN, M.; CARTER, L.; POPE, E.; TEAM, M. C. C. E. C. What determines the downstream evolution of turbidity currents? Earth and Planetary Science Letters, v. 532, p. 116023, 2020.

HERCOS, C.M., SCHREINER, S., FERREIRA, E.T.I., 2023. Deep-water seafloor geomorphic features of the Santos Basin, Southeastern Brazilian Margin, shown by analyses and integration of an extensive 3-D seismic data set. Ocean and Coastal Research 71. https://doi.org/10.1590/2675-2824071.22067cmh

HUDEC, M. R.; JACKSON, M. P. A. Terra infirma: understanding salt tectonics. Earth-Science Reviews, v. 82, p. 1–28, 2007. DOI: 10.1016/j.earscirev.2007.01.001.

JACKSON, M. P. A.; HUDEC, M. R. Salt tectonics: principles and practice. Cambridge: Cambridge University Press, 2017.

JACKSON, M. P. A. Retrospective salt tectonics. In: JACKSON, M. P. A.; ROBERTS, D. G.; SNELSON, S. (ed.). Salt tectonics: a global perspective. Tulsa: American Association of Petroleum Geologists, 1995. p. 1–28. (Memoir, 65).

JACKSON, M. P. A.; VENDEVILLE, B. C. Regional extension as a geologic trigger for diapirism. GSA Bulletin, v. 106, p. 57–73, 1994.

JOBE, Z. R.; LOWE, D. R.; UCHYTIL, S. J. Two fundamentally different types of submarine canyons along the continental margin of Equatorial Guinea. Marine and Petroleum Geology, v. 28, n. 3, p. 843–860, 2011.

KANARI, M., TIBOR, G., HALL, J.K., KETTER, T., LANG, G., SCHATTNER, U., 2020. Sediment transport mechanisms revealed by quantitative analyses of seafloor morphology: New evidence from multibeam bathymetry of the Israel exclusive economic zone. Mar. Pet. Geol. 114. https://doi.org/10.1016/j.marpetgeo.2020.10422

KUNATH, P., TALLING, P. J., URLAUB, M., BERNDT, C., CHI, W. C., & BAKER, M., 2025. Ocean-bottom seismometers document how submarine landslides develop and grow. Communications Earth & Environment, 6(1), 871. https://doi.org/10.1038/s43247-025-02918-

LI, W., ALVES, T.M., REBESCO, M., SUN, J., LI, J., LI, S., WU, S., 2020. The Baiyun Slide Complex, South China Sea: a modern example of slope instability controlling submarine-channel incision on continental slopes. Mar. Pet. Geol. 114, 104231. https://doi.org/10.1016/j.marpetgeo.2020.104231

LI, W., LI, S., ALVES, T. M., JING, S., CHEN, H., & ZHAN, W. (2023). Initiation and evolution of an isolated submarine canyon system on a low-gradient continental slope. Geomorphology, 434, 108746. doi.org/10.1016/j.geomorph.2023.10874

MASSON, D. G.; HARBITZ, C. B.; WYNN, R. B.; PEDERSEN, G. Submarine landslides: processes, triggers and hazard prediction. Philosophical Transactions of the Royal Society A: Mathematical, Physical and Engineering Sciences, v. 364, n. 1845, p. 2009–2039, 2006.

MAYALL, M.; JONES, E.; CASEY, M. Turbidite channel reservoirs—key elements in facies prediction and effective development. Marine and Petroleum Geology, v. 23, n. 8, p. 821–841, 2006.

MCHARGUE, T., PYREZ, M.J., SULLIVAN, M.D., CLARK, J.D., FILDANI, A., ROMANS, B.W., COVAULT, J.A., LEVY, M., POSAMENTIER, H.W., DRINKWATER, N.J., 2011. Architecture of turbidite channel systems on the continental slope: Patterns and predictions. Mar. Pet. Geol. 28, 728–743. https://doi.org/10.1016/j.marpetgeo.2010.07.008

MOHRIAK, W. U.; SZATMARI, P.; ANJOS, S. M. C. Sal: geologia e tectônica. São Paulo: Beca, 2008. p. 64–89.

MOHRIAK, W.U., SZAMEITAT, L., 2023. The anomalous magmatism in the southern part of the Santos basin, and the non-continuous salt layer over Abimael ridge. J. S. Am. Earth Sci., 104435. https://doi.org/10.1016/j.jsames.2023.104435

MOSCARDELLI, L.; WOOD, L.; MANN, P. Mass-transport complexes and associated processes in the offshore area of Trinidad and Venezuela. AAPG Bulletin, v. 90, p. 1059–1088, 2006.

MOSCARDELLI, L.; WOOD, L. New classification system for mass transport complexes in offshore Trinidad. Basin Research, v. 20, n. 1, p. 73–98, 2007.

NORMANDEAU, A., JENNER, K.A., DESIAGE, P.-A., DE MOURA NEVES, B., EDINGER, E., VAN NIEUWENHOVE, N., LIMOGES, A., COTE, D., and SHERWOOD, O.A., 2025, Holocene earthquake-triggered submarine landslides and turbidites in western Baffin Bay: Canadian Journal of Earth Sciences, v. 62, p. 1043–1061, https:// doi .org /10 .1139 /cjes -2024 -0068.

NORMARK, William R.; CARLSON, Paul R. Giant submarine canyons: Is size any clue to their importance in the rock record? Geological Society of America, Geological Society of America Special Paper, vol. 370, pp. 175e190.2003. DOI: 10.1130/0-8137-2370-1.175

NORMARK, W. R.; POSAMENTIER, H.; MUTTI, E. Turbidite systems: state of the art and future directions. Reviews of Geophysics, v. 31, n. 2, p. 91–116, 1993

OLUBOYO, A.P., GAWTHORPE, R.L., BAKKE, K., HADLER-JACOBSEN, F., 2014. Salt tectonic controls on deep-water turbidite depositional systems: Miocene,

southwestern Lower Congo Basin, offshore Angola. Basin Research 26, 597–620. https://doi.org/10.1111/bre.12051

PICHEL, L.M., JACKSON, C.A.L., PEEL, F., DOOLEY, T.P., 2020. Base-salt relief controls salt-tectonic structural style, São Paulo Plateau, Santos Basin, Brazil. Basin Research 32, 453–484. https://doi.org/10.1111/bre.1237

PIRMEZ, C., BEAUBOUEF, R.T., FRIEDMANN, S.J., MOHRIG, D.C., 2000. Equilibrium profile and baselevel in submarine channels: examples from Late Pleistocene systems and implications for the architecture of deepwater reservoirs. Deep-water Reservoirs of the World. GCSSEPM Foundation 20th Annual Research Conference.

POSAMENTIER, H.W., KOLLA, V., 2003. Seismic geomorphology and stratigraphy of depositional elements in deep-water settings. Journal of Sedimentary Research 73, 367–388. https://doi.org/10.1306/11130273036

PRATHER, B.E., 2003. Controls on reservoir distribution, architecture and stratigraphic trapping in slope settings. Mar. Pet. Geol. 20, 529–545. https://doi.org/10.1016/j.marpetgeo.2003.03.009

PUIG, P., DURÁN, R., MUÑOZ, A., ELVIRA, E., GUILLÉN, J., 2017. Submarine canyon-head morphologies and inferred sediment transport processes in the Alías-Almanzora canyon system (SW Mediterranean): on the role of the sediment supply. Mar. Geol. 393, 21–34. https://doi.org/10.1016/j.margeo.2017.02.009

RASMUSSEN, E.S., 1994. The relationship between submarine canyon fill and sea-level change: an example from Middle Miocene offshore Gabon, West Africa. Sediment. Geol. 90 (1–2), 61–75. https://doi.org/10.1016/0037-0738(94)90017-

SANTOS FILHO, J.R., FIGUEIREDO JÚNIOR, A.G., CARNEIRO, J.C., DIAS, G.T.M., RAMALHO, A.S. (2022). Mesophotic bioclastics and bioconstructions at the continental shelf of Santos Basin, Brazil. Sedimentary Geology, 442, 106294. https://doi.org/10.1016/j.sedgeo.2022.106294

SHANMUGAM, G., 2019. Slides, slumps, debris flows, turbidity currents, hyperpycnal flows, and bottom currents. Encyclopedia of ocean sciences, v. 4, p. 228-257.

SHANMUGAM, G.; LEHTONEN, L. R.; STRAUME, T.; SYVERTSEN, S. E.; HODGKINSON, R. J.; SKIBELI, M. Slump and debris-flow dominated upper slope

facies in the Cretaceous of the Norwegian and Northern North Seas (61–67°N): implications for sand distribution. AAPG Bulletin, v. 78, n. 6, p. 910–937, 1994.

SHIPP, R. C., WEIMER, P., & POSAMENTIER, H. W. (2011). Mass-transport deposits in deepwater settings: an introduction. SEPM Special Publication, Tulsa, OK (2011), p. 96 https://doi.org/10.2110/sepmsp.096.003

SILVA, F. C., MOHRIAK, W. U., PORTO, A. L., & GORDON, A. C. (2024). The impact of the Abimael Ridge on the salt tectonics in the southern Santos Basin, Brazil: The Esmeralda exploration block case. Journal of South American Earth Sciences, 148, 105094. https://doi.org/10.1016/j.jsames.2024.10509

SMITH, R. (2004) Silled sub-basins to connected tortuous corridors: sediment distribution systems on topographically complex sub-aqueous slopes. In: Confined Turbidite Systems (Ed. by S.A. Lomas & P. Joseph) Geol. Soc. London Spec. Publ., 222,23–44. https://doi.org/10.1144/GSL.SP.2004.222.01.03

TALLING, P. J., MASSON, D. G., SUMNER, E. J., and MALGESINI, G. (2012). Subaqueous sediment density flows: depositional processes and deposit types. Sedimentology 59 (7), 1937–2003. doi:10.1111/j.1365-3091.2012.01353.

TAYLOR, W.J., HODGSON, D.M., PEAKALL, J., KANE, I.A., FLINT, S.S., BOUWMEESTER, M.J., MARSH, J.R., SOUTTER, E.L., POYATOS-MORÉ, M., MCARTHUR, A.D., KEAVNEY, E., BRUNT, R.L., and VALDEZ-BUSO, V., 2026, Spilling into confinement: Submarine canyon-confined overbank processes and architecture: Geosphere, v. 22, no. 1, p. 70–100, https://doi.org/10.1130/GES02900.1

VENDEVILLE, B. C.; JACKSON, M. P. A. The rise of diapirs during thin-skinned extension. Marine and Petroleum Geology, v. 9, n. 4, p. 331–353, 1992a.

VENDEVILLE, B. C.; JACKSON, M. P. A. The fall of diapirs during thin-skinned extension. Marine and Petroleum Geology, v. 9, p. 354–371, 1992b.

WEIJERMARS, R.; JACKSON, M. P. A.; VENDEVILLE, B. C. Rheological and tectonic modeling of salt provinces. Tectonophysics, v. 217, p. 143–174, 1993.

WU, N., NUGRAHA, H. D., ZHONG, G., & STEVENTON, M. J. (2022). The role of mass-transport complexes in the initiation and evolution of submarine canyons. Sedimentology, 69(5), 2181-2202. https://doi.org/10.1111/sed.12987

ZEMBRUSCKI, S.G. (1979). Geomorfologia da margem continental sul brasileira e das bacias adjacentes. In: Chaves, H.A.F. (Ed.), Projeto REMAC – Geomorfologia da margem continental brasileira e das áreas adjacentes (Relatório Final). PETROBRÁS, CENPES, DINTEP, 7, 129–177.

ZHANG, J., ZHAO, J., GAO, Z., SHEN, W., WEI, F., MENG, X., YAN, X., ZHANG, X., WU, W., ZHAO, Z., CAO, L. & BAI, Y. (2026). Characterization of gravity-flow deposits in the Chang 7–9 oil groups in the Yanchang Formation, Ganquan County, Ordos Basin. Energy Geoscience, 100520. https://doi.org/10.1016/j.engeos.2026.100520

ZHANG, L. F., PAN, M., & LI, Z. L. (2020). 3D modeling of deepwater turbidite lobes: a review of the research status and progress. Petroleum Science, 17(2), 317-333. https://doi.org/10.1007/s12182-019-00415-y